

**Synthesis and characterization of activated carbon spheres SILP catalysts for the selective hydrogenation of aldehydes using a well-defined Fe(II) PNP complex**

**Rafael Amorim Leandro de Castro Amoedo**

Thesis to obtain the Master of Science Degree in

**Chemical Engineering**

Supervisors: Professor Ana Margarida Sousa Dias Martins

Professor Karl Kirchner

**Examination Committee**

Chairperson: Professor Maria Matilde Soares Duarte Marques

Supervisor: Professor Ana Margarida Sousa Dias Martins

Members of the Committee: Dr. Maria João Gomes Ferreira

Dr. Zita Csendes

**November 2017**

## Acknowledgements

First and foremost I would like to express my deepest gratitude to all my supervisors, Professor Ana Margarida Martins and Professor Karl Kirchner, without whom this work would not be possible. Furthermore, I would like to extend to Dr. Zita Csendes my warm thankfulness. Their guidance, support and enthusiasm since the first day were crucial to take this adventure on.

To my colleagues, working in Prof. Kirchner's laboratory, which helped me with the ins and outs of so many different techniques. In particular, to Dr. Zita Csendes for the constant input and constructive comments.

To my home university, Instituto Superior Técnico, and in particular to the Department of Chemical Engineering, where I belonged for 5 years that reach an end now. It was an honour and a privilege to be part of it and becoming an engineer of this prestigious university.

Last but definitely not least, to my friends and family, in particular my parents and grandmother who suffered more with my absence than I could imagine and whose unconditional love and support over these 5 years was essential for this day to happen. Finally, to Joana, who played and still plays a very important role in my life.

## Abstract

Supported Ionic Liquid Phase (SILP) systems are in a crescendo development, once they are able to provide the benefits of both homogeneous and heterogeneous catalysis, in particular, excellent selectivity and reaction rates from the former and easiness in handling and separation of the latter. Furthermore, while joining these two classic conceptions, it promotes greener solutions, contributing to the increasing demand for cleaner processes.

The aim of this thesis is to study SILP systems on carbon supports, with a special focus on activated carbon spheres, using a recently discovered and highly selective Fe(II) complex catalyst for the hydrogenation of aldehydes. Moreover, providing insight on the full structure of the porous matrix is also a major point of this work, where BET, XPS, IR and DSC techniques were employed.

Different substrates and Ionic Liquids were tested as well as different experimental conditions, in particular reaction overall pressure and substrate to catalyst ratio.

As major results, a successful SILP was obtained. Hydrogenations using this system showed better results when using 4-Fluorobenzaldehyde as a substrate and pressures above 20 bar, achieving full conversion after 2 hours. The overall conversion was found to be extremely dependent on the impregnation time. Additionally, the SILP structure is manifestly heterogeneous, with the Ionic Liquid adopting special conformations and spatial orientation when in contact with a solid support and when containing catalyst dissolved.

**Keywords:** SILP, Fe(II) PNP complex, hydrogenation, impregnation, conformational change, Ionic Liquid structure.

## Resumo

Sistemas contendo líquidos iónicos em fase suportada estão a ter um desenvolvimento exponencial, uma vez que conseguem conjugar os benefícios tanto da catálise homogénea como heterogénea, em particular a excelente seletividade e velocidade de reação da primeira com a facilidade de manuseamento e separação da segunda. Em adição, ao mesmo tempo que junta estes dois conceitos, institui-se como uma alternativa ecológica, contribuindo para a procura crescente de processos sustentáveis.

O objectivo desta tese é estudar os sistemas acima referidos usando suportes de carbono, com especial enfoco em esferas de carvão ativado, usando um catalisador de Fe(II) recentemente descoberto, que apresenta excelente seletividade para a hidrogenação de aldeídos. O estudo da estrutura porosa é também um ponto-chave do trabalho, com extensiva caracterização da mesma; para isso técnicas como BET, XPS, IR e DSC foram usadas.

Diversos aldeídos e líquidos iónicos foram testados assim como diferentes condições experimentais, em particular a pressão total do sistema e o rácio aldeído/catalisador.

Como resultados principais, um sistema de líquido iónico em fase suportada foi obtido com sucesso. As hidrogenações usando este sistema apresentam melhores resultados usando 4-fluorbenzaldeído e pressões acima de 20 bar, com conversão total em 2 horas. Foi descoberto que a conversão é extremamente dependente do tempo de impregnação na estrutura porosa. Adicionalmente, a estrutura é manifestamente heterogénea, com o líquido iónico a adotar uma conformação especial quando em contacto com o suporte sólido e quando contendo o catalisador dissolvido.

**Palavras-chave:** líquido iónico em fase suportada, complexo Fe(II) PNP, hidrogenação, impregnação, alteração conformação, estrutura do líquido iónico.

# Table of Contents

List of Tables .....	VI
List of Figures .....	VII
Abbreviations and Symbols .....	IX
1. Introduction .....	1
1.1 Motivation .....	1
1.2 Objective .....	2
2. State of the art .....	3
2.1 Supported Ionic Liquids.....	3
2.2 Ionic Liquids.....	4
2.3 Support.....	6
2.4 Catalytic function .....	7
2.5 Catalysis in IL films .....	9
2.6 Applications.....	10
2.6.1 Hydrogenation reactions.....	11
2.7 Solvents.....	12
2.8 Magnetic Ionic Liquids .....	13
2.9 Support and Impregnation .....	14
3. Materials and Methods.....	16
3.1 Substrates.....	16
3.2 Ionic Liquid selection .....	17
3.3 Support.....	19
3.4 Catalyst.....	19
3.5 Procedures .....	21
3.5.1 General procedures.....	21
3.5.2 Miscibility test.....	21
3.5.3 Carbon treatment .....	21
3.5.4 NMR measurements .....	22
3.5.5 Elemental Analysis/ICP.....	22
3.5.6 XPS measurements .....	22
3.5.7 BET measurements .....	23
3.5.8 DSC measurements.....	23
3.5.9 Infrared measurements.....	23
3.5.10 Density measurements.....	24

3.5.11 Impregnation procedure .....	24
3.5.12 Hydrogenation reactions procedure .....	24
3.5.13 Recyclability tests.....	25
4. Results and discussion .....	26
4.1 Measured properties .....	26
4.2 Homogeneous reactions.....	28
4.3 Biphasic reactions .....	29
4.4 Heterogeneous reactions.....	31
4.5 Activated Carbon Spheres .....	33
4.5.1 Support characterization .....	33
4.6 Reaction optimization .....	38
4.7 Characterization of CARB 40 .....	45
4.7.1 FTIR measurements.....	45
4.7.2 BET and density measurements.....	47
4.7.3 XPS results .....	48
4.8 Reactions using the optimized CARB 40 .....	56
4.8.1 Substrate to catalyst ratio (S/C).....	56
4.8.2 Mass transfer limitations.....	57
4.8.3 Leaching.....	59
4.8.4 Recyclability .....	59
4.9 Carbon Cloth – Activated carbon fibers .....	63
4.10 Overall resume .....	65
5. Conclusions and future work.....	66
6. References.....	68

## List of Tables

TABLE 1 - SWOT ANALYSIS OF ILS DEVELOPMENT. ....	6
TABLE 2 - APPLICATIONS OF IL PER KIND OF REACTION .....	10
TABLE 3 - COMPARATIVE BOARD FOR DIFFERENT KINDS OF SUPPORT. ....	14
TABLE 4 - PAIRS ALDEHYDE/ALCOHOL USED .....	16
TABLE 5 - ILS USED; DESCRIPTION AND STRUCTURE. ....	17
TABLE 6 - MISCIBILITY TEST AT 25 (R.T.), 60 AND 0°C.....	26
TABLE 7 - CATALYST SOLUBILITY IN DIFFERENT ILS. ....	27
TABLE 8 - HOMOGENEOUS REACTIONS RESULTS FOR 4-FBA.....	28
TABLE 9 - HOMOGENEOUS REACTIONS RESULTS; 10 BAR HYDROGEN PRESSURE .....	28
TABLE 10 - BIPHASIC REACTIONS. REACTION CONDITIONS: 2 MMOL OF 4-FBA, 0.5 MOL% CATALYST, 2 ML SOLVENT AND IL AMOUNT ACCORDING TO TABLE 7; PRESSURE: 10 BAR. ....	30
TABLE 11 - ELEMENTAL ANALYSIS SUMMARY; * - BELOW THE DETECTION LIMIT. ....	34
TABLE 12 - BET MEASUREMENTS ON PURE CARBON SUPPORT. ....	35
TABLE 13 - XPS SURFACE ELEMENTAL ANALYSIS; * BELOW DETECTION LIMIT. ....	35
TABLE 14 - SUPPORT USED AND RESPECTIVE PH.....	37
TABLE 15 - PORE FILLING DEGREE TESTING ON SUPPORTED REACTIONS; SUPPORT: 100 MG OF CC; IL#1: 50ML.....	39
TABLE 16 - PORE FILLING DEGREE TESTING ON SUPPORTED REACTIONS; SUPPORT: 100 MG OF CARB; IL#1: 50ML. ....	41
TABLE 17 - BET RESULTS FOR CARB AND CC. ....	42
TABLE 18 - BET MEASUREMENTS ON CARBON SAMPLES.....	47
TABLE 19 - DENSITY RESULTS FOR IL AND IL+CAT.....	47
TABLE 20 - XPS ELEMENTAL ANALYSIS.....	48
TABLE 21 - ICP RESULTS FOR LEACHING DETECTING; ** - LEACHING WAS DETECTED BY NMR. ....	59
TABLE 22 - SUBSTRATE SCREENING; EXPERIMENTAL CONDITION: 100 MG OF SUPPORT; 2 MMOL OF SUBSTRATE; 5 MG OF CATALYST; 2 ML OF SOLVENT (HEPTANE); 16ML OF DBU; 50 ML OF IL#1; PRESSURE: 10 BAR. ....	61
TABLE 23 - CARBON CLOTHS MAIN CHARACTERISTICS. ....	64
TABLE 24 - CARBON CLOTHS RESULTS. EXPERIMENTAL CONDITIONS: 100 MG OF SUPPORT; 1 MMOL OF SUBSTRATE (4-FBA); 2.5 MG OF CATALYST; 2 ML OF SOLVENT (HEPTANE); 8 ML OF DBU; 40 ML OF IL#1; PRESSURE: 40 BAR. ....	65
TABLE 25 - RESUME CONDITIONS: BIPHASIC: 2 MMOL OF SUBSTRATE; 5 MG OF CATALYST; 2 ML OF SOLVENT (HEPTANE); 16 ML OF DBU; IL ACCORDING TO TABLE 7; SUPPORTED: 100 MG OF SUPPORT; 2 MMOL OF SUBSTRATE; 5 MG OF CATALYST; 2 ML OF SOLVENT (HEPTANE); 16 ML OF DBU; 50 ML OF IL; PRESSURE: 10/40 BAR. * - NO DBU ADDED. ....	65

## List of Figures

FIGURE 1 - SCHEMATIC REPRESENTATION OF SUPPORTED IL; THE GREEN LINE REPRESENTS THE IL PHASE CONTAINING A HOMOGENEOUS CATALYST. ....	3
FIGURE 2 - MOST COMMON CATIONS IN IL'S STRUCTURES .....	4
FIGURE 3 - MOST COMMON ANIONS IN IL'S STRUCTURES .....	5
FIGURE 4 - DIFFERENT POSSIBILITIES FOR THE LOCALIZATION OF THE CATALYTIC FUNCTION (CF).....	8
FIGURE 5 - SCHEMATIC REPRESENTATION OF THE CATALYST ENTRAPMENT INSIDE IL CLUSTER. LINES AND DOTS REPRESENT CONNECTIONS TO LIGANDS, NOT SHOWN ON PURPOSE. ....	9
FIGURE 6 - DIFFERENT BINDING MODES EXPECTED FOR HOMOGENEOUS CATALYST IN (A) IONIC LIQUID (B) COMMON SOLVENT. ADAPTED FROM REF. 53.....	12
FIGURE 7 - SCHEMATIC REPRESENTATION OF DIFFERENT APPROACHES TO HYDROGENATION. ....	15
FIGURE 8 – IRON HYDRIDE COMPLEXES FROM REF. 76; (A) PRE-CATALYST; (B) ACTIVE CATALYST.....	20
FIGURE 9 - SIMPLIFIED CATALYTIC CYCLE FOR THE CHEMOSELECTIVE HYDROGENATION OF ALDEHYDES; ADAPTED FROM REF.76 .....	20
FIGURE 10 - AUTOCLAVE AND FISHER- PORTER TUBE.....	25
FIGURE 11 - <sup>19</sup> F NMR SPECTRA; 4-FLUOROBENZALDEHYDE PEAK (-102.30 PPM), 4-FLUOROALCOHOL (-114.69) AND NTf2 ANION (-78.22).....	30
FIGURE 12 - SIMPLIFIED DIAGRAM BLOCK OF THE OVERALL PROCESS.....	32
FIGURE 13 – SCHEMATIC REPRESENTATION OF THE DESIRED HYDROGENATION MECHANISM AND SEPARATION IN SUPPORTED CATALYSIS. ....	32
FIGURE 14 - SCHEMATIC REPRESENTATION OF SILP CATALYSIS.....	33
FIGURE 15 – LIGHT MICROSCOPIC IMAGES OF DIFFERENT CARBON PARTICLES (A) AND SEM IMAGE (B); OBTAINED FROM REF. 98....	35
FIGURE 16 - XPS PRISTINE CARBON SURFACE SPECTRA AND QUANTIFICATION; SHAKE-UP STANDS FOR OTHER $\pi$ INTERACTIONS; BLACK LINE REPRESENTS EXPERIMENTAL DATA AND RED LINES THE USED FITTINGS. ....	36
FIGURE 17 - SURFACE GROUPS ON ACTIVATED CARBON SURFACE; IMAGE FROM REF. 97 .....	37
FIGURE 18 – BEGINNING (A) AND THE END (B) OF IMPREGNATION STEP. ....	38
FIGURE 19 – MODEL REACTION FOR OPTIMIZING REACTION CONDITIONS .....	39
FIGURE 20 – MACROSCOPIC VIEW OF 2 SAMPLES WITH (A) DESIRABLE AND (B) UNDESIRABLE TEXTURE.....	40
FIGURE 21 – DSC (GREEN) AND MASS PERCENTAGE (BLACK) PLOTS FOR (A) PURE IL#1 AND (B) IMPREGNATED SAMPLE WITH A = 30% .....	41
FIGURE 22 - 40 BAR PRESSURE HYDROGENATION RESULTS; EXPERIMENTAL CONDITION: 100 MG OF SUPPORT; 2 MMOL OF SUBSTRATE(4-FBA); 5 MG OF CATALYST; 2 ML OF SOLVENT (HEPTANE); 16ML OF DBU; 24-60 ML OF IL#1. ....	42
FIGURE 23 – 10 BAR PRESSURE HYDROGENATION RESULTS; EXPERIMENTAL CONDITION: 100 MG OF SUPPORT; 2 MMOL OF SUBSTRATE(4-FBA); 5 MG OF CATALYST; 2 ML OF SOLVENT (HEPTANE); 16ML OF DBU; 30-60 ML OF IL#1. ....	43
FIGURE 24 - SUPPORT'S AMOUNT RESULTS; EXPERIMENTAL CONDITION: 50-150 MG OF SUPPORT; 2 MMOL OF SUBSTRATE (4-FBA); 5 MG OF CATALYST; 2 ML OF SOLVENT (HEPTANE); 16ML OF DBU; 24-70 ML OF IL#1; PRESSURE: 10 BAR. ....	44
FIGURE 25 – IMPREGNATION TIME EXPERIMENT; EXPERIMENTAL CONDITION: 100 MG OF SUPPORT; 2 MMOL OF SUBSTRATE (4-FBA); 5 MG OF CATALYST; 2 ML OF SOLVENT (HEPTANE); 16ML OF DBU; 50 ML OF IL#1; PRESSURE: 10 BAR; POINTS REPRESENT EXPERIMENTAL DATA; LINES WERE CREATED JUST TO FIT DATA. ....	44
FIGURE 26 – IR RESULTS OF (A) ALL SAMPLES MEASURED AND (B) CATALYST AND IL IN DETAIL; ** - RESULTS FROM SUBTRACTING CARB SPECTRUM FROM CARB 40 SPECTRUM. IN (B), THE SPECTRA WERE BASELINE CORRECTED.....	46
FIGURE 27 - REPRESENTATION OF POSSIBLE PORE CLOGGING. ....	47
FIGURE 28 – XPS SURVEY SCAN SPECTRA AND ELEMENTAL IDENTIFICATION; MEASUREMENTS AT 51° RELATIVE TO SAMPLE SURFACE NORMAL. ....	49
FIGURE 29 – XPS C 1s SPECTRA AND IL#1 STRUCTURE AND PEAK ASSIGNMENT; MEASUREMENTS AT 51° RELATIVE TO SAMPLE SURFACE NORMAL .....	50
FIGURE 30 – N1s, S2p AND F 1s XPS SPECTRA FOR MAJOR SAMPLES; MEASUREMENTS AT 51° RELATIVE TO SAMPLE SURFACE NORMAL. ....	51
FIGURE 31 – XPS ANGLE DEPENDANT RESULTS FOR CARBON ELEMENT; VALUES IN ATOMIC PERCENTAGE. ....	53
FIGURE 32 - XPS ANGLE DEPENDANT RESULTS FOR NITROGEN ELEMENT; VALUES IN ATOMIC PERCENTAGE.....	53
FIGURE 33 - XPS ANGLE DEPENDANT RESULTS FOR SULFUR ELEMENT; VALUES IN ATOMIC PERCENTAGE. ....	54
FIGURE 34 - XPS ANGLE DEPENDANT RESULTS FOR FLUOR ELEMENT; VALUES IN ATOMIC PERCENTAGE.....	54



FIGURE 35 - XPS ANGLE DEPENDANT RESULTS FOR OXYGEN ELEMENT; VALUES IN ATOMIC PERCENTAGE. ....	55
FIGURE 36 - S/C RATIO EXPERIMENTS AT (A) 10 BAR AND (B) 40 BAR; EXPERIMENTAL CONDITION: 100 MG OF SUPPORT; 2-10 MMOL OF SUBSTRATE; 5 MG OF CATALYST; 2 ML OF SOLVENT (HEPTANE); 16ML OF DBU; 50 ML OF IL#1; PRESSURE: 10;40 BAR. .	57
FIGURE 37 - SCHEMATIC REPRESENTATION OF MAJOR MASS TRANSFER LIMITATIONS; $C_{\infty}$ - CONCENTRATION OF H <sub>2</sub> IN THE GAS PHASE; $C_{SAT}$ . - MAXIMUM CONCENTRATION OF H <sub>2</sub> IN HEPTANE. ....	58
FIGURE 38 - EFFECT OF CHANGING H <sub>2</sub> PRESSURE; EXPERIMENTAL CONDITION: 100 MG OF SUPPORT; 2 MMOL OF SUBSTRATE(4-FBA); 5 MG OF CATALYST; 2 ML OF SOLVENT (HEPTANE); 16ML OF DBU; 50 ML OF IL#1; PRESSURE: 10-40 BAR. ....	58
FIGURE 39 - RECYCLABILITY TESTED; EXPERIMENTAL CONDITIONS: 100 MG OF SUPPORT; 2 MMOL OF SUBSTRATE (4-FBA); 5 MG OF CATALYST; 2 ML OF SOLVENT (HEPTANE); 16ML OF DBU; 50 ML OF IL#1; PRESSURE: 40 BAR. ....	60
FIGURE 40 - ILS TESTING; EXPERIMENTAL CONDITION: 100 MG OF SUPPORT; 2 MMOL OF SUBSTRATE(4-FBA); 5 MG OF CATALYST; 2 ML OF SOLVENT (HEPTANE); 16ML OF DBU; 50 ML OF IL; PRESSURE: 10 BAR. ....	63
FIGURE 41 - CARBON CLOTH EXAMPLE. ....	64

## Abbreviations and Symbols

IL – Ionic liquid

MIL – Magnetic Ionic Liquid

4-FBA – 4-Fluorobenzaldehyde

SILP – Supported Ionic Liquid Phase

NMR – Nuclear Magnetic Resonance

XPS – X-ray photoelectron spectroscopy

BET – Brunauer-Emmett-Teller

DSC – Differential Scanning Calorimetry

Cat. – Catalyst

R.T. – Room temperature

DBU - 2,3,4,6,7,8,9,10-octahydropyrimido[1,2-a]azepine or 1,8-Diazabicyclo[5.4.0]undec-7-ene

$C_{\text{sat}}$  – Saturation concentration

$C_{\infty}$  - Infinite concentration

*i*-Pr – Isopropyl

KE – Kinetic Energy

BE or B.E. – Binding Energy

*h* - Plank constant

$\nu$  – Frequency

Eq. – equation

UHV – Ultra High Vacuum

NTf<sub>2</sub> – Bis(trifluoromethylsulfonyl)imide

*j* – Azimuthal quantum number

$m_j$  – Magnetic quantum number

min. – minute

TON – Turnover Number

TOF - Turnover Frequency

LiOTf - Lithium trifluoromethanesulfonate

OTf – Trifluoromethanesulfonate

S:C – Substrate to Catalyst ratio

$\alpha$  – Pore filling degree

at.% - Atomic percentage

CC – Comercial Carbon

CARB – Comercial Carbon after thermal treatment

# 1. Introduction

## 1.1 Motivation

Both homogeneous and heterogeneous catalysis are largely studied worldwide; their advantages and drawbacks are known. The main benefits of homogenous catalytic processes are the high selectivity, often achieved by using asymmetric metal complexes that introduce chirality and produce enantiomeric pure organic compounds [1], associated with high yields due to molecular dispersion. On the other hand, the very hard separation of the catalyst, not only but more pronounced in industrial applications, constitute the main setback of this type of catalysis. For the heterogeneous systems, the ease of separation is undoubtedly the major advantage. The catalyst must be recycled, not only because of cost issues, but also because of waste and environmental considerations. In this way recycling of the catalyst is part of an environmentally adapted and sustainable chemistry [2]. The lack of good selectivity (associated with active sites distribution and affinity to different molecules) as well as low global yields are on the list of disadvantages of heterogeneous catalysis.

There is a natural feeling, transversal to all fields of knowledge, to adapt an existing theory or mix two theories in order to accommodate the new results. This mechanism of building over an existing set of results is logical. The same happens to catalysis. Curiously the weak points of homogenous catalysis are the strong points of heterogeneous and vice-versa.

A possible approach consists in immobilizing organometallic complexes, including cross-linking with organic [3] or inorganic groups [4], fixation on solid supports, like oxides [5] or even polymers [6]. The results though were not what it was expected, once enantioselectivity was often lost in the majority of immobilisation methods [7].

The idea was simple, but a bridge was needed in order to bring the best of both worlds together. In a first approach Ionic Liquids (ILs) were tested, in order to be the liquid phase in which the catalyst could be dissolved, while being stable and active. In general the rate of those reactions was in line with that of using only homogeneous catalysts and a high enantioselectivity was obtained [8]. The first steps were laid down for an all new subtopic inside catalysis where in the last 20 years a tremendous research work not only in academia but also in the industry [9,10] has been achieved. Primarily and due to some catalysts excellent immobilization in the IL, liquid-liquid biphasic processes were optimized, changing the common organic solvent by ILs. In this way ILs were regarded as alternative solvents [11]. Also, desirable low miscibility with reaction products was observed. Two problems were to be solved: the price and the reaction rate limitation. For the first little was to be done, once large quantities were required. For the second, the viscosity of the IL is a key parameter in ensuring the good diffusion of both reagents and products inside the IL phase. In some cases the reaction occurred only in a small layer, due to severe mass limitation. The correct choice of ILs would tune the properties but ensure that all the volume was active was a difficult task.

The fact that ILs presented better performances in liquid-liquid biphasic applications, was not enough *per se*, to change any industrial purposes for the aforementioned reasons. Furthermore, it lacked an important characteristic: it was not "green". The current environmental concerns, that get stricter as the years pass by, demanded an alternative sustainable suggestion. In this way, the immobilization of ILs in different supports solved both, the environmental and the economic issues. This has become known as Supported Ionic-Liquid-Phase (SILP) [12], firstly developed by Mehnert et al. [13]. Mass transfer limitations concerns were also solved, once the layer inside the porous material

or on top of it, is normally thin (about 0.5 nm) [14] and the whole IL volume is within the diffusion layer. Furthermore, the supported ionic liquid catalyst shows a greater activity when compared to biphasic ionic liquids reaction, with TOFs at least 3 times higher [8]. These results were ascribed essentially to a higher concentration of the catalyst species at the interface, associated with an enhanced surface area provided by the support. For sure the main drawback of biphasic reactions is mass transfer limitation, due to the relatively high viscosity of the IL catalytic phase [15]. Due to this fact the majority of the IL phase is not in contact with the substrate [16] and so the overall rate of reaction is reduced.

## 1.2 Objective

The objective of this work is to shed some light on the selective hydrogenation of aldehydes using a recently synthesized iron(II) homogeneous catalyst. It constitutes an approach, from classical homogenous catalysis, towards a more heterogeneous process, using for that purpose a carbon based support.

The challenge of the project is to be able to choose a proper ionic liquid to dissolve the catalyst and impregnate inside a porous carbon matrix, creating a supported ionic liquid phase (SILP) to perform hydrogenation reactions. Having in mind a green and sustainable chemistry, being able to recycle the SILP is most desirable. Furthermore, by means of different techniques, being able to characterize the support (pure and impregnated) is also part of what is intended.

## 2. State of the art

### 2.1 Supported Ionic Liquids

A rough estimation points out that there must be around  $10^{18}$  Ionic Liquids (IL) available [17]. This number results from the combination of the known anions and cations typically used for this purpose and applications on unexpected and interesting new fields are coming out [18,19].

An IL is defined as a melting salt, having its melting point below  $100^{\circ}\text{C}$  and extremely low vapor pressure (low volatility). Associated with these properties, an extensive mixability with several organic compounds, makes it a suitable candidate for a catalyst phase [10,20,21]. For the majority of the reactions it would be interesting to use an IL with special features, namely polarity and solubility for several components (reactants, products, catalysts, and so on) [22]. This possibility is real due to the large amount of available ILs. A key issue though, in the search procedure for ILs, is the affinity and stability of the catalyst. Typically, catalysts are very sensitive to the surroundings and their deactivation is a serious problem when to choose the appropriate IL. Catalysts' properties such as nucleophilicity, Lewis acidity and basicity [23] are to be analysed. Furthermore, the macroscopic properties of the mixture (IL+catalyst) such as viscosity and density take their role in the overall system and need to be considered as well.

Inspired by heterogeneous processes and in the easy use of a support, a concept for designing catalysts aroused. It consisted in coating a solid support with one (or several) layer(s) of IL (thin preferably). The former would be mainly responsible for the structure (exceptionally the catalytic activity may be associated with the surface) and the latter would transport the catalyst that would be dispersed, acting as a homogeneous catalyst, Figure 1. Another possibility is the IL itself be the catalyst, with one of its ions playing that role [24]. As one may conclude by the almost infinite choices of IL, catalysts and supports interesting results and tailor-made catalysis may be achieved.



**Figure 1** - Schematic representation of supported IL; the green line represents the IL phase containing a homogeneous catalyst.

## 2.2 Ionic Liquids

With a melting point below 100°C [25] Ionic Liquids (ILs) are an extraordinary new class of materials. They consist of self-dissociated ions, which, in other words, means that there is no need of a solvent, like water e.g., to obtain the dissociated ions. ILs applications are several and ranging from electrolytes in batteries [26], active components in sensors [27], extraction solvents [28], lubricants [29] and much more [11].

The first salt facing the required conditions to become an IL was ethanolammonium nitrate and ethylammonium nitrate [30] with melting points ranging from 52-55°C and 12°C, respectively. The biggest input arrived some years after when Wilkes [31] described an electrochemically stable IL, that resulted from the mixing between chloroaluminate  $[\text{AlCl}_4]^-$  and 1-ethyl-3-methyl imidazolium. However, this IL was not stable in water. Later [32] the same author reported the synthesis of imidazolium cations with weakly coordinating anions like  $[\text{PF}_6]^-$ ,  $[\text{BF}_4]^-$ , and others, obtaining water and air stable ILs. Logically this input contributed enormously to the proliferation of ILs and its' applications.

In general, the majority of ILs are designed through the combination of: **a)** an organic heterocyclic cationic structure, like imidazolium, pyrrolidinium, tetraalkylammonium, tetraalkylphosphonium, among others. The most common structures are represented in Figure 2; **b)** an anion that could be either organic or inorganic, such as a halide, nitrate, tetrafluoroborate, and so on. The most commonly used anions are represented in Figure 3.

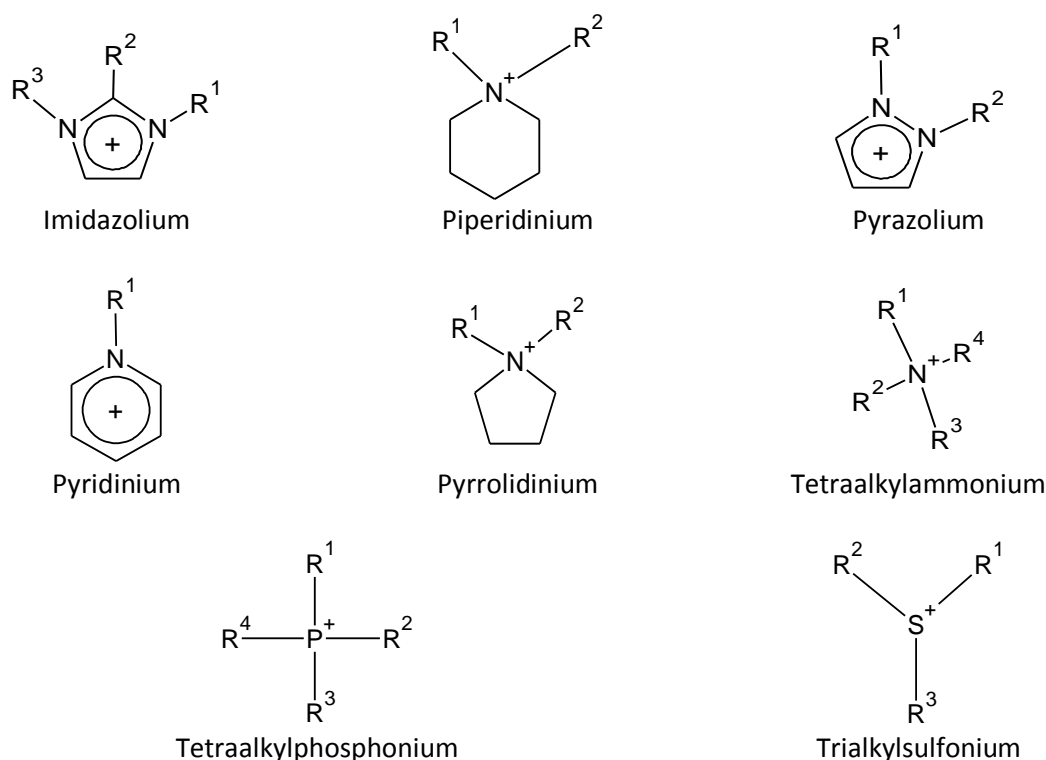


**Figure 2** - Most common cations in IL's structures

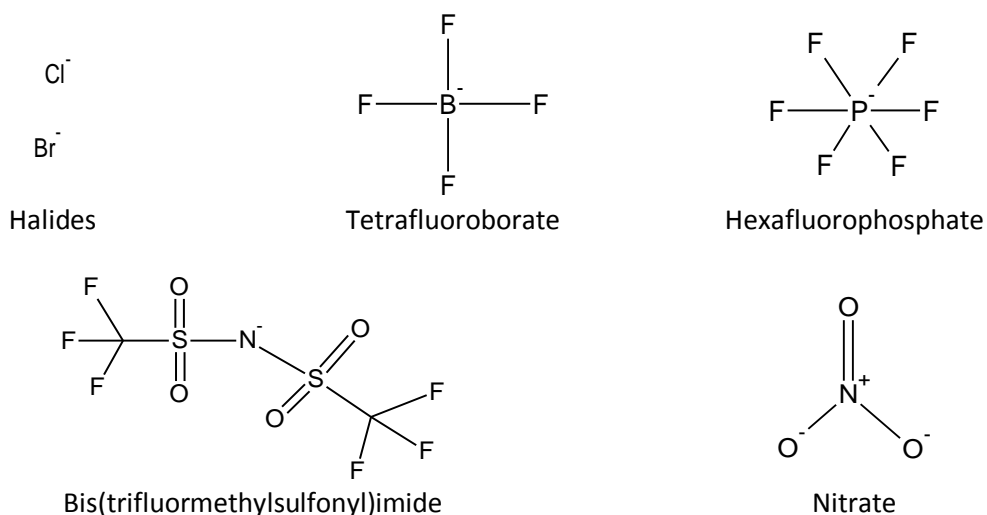


**Figure 3** - Most common anions in IL's structures

ILs have some significant physical and chemical properties that grant them a special research field. The most important ones are listed below.

- High conductivity, due to high mobility of ions.
- High polarizability.
- Exceptional thermal conductivity and heat capacity.
- High thermal stability, having melting point below 100°C and being in the liquid form for a wide range of temperatures.
- Low vapor pressure, once ion interactions are strong.
- Multiple combinations between anions and cations.

As previously reported, the properties of IL range from polar to nonpolar, hydrophilic to hydrophobic, complete miscibility with water or any other solvent to complete immiscibility with both. It all resumes to the appropriate choice of cation and anion. Typical cations are for example imidazolium or pyridinium. As for anions, almost all may be selected; because of all this list of tuneable properties ILs are known as designer solvents [33].

Nucleophilic aromatic substitution (due to its industrial application) was severely studied concerning the choice of IL as the liquid catalytic phase [34]. The myriad of possibilities turned out to some rather odd results once a small modification can have tremendous effects on the overall reaction.

ILs are for sure a good alternative to classic solvents, but like every area in science a “dark” side is always present. Table 1 provides a SWOT analysis of processes based or combining ILs.



*Table 1 - SWOT analysis of ILs development.*

<b>Strengths</b>	<b>Weaknesses</b>
<ul style="list-style-type: none"> <li>• Flexibility to be used in different settings</li> <li>• Eco-friendly processes</li> </ul>	<ul style="list-style-type: none"> <li>• Leaching in SILPs</li> </ul>
<ul style="list-style-type: none"> <li>• High purity production</li> <li>• Improved stability for specific catalysts</li> </ul>	<ul style="list-style-type: none"> <li>• Industrial scale-up</li> <li>• Insoluble substrates</li> <li>• Full recovery</li> </ul>
<b>Opportunities</b>	<b>Threats</b>
<ul style="list-style-type: none"> <li>• Innovative processes</li> <li>• Intensification of production</li> <li>• New technologies</li> </ul>	<ul style="list-style-type: none"> <li>• Toxicity/Safety of ILs</li> <li>• Cost of production and treatment</li> <li>• Durability</li> </ul>

## 2.3 Support

Depending on the IL choice, the support may be used without any chemical modification or some surface chemical treatment may be needed. In the first situation, a physical coating strong enough to hold the IL in the desired porous matrix is involved. This is possible due to strong attractive forces between the IL and the support, specifically –OH bridges and Van der Waals interactions. Helping fixation, the generally high viscosity of IL plays its part as well. For catalysis purposes, supposing recyclability of the catalyst is intended, a physical coating may not be enough. In reality if the IL is intended to be stationary for long periods, the effect of gravity becomes important, and may lead to a change in the IL pattern. To accommodate this situation there are 2 major options.

The first approach is to coat the support for which two options are made available. A different IL that presents an enormous affinity to the support and to the support's interface [35], or a polar dendrimer [36]. This will create a first layer in which the catalyst phase may easily attach. The purpose of this surface modification goes sometimes behind fixation. In some supports like Silica, in which –OH groups dominate the surface, if this treatment is not completed, the catalyst will not endure inside the catalytic phase, once the majority of organometallic catalyst are readily deactivated in presence of the hydroxyl groups. The immobilization of the IL phase has been done in several ways. For sure impregnation [37] is the easiest method, but others such as polymerization, sol-gel method and grafting were also used [38,39]. A second approach, used in smaller scale, is to encapsulate the IL in semi-open pockets simultaneously with support formation [38,40]. Sometimes this encapsulation is known as pore trapping.

As one might anticipate a large surface area is most desirable for catalytic purposes, once the thickness of the catalytic phase must be as thin as possible to avoid diffusion limitations and allow for the reaction to take place inside the bulk phase, taking profit of the molecular dispersion of the catalyst. Naturally porous materials are the first choice, once they are able to provide large internal surface area and good pore volume.

Porosity is one key parameter and plays a major role in the choice of the support. Generally, materials are can be divided into 3 categories:

- **Nonporous or macroporous supports:** The IL film coating is in general thick (diffusional problems may be involved), and the area exposed to the reaction medium is smaller than in other cases. Additionally, once the coating is on the surface or near to it, a accidental mechanical action may lead to the displacement of the IL and the catalyst, leading to a

decrease in activity. This situation is particularly aggressive in fixed-bed reactors, where the medium reaction is a liquid.

- **Mesoporous supports:** The mechanical problems are avoided and the pore size (2-50 nm) is enough to adsorb a layer of thin IL ( $\approx 0.5$  nm) without filling completely the pore, leaving enough space for the involved species to interact. Moreover, the layer size is sufficient to avoid major diffusional problems. 2 main effects led the IL to enter the pores: intermolecular forces within the IL and capillary forces. Some reports point out that even at high loads of IL ( $\approx 40$  wt%), textural properties are kept, namely easiness in handling and working [41]. Some leaching is plausible to happen though.
- **Microporous supports:** Albeit interest for a bunch of applications, in this situation due to the small pore size ( $< 2$  nm), a complete fill of the pore could be ascribed, leading to some mass transfer limitations. The reaction would perform appropriately on the catalyst phase near the outer surface of the support, reducing significantly the surface area available. However, good adsorption properties constitute a positive point for this pores.

For the aforementioned reasons mesoporous supports with a degree of micropores (in particular carbon) will take the major attention in this work. A myriad of materials have been explored and are available though [42]. Mesoporous silica [43], flame-dried silica [41], diatomic earth [37], carbon nanotubes after suitable surface modification [44] and even polymeric resins after covalently bounding an IL layer [35,45–47] are some examples.

## 2.4 Catalytic function

Of the uttermost importance to understand the mechanism involved, and available possibilities to improve overall performance, is to know where is located the catalytic function. In general, 3 major scenarios are available and depicted in Figure 4.

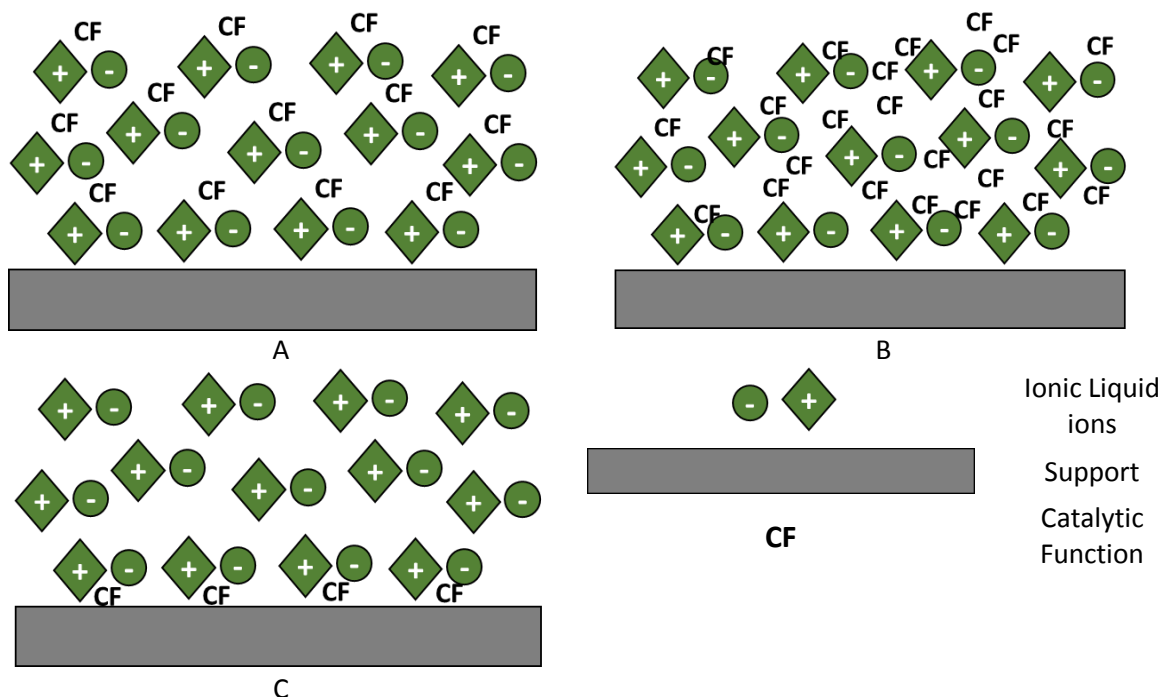


**Figure 4** - different possibilities for the localization of the catalytic function (CF).

**Situation A** – In this situation the catalytic active function is placed on one of the ions, with the possibility of one of them being the catalyst itself. In general, the layer is thin to prevent mass limitations and the support must not interact with the catalytic function. Additionally, a layer of a different IL may be used to coat the support’s surface first to avoid the referred problems. This concept also includes the monolayer situation.

**Situation B** – When organometallics components are involved this is the characteristic situation, once the molecular catalyst is dissolved in the IL and can act as a homogenous catalyst. Logically the catalyst must be highly soluble in the IL and present a low solubility in the reaction medium, to avoid leaching. Similarly to situation A, the catalyst must not interact with the support, which could in turn mean the poisoning of the former. Organometallic complexes present here an important advantage that makes this kind of catalysis particularly effective. It has been reported [48] that these complexes, when dissolved in IL, are rapidly enclosed by ion pairs of the IL (similar to solvation) forming a “cage” that traps the active catalyst, Figure 5. This prevents not only possible links between metal centres but also stabilizes the catalytic specie. Consequently, a long-range order could be detected in this organization pattern. Metal nanoparticles have also been reported showing the same kind of behaviour [49].

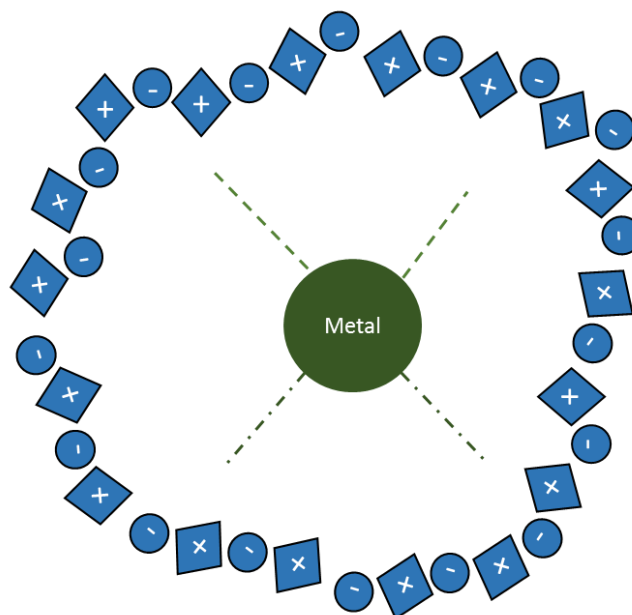


**Figure 5** - schematic representation of the catalyst entrapment inside IL cluster. Lines and dots represent connections to ligands, not shown on purpose.

**Situation C** – This situation is essentially a heterogeneous catalyst covered with a layer of Ionic Liquid. One may wonder that this layer may increase the difficulty of the involved species to reach the active site (that is carved on the surface). However, the major role of this layer is to change the access to the active centres (shape selectivity), leading to the enhancement of one reaction among several others, overcoming a traditional problem of heterogeneous catalysis: the lack of selectivity. For this to happen a cautious choice of the IL must be previously done as well as a comparison with the uncoated heterogeneous catalyst, once for sure mass limitations would increase.

At first sight it could be interesting to “by-pass” all the IL-phase and impregnate straightforwardly the catalyst into a chosen support. However, it is preferable to immobilize the catalyst in an IL-phase due to a series of advantages. **(a)** no further modification of the catalyst is needed once catalysts are typically soluble in ILs [11]; **(b)** IL’s ions may contribute to the activation of the catalyst; **(c)** IL phase may contribute to the effective stabilization of the catalyst [50]**(d)** small changes in side chains of the IL may be of big importance in controlling the overall yield of a reaction;

For any kind of the above mentioned situations, co-catalysts, additives or any other substances may be dissolved in the thin film of IL in order to promote the best conditions for the performance of the catalyst.

## 2.5 Catalysis in IL films

The solvent is a key parameter in catalytic chemical reactions, once its interaction with the catalyst and all the species involved, may greatly influence the chemical process. Solvents may be readily divided into 2 categories: non-polar and polar solvents. The formers are randomly oriented and may have their local dipoles oriented by applying an electric field. The latter, and especially those that may establish H-bonds, are structured, frequently exhibiting formation of clusters though

remaining randomly spread. When a charged specie is placed in this medium a redistribution occurs in order to accommodate the new neighbour [51]. ILs' dielectric constants are in general high and the introduction of a charged metal complex will induce the re-orientation of the ion pairs of the ILs [52] in order to “cage” the new specie (Figure 5). The formation of ordered structures [41,53] leads to an increase in viscosity of the catalytic phase and of course generates a long-range ordered system [54,55]. It has also been reported that these structures around the molecular complexes comprise up to 33 ion pairs of the IL [41] and are similar to metal nanoparticles in imidazolium ILs [56]. Only at higher temperatures ( $\approx 70^\circ\text{C}$ ) these structures are broken [48].

The consequences of an increase in viscosity are negative for the reaction itself, once mass diffusion limitations are known to increase. This aspect also reinforces the requirement of a thin layer of IL, so that the diffusion path is as small as possible. If this imposition is not achieved, the reaction will take place in the boundary of the system instead of using all the IL medium. This would unavoidably mean lower yields and even a change in the expected kinetics. This effect can be compared to that of lower reactant solubility in the IL film, yielding severe mass limitations.

## 2.6 Applications

Although a recent research topic, ILs supported phase have been applied to the most important chemical industrial reactions with good results. Table 2 resumes the information available, including supports tested and references.

**Table 2** - applications of IL per kind of reaction

Reaction	Support	Catalyst(s)	Type	Reference
<b>Hydrogenation</b>	Silica	Ru and Rh complexes	Slurry	53
	Molecular sieves	Palladium NPs	Slurry	57
	Membranes	Rh complexes	“Fixed bed”	58
	Mercaptopropyl silica gel	Pd complex	Slurry	59
	Porous Ni	Ni	Slurry	60
	Carbon nanotubes	Rh complex	Slurry	61
	Carbon cloth	Pd complex	Slurry	62
	Carbon nanofiber network	Pd NPs	Slurry	63
<b>Hydroamination</b>	Silica	Ru complex	Fixed bed	64
	Diatomic earth	Rh(I), Pd(II), Zn(II)	Slurry	37
	Silica	Pd(II) complex	Slurry/Fixed bed	41
<b>Hydroformylation</b>	Silica	Palladium complex	Slurry	65
	Silica gel	Rh complex	Fixed bed	12
<b>Carbonylation</b>	Silica	Rh complex	Fixed bed	66
	Spherical activated carbon	Cu	Fixed bed	67
<b>Carboxylation</b>	Silica	Rh complex	Fixed bed	68
	Silica	1-butyl-3-methyl-imidazolium ILs	Slurry	69

<b>Michael reaction</b>	Silica	Sodium materials	Slurry	70
	Silica	Sc complex	Slurry	71
<b>Mukaiyama reaction</b>	Silica	Sc complex	Slurry	71
<b>Fluorinations</b>	Polystyrene resin	Imidazolium ILs	Slurry	72
<b>Enzymatic reactions</b>	Silica	Enzymes	Slurry	73
	Acrylic resin	Enzymes	Fixed bed	74

A special focus will be given to organometallics complexes as the active catalytic function, once the experimental work developed aimed at the introduction of an iron (II) complex in a range of ILs for the selective hydrogenation of aldehydes to alcohols.

### 2.6.1 Hydrogenation reactions

Carbonyl groups and in particular their catalytic reduction using Hydrogen represents a way to get valuable alcohols used for the manufacture of bulk and fine chemicals [75]. The selective hydrogenation of aldehydes over other carbonyl compounds persisted a main challenge until 2016 extraordinary publication of a well-defined Fe(II) catalyst for a highly efficient and selective hydrogenation of aldehydes [76]. More details of the catalyst will be discussed in a proper section ahead in this work.

The big challenge is to be able to accomplish all the optimal results achieved in a homogeneous medium and enable the catalyst to work inside an IL confined in a porous structure. As an example of what can be achieved, the hydrogenation of acetophenone (using chiral Rhodium and Ruthenium complexes) is used to shed some light on what is happening; in a “classic” solvent, like ethanol or methanol, the hydrogenation of acetophenone showed no enantioselectivity, whereas using an IL promoted a 74% enantioselectivity [53], leaving all the other parameters of the reaction unchanged. What provoked this change?

The most accepted explanation [77] is briefly illustrated in Figure 6. It is probable that, in the IL cluster, acetophenone is binding to the metal via both the carbonyl group and the phenyl ring. This binding mode allows for transferring stereo chemical information to the metal. In contrast, the binding mode in common solvents only allows for the connection of the carbonyl group, impeding any conformational information to reach the metal centre.

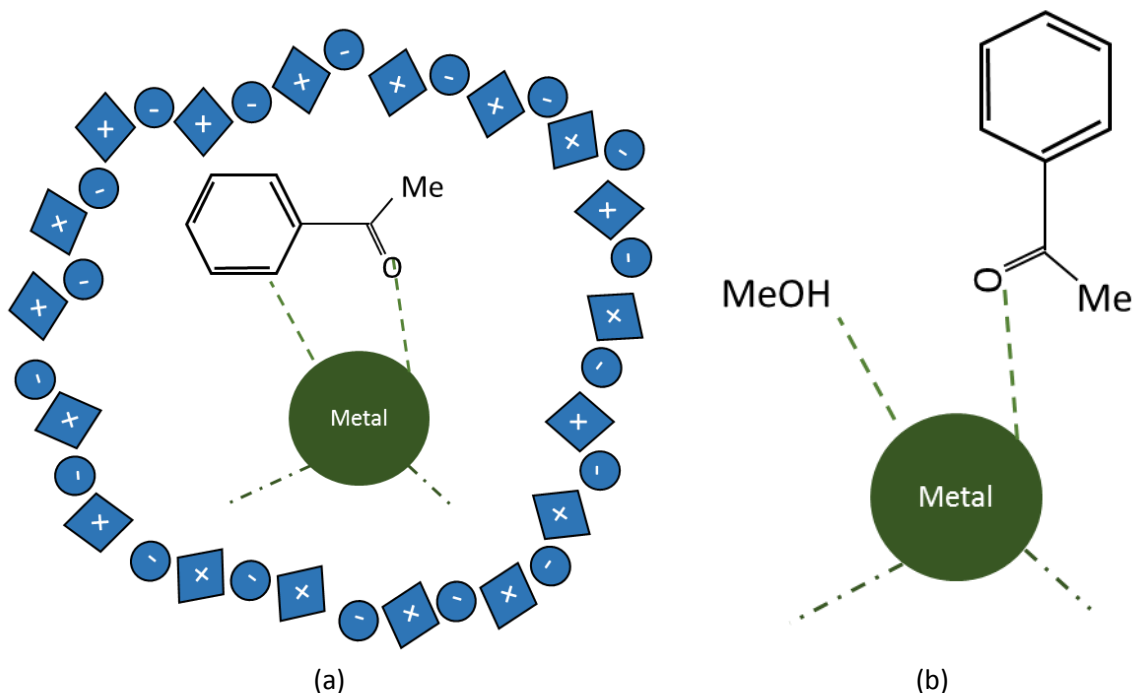


**Figure 6** - different binding modes expected for homogeneous catalyst in (a) Ionic Liquid (b) common solvent. Adapted from ref. 53

It is important to bear in mind that a repulse of the reaction product must happen or the efficiency of all the system is wasted. In other words, the IL and the alcohol (in this particular case) must be immiscible. However, some degree of miscibility should exist between the former and the substrate, otherwise the reaction would perform only at the interface and all the bulk desirable effect would be lost.

As one may immediately forecast the main issues are the choice of the ionic liquid and the support. Mixability results are important and a vast list of possible combinations was reported [78,79], although for alcohols oxidations and not hydrogenation of aldehydes. For the support itself the main point is to be sure that a good impregnation is possible based on the affinity to the IL. The majority of the supports were previously treated before use, in order to tune surface groups.

## 2.7 Solvents

Solvents must meet several criteria such as:

1. Compatible with the homogeneous catalyst to allow the reaction to occur. Typically, catalysts are extremely sensitive to the environment.
2. Hydrophilic to remain outside the support and let the aldehyde (reactant) penetrate the pore structure. In addition, the solvent should be capable of collecting the alcohol (product) without severe loss of material in the pores.
3. Not mixable with the ionic liquid and not react with any of the intervenients.
4. Being cheap, safe and readily available

The first choice is unquestionably water. One of the cheapest, safe and available solvents available. The aforementioned properties have to be checked.

1. The catalyst used in the reaction is an iron complex synthesized by the Kirchner group [76,80], extremely sensitive to oxygen but reported to be active in water as a solvent.
2. There is nothing more hydrophilic than water, so the introduction of the aldehyde inside the pore structure is assured. On the other hand, the collection of the alcohol is a critical step that must be studied for each substrate.
3. The IL must be hydrophobic, which is easily done choosing cations with long alkyl chains and not choosing anions that may be reacting in water. For both the reactant and the product a reaction is not expected to occur with water.
4. For sure the safest, reliable, available and cheap of the solvents.

Although desirable as it may seem, water presents a critical issue in recovering the product. Some alcohols tested are not miscible with water, which makes difficult its choice. Essentially two solvents are immediately in line: ethanol and heptane. The first is known to dissolve both catalyst and ILs and so for sure the reaction would work (although homogeneously); furthermore, no problems were expected in mixing with the reaction product. The second, representing an all class of hydrophobic hydrocarbons, will not dissolve the catalyst and is able to dissolve the majority of the alcohols formed. As a setback a certain degree of solubility with the used ILs may be pointed out.

## 2.8 Magnetic Ionic Liquids

In some recent reviews [81,82] of Magnetic Ionic Liquids (MILs) lots of applications for this special ILs have been resumed. MILs are magnetic solvents similar to a classic IL, but for some magnetic properties incorporated either in the cation or the anion [83]. These interesting ILs present by themselves magnetic properties but, although being magnetic, there are no magnetic nanoparticles involved.

The first magnetic IL ever synthesized was 1-butyl-3-methylimidazolium tetrachloroferrate ([BMIM][FeCl<sub>4</sub>]) [84]. Following this discovery the properties of 1-ethyl-3-methylimidazolium tetrachloroferrate ([EMIM][FeCl<sub>4</sub>]) [85] were studied and an increasing consciousness for this subject was starting to come up, especially when separation and recovery from a mixture of MILs and water was achieved. Ever since, several types of MILs have been developed, from imidazolium to phosphonium cations and Cobalt, Chromium, Manganese, Iron, Gadolinium based anions, all of them show some degree of paramagnetism [86].

For catalysis purposes this ILs show huge applicability, once recycling can be much more easily done. In the present research the aim of using this kind of ILs is clear. If magnetic ILs can be successfully impregnated into a porous support and the bulk magnetic properties be transferred to it in enough strength this could be a very simple way of performing a reaction and separate the catalyst from the reaction medium.

Several problems are on the table with this approach.

1. What Magnetic Ionic Liquid is to be chosen?
2. Can the MIL be successfully impregnated into the support?



3. Can the Catalyst be active inside the MIL structure?
4. What is the better MIL:support ratio in order to have macroscopic magnetic properties?
5. Will the MIL leach after some reaction cycles?

## 2.9 Support and Impregnation

There are many possibilities of bringing Ionic liquids and supports together [77]. Among them, wet impregnation is probably one of the simplest ways to do it. The technique [87] consists in mixing at the same time the support, the IL and the catalyst in presence of a suitable solvent, that should be miscible with the IL. Time of mixing and vacuum are crucial parameters. The first can be up to one week [87], depending on the support's affinity to the Ionic Liquid. The second has been reported [88] as an essential driving force to lead the IL inside the pore structure. It goes without saying that the impregnation process used is based on physical adsorption interactions between the support and the IL, helped by capillary forces. It is convenient though to elucidate some terms by which the IL is inserted in a porous structure. Some authors [88] present the designation adsorption when the IL is on the outer surface of the porous material and there is no special order, leading to an amorphous state of the IL. On the other hand, confinement is similar, but the IL effectively penetrates the porous material and in some cases presents a crystalline structure inside the pores. For the latter, vacuum is needed. In the present research and for the sake of uniform language, confinement is used to mean that the wet impregnation technique was applied.

Although easy to describe, the nuances involved make the process very difficult. First and foremost, the support and its pore size distribution. Undeniably a porous material is needed, taking advantage of an enhancement in the surface area available. Table 3 summarizes some concerns when using different kinds of porous materials. A solution between micropores and mesopores seems being a good fit, minimizing somehow the clogging of the first [87].

*Table 3 - Comparative board for different kinds of support.*

Type of pores	Advantages	Disadvantages	Solutions
<b>Micropores</b>	Very good adsorption capacity	Pores clogging or completely filled leading to mass transfer limitations	Tuning the properties of the IL, in particular the size of the side chains
<b>Micro/Mesopores</b>	Good adsorption capacity	Same as micropores but in less scale	Tuning the properties of the IL, in particular the size of the side chains
<b>Mesopores</b>	Good rates of reaction	Acceptable adsorption capacity	Support's surface treatment

The second important issue has to do with the ionic liquid itself. In order to promote a good physical adsorption, the IL must be as hydrophobic (or hydrophilic) as the support, to be able to migrate from the solvent to the support. In the majority of the cases, the support needs to be previously washed in order to remove impurities or even in order to tune its properties to be

compatible with the IL. The IL on its turn must be able to enter the pores and form a thin layer, helped by capillary forces and strong vacuum that at the same time removes the solvent.

After impregnation, the filled support may be washed in order to ensure that only the strongly adsorbed/confined material remains. Performing or not this step will lead to some leaching during the reaction [8] (though in different amounts), due to mechanical action, at least. The support's choice is of course determinant for this situation.

The filling amount is also a key parameter. The amount generally reported to optimize this issue is between 10 and 30% weight of IL to the support's pore volume [89]. However, this question is far from being linear; there are reports [64] where 80% impregnation loading proved not to cause visible mass transfer limitation and hence, coating all the supports surface, would ensure that the substrate would not "stick" to the available support instead of penetrating the IL and keeping the reaction going.

Figure 7 shows a schematic summary of several possibilities in order to perform hydrogenated catalytic reactions.

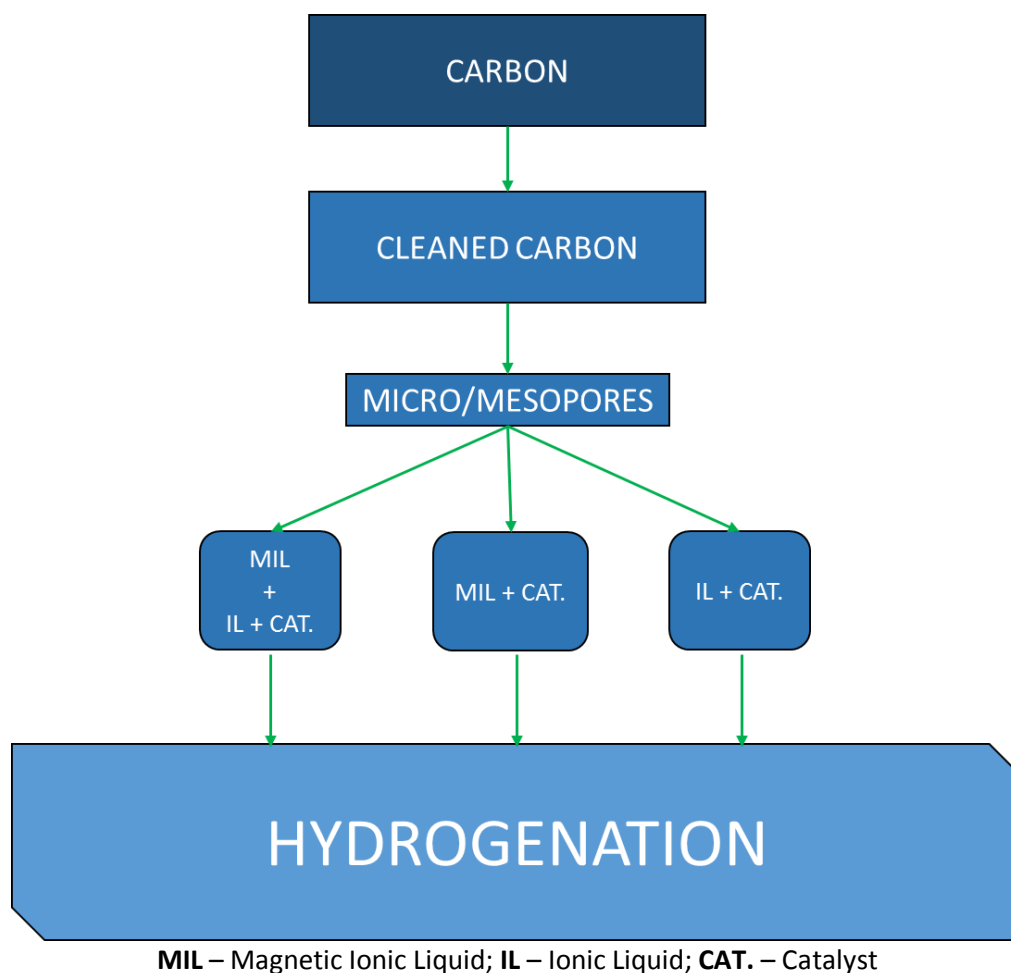


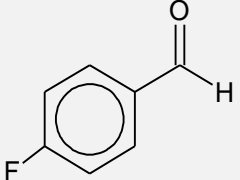
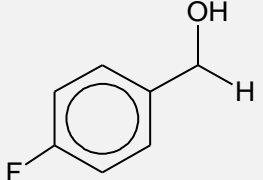
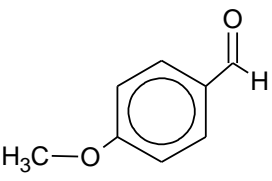
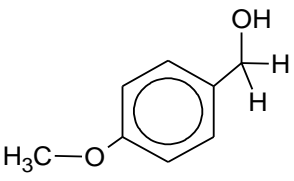
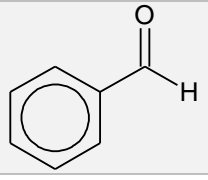
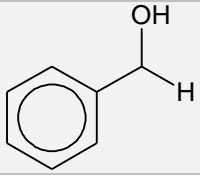
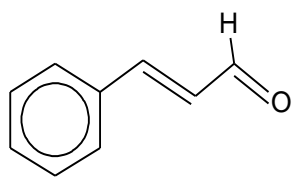
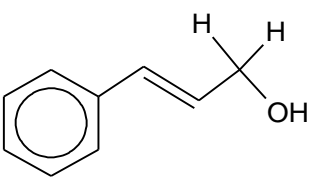
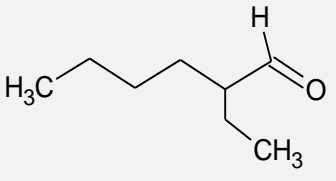
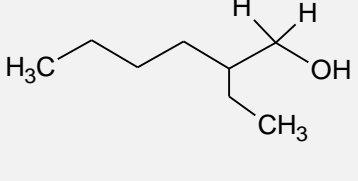
*Figure 7 - Schematic representation of different approaches to hydrogenation.*

### 3. Materials and Methods

#### 3.1 Substrates

The first issue to address was to choose the pairs aldehydes/alcohols to be tested under hydrogenation conditions. We have selected four aromatic aldehydes, (i) with an electron withdrawing halogen substituent (4-fluorobenzaldehyde), (ii) with an electron donating OMe group (4-anisaldehyde), (iii) without substituent (benzaldehyde), (iv) a challenging  $\alpha,\beta$ -unsaturated substrate (cinnamaldehyde), and one aliphatic aldehyde (2-ethyl-hexanal) They are also commonly used in industrial applications, widely reported [16,62,76], and easy to detect. Table 4 summarizes the pairs used under experimental conditions.

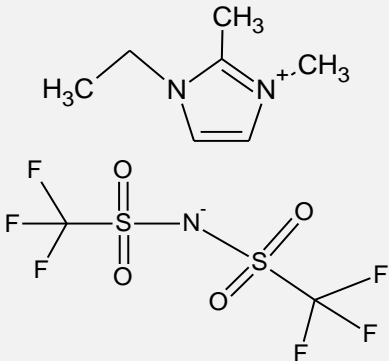
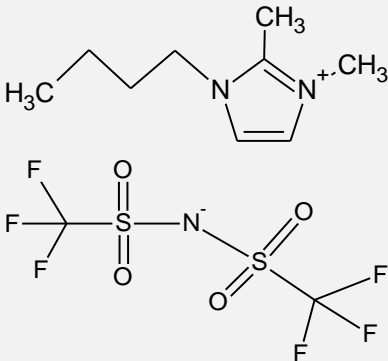
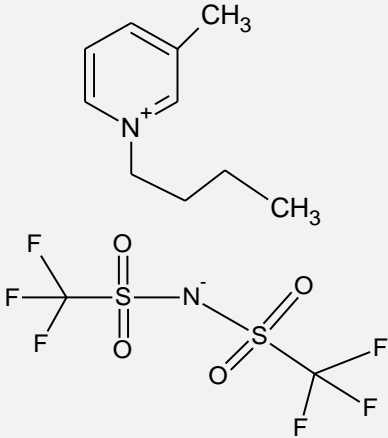
**Table 4 - Pairs Aldehyde/Alcohol used**

Aldehyde	Schematic drawing	Alcohol	Schematic drawing
<b>4-Fluorobenzaldehyde (4-FBA)</b>		<b>4-Fluorobenzyl alcohol</b>	
<b>4-Anisaldehyde</b>		<b>4-Anisyl alcohol</b>	
<b>Benzaldehyde</b>		<b>Benzyl alcohol</b>	
<b>Cinnamaldehyde</b>		<b>Cinnamyl alcohol</b>	
<b>2-Ethyl-hexanal (2-EH)</b>		<b>2-Ethyl-hexanol</b>	

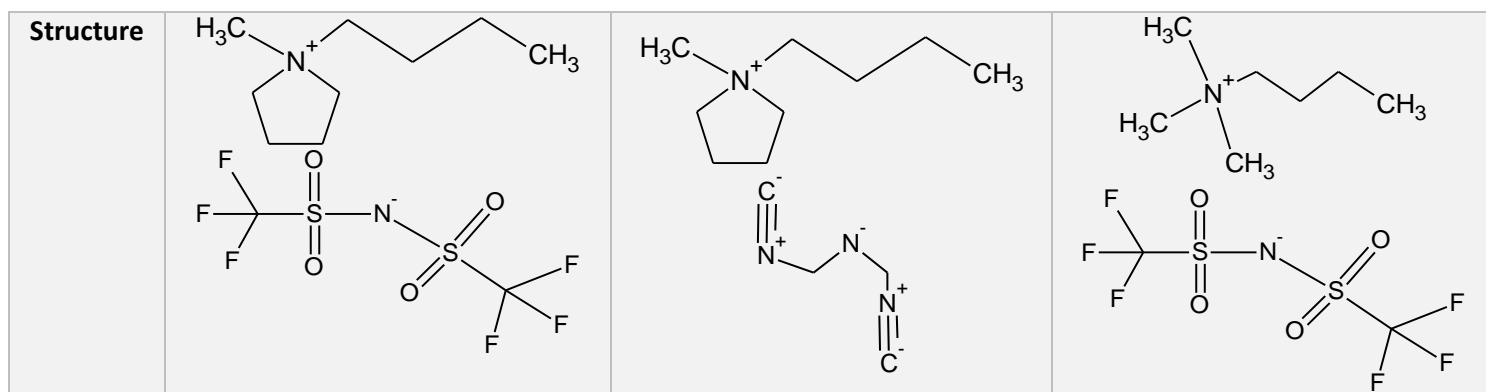
### 3.2 Ionic Liquid selection

The second issue to be addressed concerns ILs. It was previously referred that the wide variety of combinations between anions and cations makes it a challenge to be able to provide the best choice for the reaction in study. Having in mind that the carbon supports are hydrophobic, the ILs choice had to be in line with that fact. This guarantees a strong hydrophobic interaction between the support and the IL, as well as the possibility of using water as reaction solvent. Bis(trifluoromethylsulfonyl)imide anion [NTf<sub>2</sub>] has been chosen for the anion, since it is a weakly coordinating anion. Imidazolium, pyridinium, pyrrolidinium, ammonium, phosphonium, DBU and pyridine based were chosen as cations. One magnetic IL with FeCl<sub>4</sub> anion was also used (IL#10). On the other hand, it is common that the characteristics of the support need to be tuned, which accounts for two hydrophilic ILs chosen. These ILs (IL#5 and 9) are basic and could have a positive impact on the reaction. Moreover, dicyanamide based ionic liquids have shown excellent selectivity in citral (acyclic monoterpene) hydrogenation [62] with dicyanamide based ionic liquid promoting the selective hydrogenation of the aldehyde. However, dicyanamide anion is a strongly coordinating anion which can poison the catalyst. Table 5 resumes the chosen ILs with their used numerical system in order to facilitate further discussions.

**Table 5** - ILs used; description and structure.

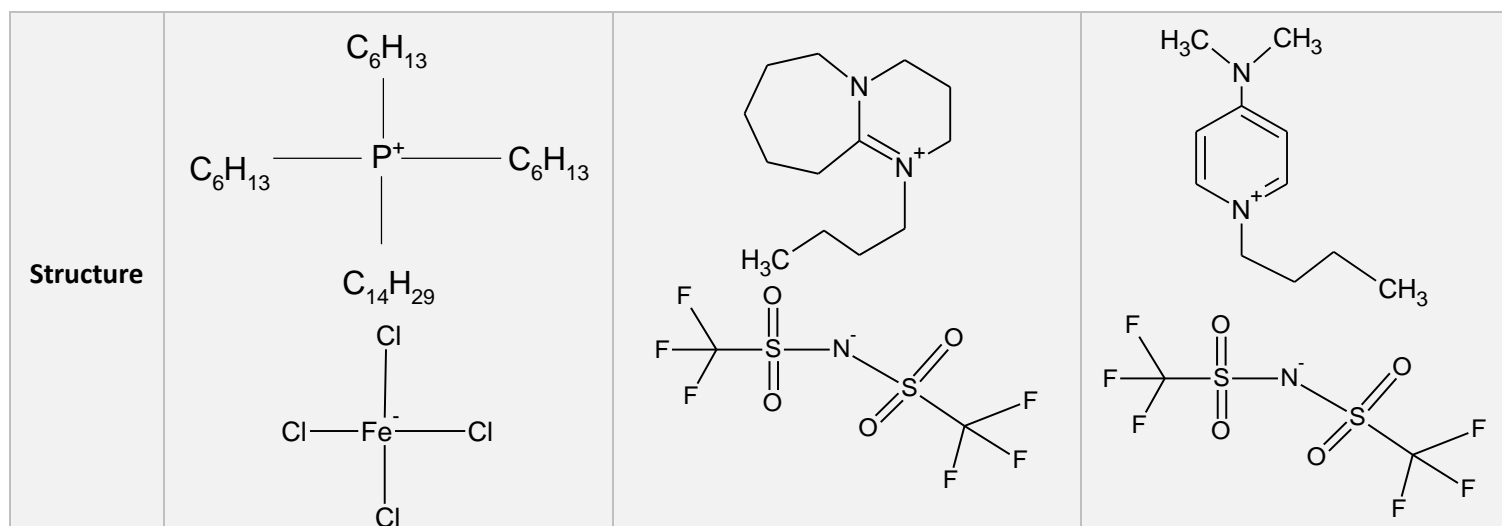
Number	IL#1	IL#2	IL#3
Name	1-Ethyl-2,3-methylimidazolium bis(trifluoromethylsulfonyl)imide	1-Butyl-2,3-methylimidazolium bis(trifluoromethylsulfonyl)imide	1-Butyl-3-methylpyridinium bis(trifluoromethylsulfonyl)imide
Short Name	EMMIm NTf <sub>2</sub>	BMMIm NTf <sub>2</sub>	BMPyr NTf <sub>2</sub>
Structure			

Number	IL#4	IL#5	IL#6
Name	1-Butyl-1-methylpyrrolidinium bis(trifluoromethylsulfonyl)imide	1-Butyl-1-methylpyrrolidinium dicyanamide	Butyltrimethylammonium bis(trifluoromethylsulfonyl)imide
Short Name	BMPyrr NTf <sub>2</sub>	BMPyrr N(CN) <sub>2</sub>	N <sub>1114</sub> NTf <sub>2</sub>



Number	IL#7	IL#8	IL#9
<b>Name</b>	Methyl-trioctylammonium bis(trifluoromethylsulfonyl)imide	trihexyltetradecylphosphonium bis(trifluoromethylsulfonyl)imide	Trihexyltetradecylphosphonium dicyanamide
<b>Short Name</b>	N <sub>1888</sub> NTf <sub>2</sub>	P <sub>66614</sub> NTf <sub>2</sub>	P <sub>66614</sub> N(CN) <sub>2</sub>
<b>Structure</b>			

Number	IL#10	IL#11	IL#12
<b>Name</b>	Trihexyltetradecylphosphonium iron(III) chloride	1-Butyl-1,8-diazabicyclo[5.4.0]undec-7-en-8-ium bis(trifluoromethylsulfonyl)imide	1-Butyl-4-dimethylaminopyridine bis(trifluoromethylsulfonyl)imide
<b>Short Name</b>	P <sub>66614</sub> FeCl <sub>4</sub>	BDBU NTf <sub>2</sub>	BDMAP NTf <sub>2</sub>



### 3.3 Support

Activated carbon spheres and activated carbon cloth were used as support. The first is 50% micro and 50% mesoporous and was gently offered by Blucher<sup>®</sup> Company. The second is fully microporous and gently offered by Kynol<sup>®</sup> Company. Both were used after further treatment. For spheres, a wide range of treatments were applied and described in section 3.5.3. For carbon cloth, only thermal treatment was used.

### 3.4 Catalyst

There are a lot of hydrogenation catalysts; some contain precious or noble metals while some of them are more modest and based on abundant first-row transition metals. It is undeniably attractive to replace scarce, toxic and expensive noble metals by more plentiful and eco-friendly first-row transition metals. Iron, being the most abundant transition metal in earth's crust and displaying readily availability, is an excellent candidate. In the present situation the catalyst choice was evident, since our group recently reported an inexpensive and robust homogenous catalyst for the highly selective and efficient hydrogenation of aldehydes [76]. The pre-catalyst  $[\text{Fe}(\text{PNP}^{\text{Me}}i\text{Pr})(\text{CO})(\text{H})(\text{Br})]$  and the catalyst  $[\text{Fe}(\text{PNP}^{\text{Me}}i\text{Pr})(\text{H})_2(\text{CO})]$  – both a mixture of cis and trans isomers - depicted in Figure 8 are based on 2,6-diaminopyridine scaffold where  $PiPr_2$  moieties of the PNP ligand connect to the pyridine ring via NMe spacers.

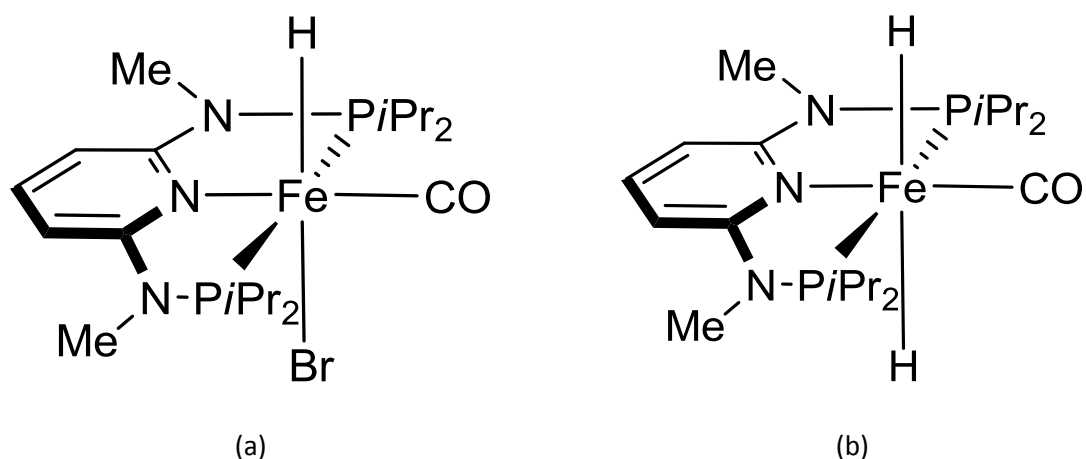


**Figure 8** – Iron hydride complexes from ref. 76; (a) pre-catalyst; (b) active catalyst

The reactions' mechanism proposed by the authors is interesting. The substrate insertion proceeds through a mechanism in which the dihydride makes a nucleophilic attack on the aldehyde's carbonyl group to give an alkoxide intermediate that is further expelled to originate the expected alcohol. For elucidative purposes the mechanism is showed in Figure 9 and is an exact copy of the model purposed by our group.

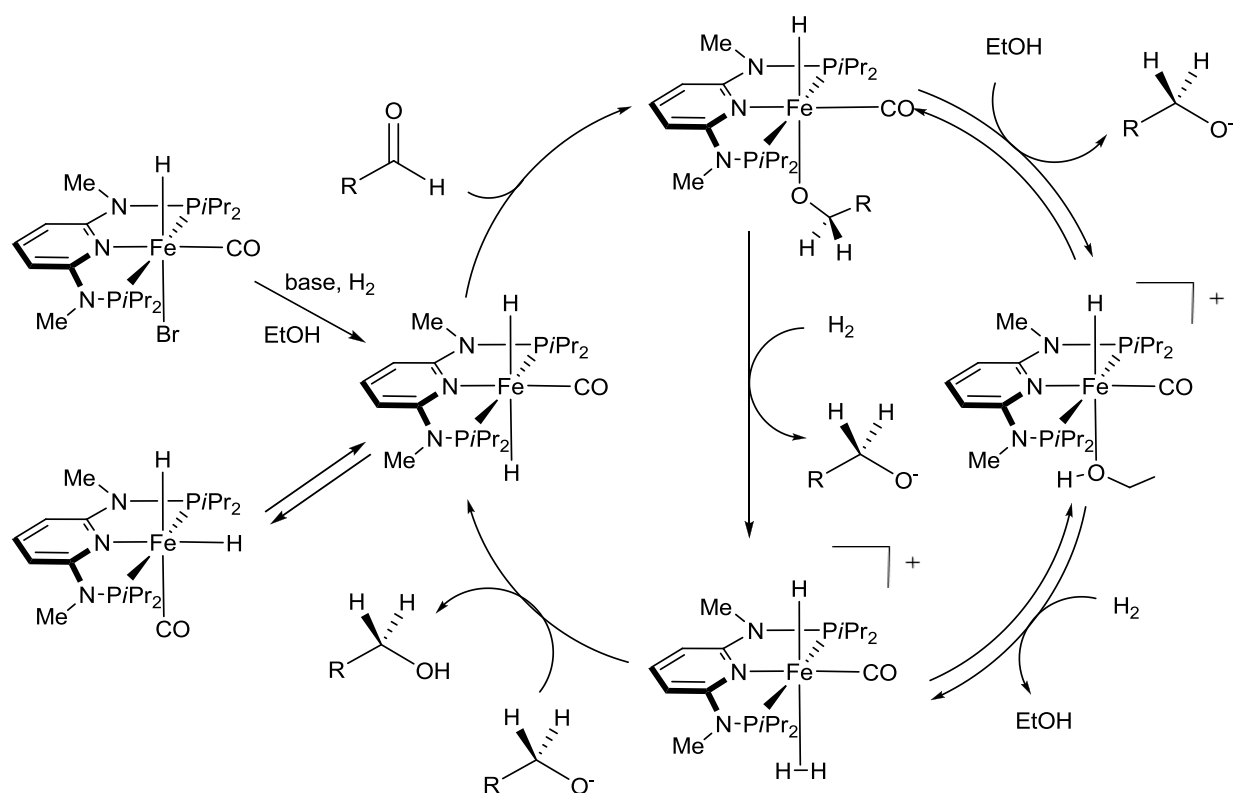


**Figure 9** - Simplified catalytic cycle for the chemoselective hydrogenation of aldehydes; adapted from ref.76

In the proposed mechanism the role of each intervenient is clear and justifies some experimental decisions that were made. Firstly the use of a base is clarified; the heterolytic cleavage of diatomic hydrogen stimulated by the metal centre and external base lead to the formation of the active catalyst that is in a pseudo-equilibrium with the cis isomer. In the second place the role of a polar protic solvent (ethanol in this situation) is responsible for the protonation in order to obtain the product or is directly involved in expelling the alkoxide intermediate of the coordinating Fe sphere by simple replacement with the alkoxide. However, this issue is questioned by the authors on whether the compound with the solvent in the alkoxide place is part of the catalytic cycle or a mere resting situation, once there is evidence of its existence in NMR spectra.

It is pertinent to note that the possibility of using a polar protic solvent may be relaxed to a strong polar solvent like an IL. This situation has been here reported, and constitutes another advantage of this catalyst. However, the activated catalyst is especially sensitive to oxygen environment that could lead to its deactivation.

Based on this reference, DBU was definitely chosen as the base to be used in all hydrogenations performed, once it is the one that reports better results. The used amount was 5 mol% using substrate as a reference, which was 2 mmol, while 0.5 mol% catalyst was applied.

## 3.5 Procedures

### 3.5.1 General procedures

All manipulations were performed under Argon atmosphere by using Schlenk techniques or/and in a MBraun inert-gas glovebox. All solvents and substrates were purified according to standard procedures [90]. The deuterated solvents were purchased from Sigma-Aldrich and dried over 4 Å molecular sieves. Ionic liquids were acquired from Iolitec and used as received. Solvents purchased from Sigma-Aldrich and used after distillation.

### 3.5.2 Miscibility test

All miscibility tests were performed by mixing 2 mmol of alcohol with 125 µL of IL inside a suitable tube. After 10 minutes the number of phases was noted down. The tube was agitated again and inserted inside an oven at 60°C for 1 hour. After that period the number of phases or any possible degradation was noted down. The procedure was repeated but using an ice bath (at 0°C).

### 3.5.3 Carbon treatment

The carbons were subjected to one or several treatments in order to make them suitable for catalytic purposes.

#### 3.5.3.1 Oxygen removal

Under vacuum conditions, carbon spheres/carbon cloth were stirred for 24h with a temperature of approximately 50°C. After that, storing in a MBraun inert-gas glovebox.

#### 3.5.3.2 HCl treatment

Concentrated HCl (35 w%) was added to the carbon sample; the mixture was stirred for 24h in order to remove any acid soluble impurities. Then, it was washed with deionized water until reaching a neutral solution and no chloride anions were detected using silver nitrate test. After that, the carbon was stirred under vacuum for 12h with argon flushing at least 3 times. Finally, it was



transferred to the glovebox. When this treatment is performed the commercial carbon spheres (CC) are designated by CC, HCl.

#### 3.5.3.3 NaOH treatment

Addition of 1M NaOH solution to the support (enough to cover all the sample), stirring for 24h and wash with water until constant pH is reached. After that, stirring under vacuum for 12h with Argon flushing at least 3 times. Transfer to the glovebox. When this treatment is performed the commercial carbon spheres (CC) are designated by CC, NaOH.

#### 3.5.3.4 Thermal treatment

Under vacuum conditions, carbon spheres/carbon cloth were stirred for 6h with a temperature of approximately 300°C provided by an oil bath, with Argon flushing at least 3 times. Following that period, 12h of vacuum at room temperature. After that, storing in a MBraun inert-gas glovebox.

#### 3.5.4 NMR measurements

$^1\text{H}$ ,  $^{19}\text{F}\{^1\text{H}\}$ , and  $^{31}\text{P}\{^1\text{H}\}$  NMR spectra were recorded on Bruker AVANCE-250 spectrometer controlled by Topspin and the resulting spectra were analysed using MestReNova version 6.0.2-5475.  $^1\text{H}$  NMR spectra were referenced internally to residual proto-solvent, and reported relative to tetramethylsilane ( $\delta = 0$  ppm).  $^{19}\text{F}\{^1\text{H}\}$  and  $^{31}\text{P}\{^1\text{H}\}$  NMR spectra were referenced externally to  $\text{CFCl}_3$  ( $\delta = 0$  ppm) and  $\text{H}_3\text{PO}_4$  (85%) ( $\delta = 0$  ppm), respectively.

#### 3.5.5 Elemental Analysis/ICP

The determination of the Fe, Co, Ni and Mn concentration was done using an inductively coupled plasma optical emission spectrometer PerkinElmer OPTIMA 8300 equipped with an SC-2 DX FAST sample preparation system. In general, non-matrix elements are determined via axial view and triple determination followed by an arithmetic averaging. A customized single-element (Merck, Roth) standard was used for the calibration. C, H, N, S and O contents were double-determined utilizing an ELEMENTAR Vario Macro elemental analyzer (CHNS-mode, WLD) and an ELEMENTAR Vario EL (O2-mode, WLD). The provided results are arithmetic mean values.

#### 3.5.6 XPS measurements

XPS is a powerful technique to get an insight into the properties on, and up to roughly 10 nm deep (in the present situation), of the surface. It is part of a class of surface analysis techniques, which involves irradiating the sample with photons, under vacuum, and determine the kinetic energy of possible emitted electrons. The scope of information this technique may provide is tremendous, ranging from quantitative data (for example, atomic percentage) to qualitative (for example, oxidation states). The advent of new materials and technologies is enlarging the spectra of applications. However, the underlying principle is the famous photoelectric effect, where photons penetrate the sample and the energy of any possibly emitted electrons is detected. This technique is commonly labelled as a surface technique, once the level of penetration is in the order of micrometers. Essentially, the excited electrons which strongly interact with matter, have a short inelastic free path, meaning that deeper electrons will lose their energy by several interactions with matter. As a consequence, only surface emitted electrons are able to be detected. Eq. 1 represents the basic equation modelling the technique. KE stands for kinetic energy, BE for Binding Energy,  $h$  is Plank constant,  $\nu$  is the frequency and  $\phi_{\text{analyser}}$  is the working function of the electron analyser.

$$KE = h \cdot \nu - BE - \phi_{analyser} \quad (1)$$

The emitted (photo)electrons should find no gas molecules in the path towards the analyser. This reason justifies the use of Ultrahigh vacuum (UHV). If not, these electrons would be scattered and possibly lost. Moreover, the number of gas molecules upon the sample surface is practically inexistent and possible dissolved gases and impurities, like water or any kind of common solvents, would be quickly vaporized. In the present situation a vacuum of  $10^{-10}$  mbar is available to ensure the required conditions. Lastly a reliable source of photons is essential. Common X-ray sources for XPS have either Mg or Al anodes, using Mg KR radiation at 1253.6 eV or Al KR radiation at 1486.6 eV, respectively.

All X-ray photoelectron spectroscopy (XPS) were carried out on a SPECS XPS-spectrometer equipped with a monochromatised Al-K $\alpha$  Xray source ( $\mu$ Focus 350) and a hemispherical WAL-150 analyser (acceptance angle: 60°). Samples were mounted onto the sample holder using double sided Cu tape or Ta. Pass energies of 100 eV and 30 eV and energy resolutions of 1 eV and 100 meV were used for survey and detail spectra respectively (excitation energy: 1486.6 eV, beam energy and spot size: 70 W onto 400  $\mu$ m, angle: 51° to sample surface normal, base pressure:  $6 \times 10^{-10}$  mbar, pressure during measurements:  $2 \times 10^{-9}$  mbar). Data analysis was performed using CASA XPS software packages employing Shirley backgrounds [91] and Scofield sensitivity factors [92]. Charge correction was applied so the adventitious carbon peak (C-C peak) was shifted to 284.8 binding energy (BE). Curve fits using combined Gaussian-Lorentzian peak shapes were used to discern the components of detail spectra. To reduce charging effects a broad spot low energy electron source (SPECS FG 22 flood gun) was used for charge compensation (5eV/25 $\mu$ A).

The detection limit in survey measurements lies around 0.1-0.5 at%, depending on the element. The accuracy of XPS measurements is around 10-20% of the values shown and the maximum depth is about 7-10 nm.

### 3.5.7 BET measurements

Textural properties were analyzed by N<sub>2</sub> physisorption (ASAP 2020 Micrometetics GmbH), using the Brunauer–Emmett–Teller (BET) theory for determining the surface area and the Barret–Joyner–Halenda (BJH) method for obtaining the pore size distribution.

### 3.5.8 DSC measurements

Thermal behaviour by Differential Scanning Calorimetry (DSC) was investigated using NETZCH analyser (STA 449 F1) and software Proteus Thermal Analysis version 7.1. Samples were heated using alumina crucibles under air atmosphere and a heating rate of 10°C/min from -50 to 400°C. The instrument was calibrated using melting points of Indium, Aluminium and Lead.

### 3.5.9 Infrared measurements

Infrared spectra were recorded with a Bruker Vertex 80 FTIR spectrophotometer using a narrow band MCT detector, measuring diffuse reflectance. 256 scans were collected for each spectrum with  $4\text{ cm}^{-1}$  resolution. The data is provided using Kubelka Munk conversion and OPUS software version 7.5.

The use of solid samples led to the use of Potassium Bromide (KBr) as the reference spectrum as well as the support to grind all the samples. The grinding was manually done for 10 minutes in order to obtain a homogeneous powder.

#### 3.5.10 Density measurements

Density of IL+Catalyst was measured using an analytical balance and an automatic pipette, considering  $100\ \mu\text{L}$  volume. This volume was removed with an automatic pipette and weighted in order to indirectly obtain a density value.

#### 3.5.11 Impregnation procedure

In a flask, a mixture containing the support, IL and catalyst was stirred in 2 mL of ethanol for approximately 5 minutes, under inert atmosphere. After that period, evaporation under vacuum (about  $10^{-2}$  mbar) was used in conjunction with an oil bath at  $60^\circ\text{C}$  until the spheres presented rolling behaviour again (about 10 minutes).

#### 3.5.12 Hydrogenation reactions procedure

All hydrogenation reactions were performed in an autoclave (Figure 10) at room temperature ( $25^\circ\text{C}$ ), exceptionally at  $75^\circ\text{C}$ , under Hydrogen atmosphere between 10 and 40 bar using a 90 mL Fisher- Porter tube, which was flushed several times with Hydrogen prior to the addition of the reaction solution. For the preparation of the reaction solutions a vial was charged with the specified amount of impregnated support and several times flushed with Argon and vacuum. Subsequently, DBU, solvent and substrate were taken up into a syringe and transferred to the Fisher- Porter tube. After flushing 3 times with hydrogen, the desired pressured was established. After stirring the solution for the stated time, pressure was carefully released, and a sample for NMR was taken. If pressure was needed again, the procedure of gas admission was repeated.

In all experiments, except when stated otherwise, 2 mmol of substrate was used and 0.5 mol% of catalyst as well, leading to a Substrate to Catalyst ratio (S/C) of 200. The first value was chosen with the requisite of being enough to allow NMR measurements without compromising the reaction. The value for the catalyst is to ensure that the reaction is indeed catalytic and the value goes according to some homogenous data provided on this catalyst [76,80].



**Figure 10** - autoclave and Fisher- Porter tube.

### 3.5.13 Recyclability tests

Aiming to recycle the SILP system, recyclability tests were performed at 40 bar. After 2 hours the autoclave was open and all the possible supernatant was pulled out with a syringe and fresh substrate/DBU/heptane was added, replicating the steps followed in the previous rubric.

## 4. Results and discussion

### 4.1 Measured properties

Miscibility conditions were the first to be tested between the IL and the alcohol (at different temperatures) in order to find out how many phases were formed. Table 6 summarizes the results observed, where number 1, 2 are 1 phase or 2 phases observed, respectively. D and F mean Decomposition and Frozen, respectively.

**Table 6** - Miscibility test at 25 (R.T.), 60 and 0°C.

	IL#1	IL#2	IL#3	IL#4	IL#5	IL#6	IL#7	IL#8	IL#9	IL#10	IL#11	IL#12
4-Fluorobenzyl alcohol T = 25°C	1	1	1	1	1	1	1	1	1	1	1	1
4- Fluorobenzyl alcohol T = 60°C	1	1	1	1	1	1	1	1	1	1	1	1
4- Fluorobenzyl alcohol T = 0°C	1	1	1	1	1	1	1	1	1	1	1	1
Cinnamyl alcohol T = 25°C	1	1	2	1	1	1	1	2	1	1	1	2
Cinnamyl alcohol T = 60°C	1	1	1	1	D	1	1	2	D	D	D	1
Cinnamyl alcohol T = 0°C	1	1	2	1	1	1	F	F	1	F	1	2
2-EthylHexanol T = 25°C	1	1	1	2	1	2	1	1	1	1	1	1
2-EthylHexanol T = 60°C	1	1	1	2	1	2	1	1	1	1	1	1
2-EthylHexanol T = 0°C	F	F	2	2	1	2	1	1	1	1	1	2
4-Anisalcohol T = 25°C	1	1	1	1	1	1	1	D	1	1	1	1
4-Anisalcohol T = 60°C	1	1	1	1	1	1	1	D	1	1	1	1
4-Anisalcohol T = 0°C	F	F	F	F	2	F	F	F	F	F	F	F
Benzaldehyde T = 25°C	1	1	1	1	1	1	1	1	1	1	1	1
Benzaldehyde T = 60°C	1	1	1	1	1	1	1	1	1	1	1	1
Benzaldehyde T = 0°C	1	1	1	1	1	1	1	1	1	1	1	1

These measurements were only preliminary data in order to discover possible outcomes. If an alcohol was found that was not miscible with an IL, it was possible to have a spontaneous separation after the reaction, thus avoiding the use of a solvent. For example 4-Fluorobenzyl alcohol is soluble in all IL thus a solvent is needed, which dissolves the alcohol better than the IL. For example, heptane may be used, in order to have the driving force to release the product to the solvent medium. Cinnamyl alcohol is readily released when using IL#3 and IL#8 and the temperature is close to 25°C. For 2-EthylHexanol, IL#3, 4, and 6 seem to be the most appropriate for a reaction with spontaneous separation. Finally, 4-Anisalcohol seems to have a change in solubility for IL#5 when the temperature decreases. This first information was taken into consideration on the set of experiments. However, from these results nothing is stated on the suitability of the catalyst to work with these substrates and ILs, and of course these results do not ensure that the spontaneous separation will occur after the reaction, since there are some additional species (catalyst, base) that can change the solubility properties of the alcohols.

Then, the solubility of catalyst in the ILs was tested. In order to ensure that the reaction follows a classic homogeneous path, the catalyst must be completely solubilized in the IL phase, regarding biphasic or supported catalysis as well. Table 7 provides the values for all the ILs studied. Density values were obtained from supplier's catalogue [93] but for the magnetic IL, IL#11 and 12 whereas the values were obtained by experimental measurement.  $V_1$  means the volume of IL that is needed to completely dissolve, under ultrasonication in 30 minutes, 5 mg of catalyst, which is further used in homogeneous and biphasic reactions. However, during the preparation of the heterogeneous SILP catalysts, ethanol is used to dissolve the catalyst and IL, which is further evaporated to ensure the impregnation of carbon with IL + catalyst. The solubility of catalyst under similar conditions was investigated. By adding 2 ml ethanol to 5 mg of catalyst and a certain amount of IL, and subsequently performing ethanol evaporation, it was observed that ethanol promoted the dissolution of catalyst in IL since in this way less amount was needed ( $V_2$ ) This fact really decreases the amount of IL that has to be used in the SILPs.

*Table 7 - catalyst solubility in different ILs.*

<b>Ionic Liquid</b>	<b>Density (g/cm<sup>3</sup>)</b>	<b>V<sub>1</sub> (μL)</b>	<b>V<sub>2</sub> (μL) adding ethanol</b>
<b>IL#1</b>	1.49	300	50
<b>IL#2</b>	1.42	300	50
<b>IL#3</b>	1.41	350	50
<b>IL#4</b>	1.40	150	50
<b>IL#5</b>	1.02	100	50
<b>IL#6</b>	1.40	250	50
<b>IL#7</b>	1.15	400	50
<b>IL#8</b>	1.07	300	50
<b>IL#9</b>	0.90	300	50
<b>IL#10</b>	1.08	250	50
<b>IL#11</b>	1.45	300	50
<b>IL#12</b>	1.46	350	50

## 4.2 Homogeneous reactions

Homogeneous reactions were performed in order to obtain answers to the following major questions. Does the catalyst survive in IL? Does the catalyst survive in the presence of substrates? Can spontaneous separation be performed with suitable candidates? For the reactions, in a hydrogenation flask, 5 mg of catalyst, the corresponding amount of IL according to Table 7 ( $V_1$ ), 2 mmol of substrate and 16  $\mu\text{L}$  of DBU were mixed. Reactions were performed using 10 or 40 bar  $\text{H}_2$  pressure. 4-Fluorbenzaldehyde was chosen in order to investigate if the catalyst survives the corresponding IL. Table 8 shows the results obtained.

**Table 8** - Homogeneous reactions results for 4-FBA.

4-FBA	Conversion
	10 bar
IL#1	100% - 7 min.
IL#2	100% - 1h
IL#3	100% - 1h
IL#4	100% - 1h
IL#5	0% - 24h
IL#6	100% - 1h
IL#7	100% - 1h
IL#8	100% - 1h
IL#9	0% - 24h
IL#10/MIL	0% - 24h
IL#11	100% - 1h
IL#12	100% - 1h

It is evident that IL#5, IL#9 and IL#10/MIL do not allow for the catalyst to be active. This suggests a coordination of the dicyanamide anion to the iron complex in the two former cases and a coordination by  $\text{FeCl}_4^-$  to the iron complex in the MIL case.  $^{31}\text{P}$  NMR confirmed the coordination of the anions to the complex since the  $^{31}\text{P}$  peak of the catalyst was shifted from the expected position (164.1 ppm) to 63.2 ppm. All the others work once  $\text{NTf}_2^-$  anion is a very weakly coordinating anion. Interestingly, in basic ILs (#11, #12), the catalyst could catalyse the reaction without adding DBU to the reaction mixture.

According to the miscibility testes, Cinnamaldehyde was used particularly with IL#3 and IL#8, while 2-EthylHexanal with 3, 4, 6, to determine whether spontaneous separation occurs after the reaction. 4-Anisalcohol showed spontaneous separation with IL#5 which coordinates to the catalyst, thus it was not tested. Table 9 shows the aforementioned results.

**Table 9** - Homogeneous reactions results; 10 bar Hydrogen pressure

Substrate	Cinnamaldehyde	2-EthylHexanal	4-Anisaldehyde	Benzaldehyde
IL#1	100% - 1h	--	100% - 1h	100% - 1h
IL#2	100% - 1h	--	100% - 1h	100% - 1h

<b>IL#3</b>	93% - 1h	0% - 24h	--	--
	98% - 2h			
	99% - 3h			
	100% - 4h			
<b>IL#4</b>	100% - 1h	0% - 24h	--	--
<b>IL#5</b>	0% - 24h	--	--	--
<b>IL#6</b>	100% - 1h	0% - 24h	--	--
<b>IL#7</b>	100% - 1h	--	--	--
<b>IL#8</b>	21% - 1h	--	--	--
	33% - 2h			
	50% - 3h			
	71% - 4h			
	99.2% - 5h			
<b>IL#9</b>	0% - 24h	--	--	--
<b>IL#10</b>	0% - 24h	--	--	--

Unfortunately, after the reactions, Cinnamyl alcohol did not show spontaneous separation, with only one phase observed. Moreover, it can be seen that the hydrogenation of cinnamaldehyde in some ILs is slower than in others, due to the low solubility of the aldehyde. The hydrogenation of 2-EthylHexanal was not successful. This substrate contains some ethylhexanoic acid impurity which could not be removed by distillation, and the acid decomposed the Fe(II) complex ( $^{31}\text{P}$  NMR shifted to 64.3 ppm).

As a conclusion for homogeneous reactions, 4-FBA is a good substrate to quickly test conversions. ILs with strongly coordinating anions are coordinating to the Fe(II) complex blocking its activity. Spontaneous separation could not be performed after the reactions, thus a solvent is required for product extraction.

### 4.3 Biphasic reactions

Successful testing in homogeneous reactions revealed the need for a solvent, which dissolves the product better than the IL and (conveniently) is not miscible with the IL. Biphasic reactions are the following logical step in order to test interactions between IL phase and substrate/product, as well as between those and the solvent.

The troubled question of the solvent needs to be faced. Bearing in mind the importance of green chemistry nowadays as well as safety, water is undoubtedly the first solvent to be taken into consideration. Water would be a good candidate, however it is not miscible with the ILs. Furthermore, it does not dissolve the used organic alcohols properly, thus using water makes the extraction of the product difficult, if not impossible. The second possibility was to use a hydrocarbon that would allow for the extraction of the alcohol. Heptane was used, since it is apolar and not miscible with most of polar ILs; however ILs with long carbon chains would definitely mix with heptane taking into consideration the hydrophobic character of both, the chain and the heptane.



4-fluorobenzaldehyde was chosen as substrate, taking into account the fact that both the substrate and the product were very easy to identify via  $^{19}\text{F}$  NMR (Figure 11). In addition the fact of showing the best performance in the homogeneous reactions with different ILs as well as in previous studies of the catalyst [76,80], deem this substrate the most suitable. Additionally, if the IL leaches to the solvent phase, it is easily identifiable by the  $^{19}\text{F}$  NTf<sub>2</sub> anion peak.

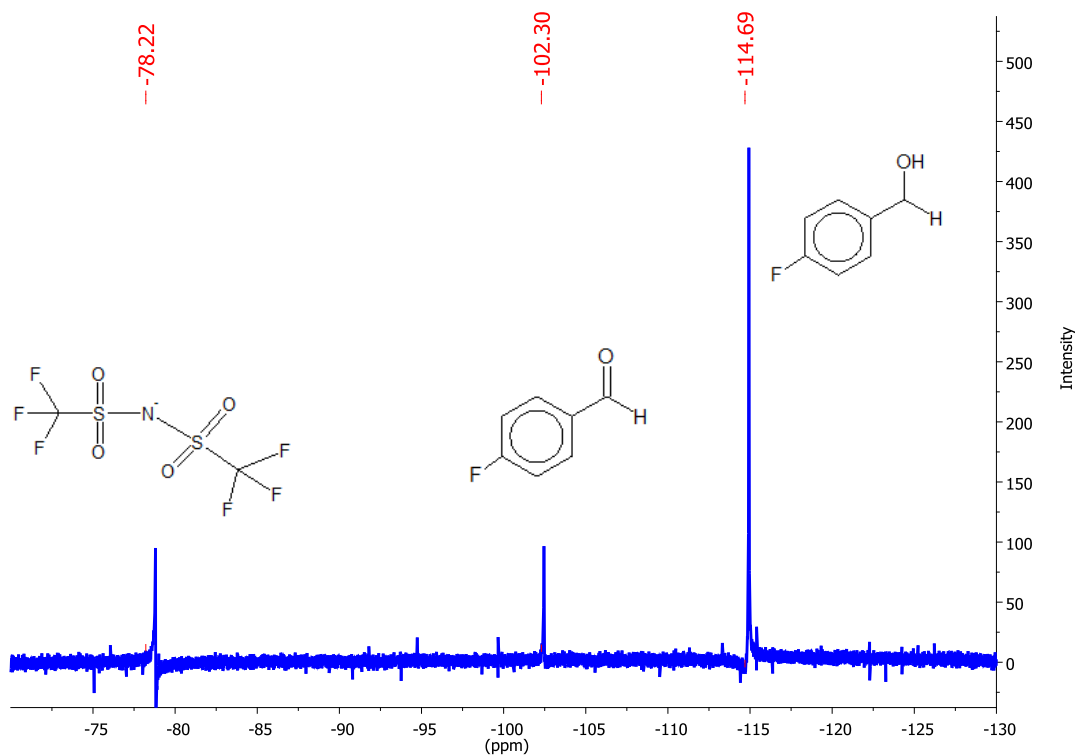


**Figure 11** -  $^{19}\text{F}$  NMR spectra; 4-fluorobenzaldehyde peak (-102.30 ppm), 4-fluoroalcohol (-114.69) and NTf<sub>2</sub> anion (-78.22).

Table 10 provides the results obtained, using different ILs and solvents. It can be concluded that the Fe(II) complex catalyses the hydrogenation of 4-FBA under biphasic conditions as well. As it was expected, the product stayed in the IL phase using water as solvent, both with long and short chain ILs, despite the addition of enough water (12 ml) to dissolve the amount of produced alcohol, due to the low solubility of the corresponding alcohol in water compared to the IL. Using heptane as solvent resulted in the extraction of alcohol from the IL, with only slight amounts of product remaining in the IL phase. As it was expected long chain ILs dissolved in heptane. For this table and the next to come conversion was calculated by NMR integration, being 4-fluorobenzyl alcohol the only reaction product.

**Table 10** - Biphasic reactions. Reaction conditions: 2 mmol of 4-FBA, 0.5 mol% catalyst, 2 mL solvent and IL amount according to Table 7; Pressure: 10 bar.

IL	Solvent	Conversion	Comments
IL#1	heptane	>99%	--

<b>IL#2</b>	heptane	>99%	--
<b>IL#2</b>	water	>99%	Alcohol in IL phase
<b>IL#3</b>	heptane (2ml)	45 %	--
<b>IL#4</b>	heptane	95%	--
<b>IL#6</b>	heptane	>99%	--
<b>IL#7</b>	heptane	>99%	IL in heptane phase
<b>IL#8</b>	heptane	>99%	IL in heptane phase
<b>IL#8</b>	water (12 ml)	>99%	Alcohol in IL phase
<b>IL#11</b>	heptane	>99%	No DBU
<b>IL#12</b>	heptane	>99%	No DBU

These results are in perfect agreement with the majority of reports on biphasic reaction using ILs, and are to a certain extent what motivates searching for a supported solution, that retains the IL and allows for the reaction to be smooth and efficient.

#### 4.4 Heterogeneous reactions

As already pointed out, starting from the classical homogeneous reaction and introduce some characteristic elements of heterogeneous reactions, is the core of this thesis. In order to do such, supported reactions were performed. Figure 12 tries to illustrate in a simplified way the overall process.

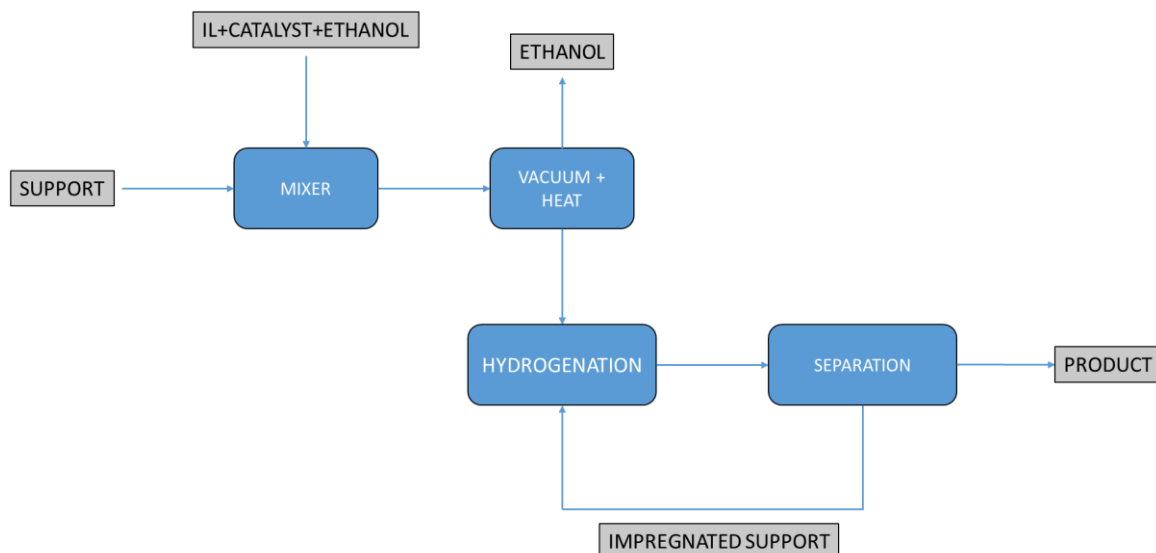
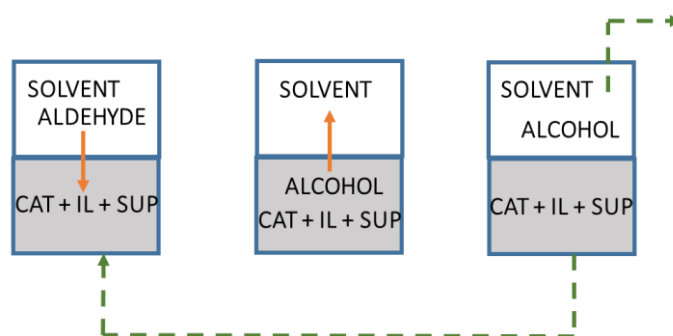


**Figure 12** - Simplified diagram block of the overall process

The heart of the all process is the hydrogenation; in an industrial scenario it would be a reactor. However in the present situation and since the reaction is in batches, an auto-clave was used as the one depicted in Figure 10 (vide section 3.5.12). With an overall limit of 200 bar of pressure and all made of stainless steel, it is a suitable equipment in where the reaction can be performed.

After the reaction itself, the separation between impregnated support and product is of great importance. The following diagram (Figure 13) tries to illustrate the desirable situation in the supported reaction. The reaction is to be carried at room temperature ( $\approx 25^{\circ}\text{C}$ ) and absolute pressures ranging from 10 to 40 bar.



**CAT** – Catalyst; **IL** – Ionic Liquid; **SUP** – Support

**Figure 13** – Schematic representation of the desired hydrogenation mechanism and separation in supported catalysis.

A schematic representation of the SILP concept applied to the present case is depicted in Figure 14. A thin layer is formed which contains the catalyst dissolved in the IL and allows for the

substrate's penetration and consequent reaction. Although an easy to understand concept, the presence of a support may change dramatically any conclusion based either on homogeneous or biphasic reactions.

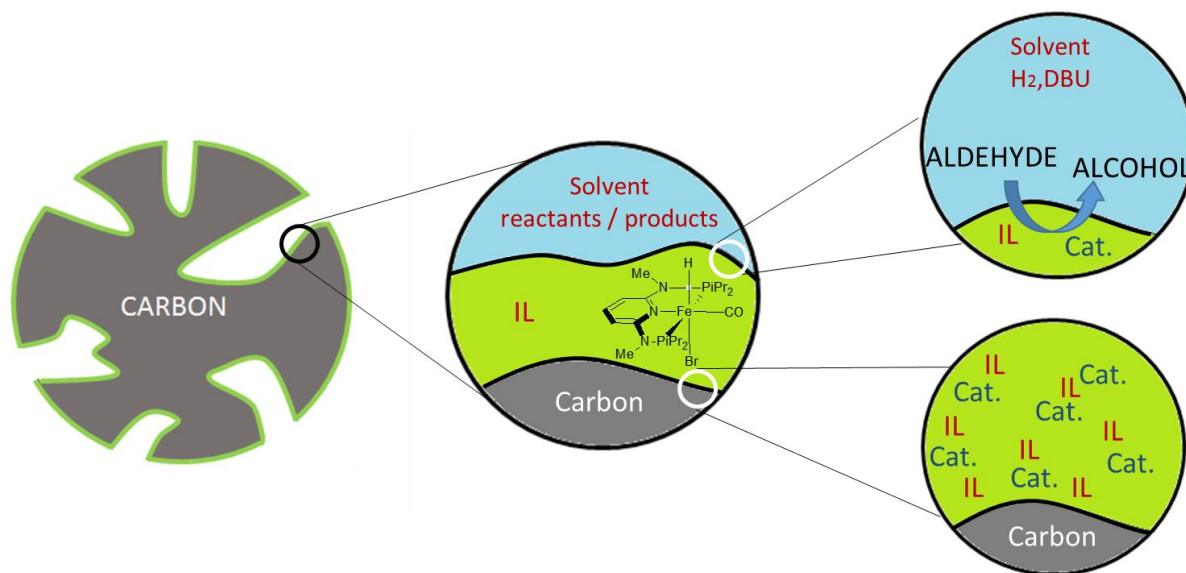


**Figure 14** - Schematic representation of SILP catalysis.

## 4.5 Activated Carbon Spheres

### 4.5.1 Support characterization

A commercial carbon was used, based on previous reports [94] of its suitability for catalytic purposes, in particular, an excellent surface composition (with basic groups dominating the surface), an appropriate porosity and pore size distribution and finally a good BET surface area. The commercial carbon was gently ceded by Blucher<sup>®</sup> Company; the core business of the company is water treatment plants and so this carbon was developed to suit that specific application.

The spherical activated carbon, also referred as commercial carbon, is protected by 2 patents [95,96] where the process of synthesis is described. As an overview, the carbon spheres are produced by a non-porous polymer (based on styrene and divinylbenzene) that is treated/activated using an oxidizing agent and carbonized above 900°C for a certain amount of time. All this process is enough to create rolling spheres with the desired degree of porosity, by controlling the different concentrations, time of exposure and range of temperatures.

It is crucial to have a full picture of the used support, once the addition of a third element to the classic biphasic reaction may have, at first look, unpredictable results. For a start, both the

elemental composition as well as the surface chemistry are of uttermost importance. They both decisively influence the adsorptive characteristics and selectivity. On the one hand oxygen groups on the carbon surface affect polarity and acid-base properties. On the other hand organic impurities have an influence on both physical and chemical adsorption [97].

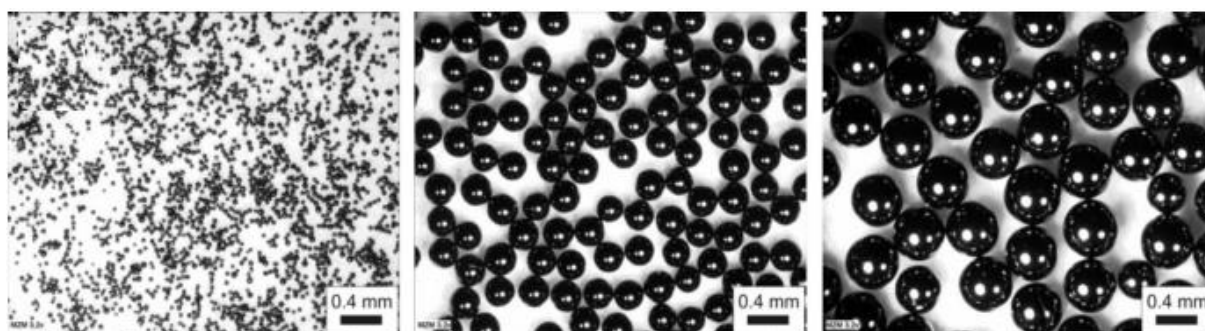
The company assured 99.9% carbon content based on their research paper [98]. We also performed elemental analysis on the provided carbon. Table 11 summarizes the values obtained.

**Table 11** - elemental analysis summary; \* - below the detection limit.

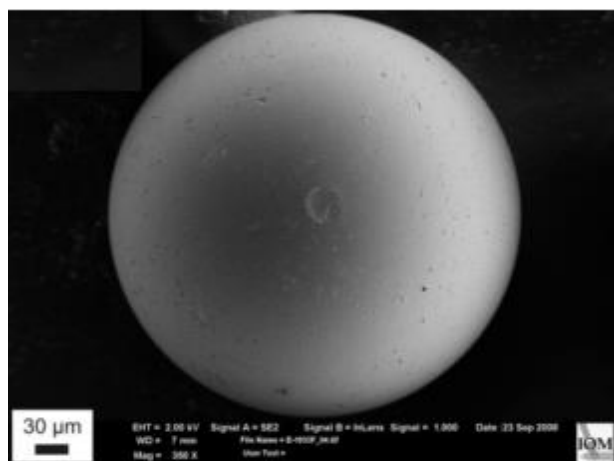
Element	Ref. 98	Elemental analysis
<b>Carbon (C)</b>	99.88%	97.88%
<b>Iron (Fe)</b>	0.1 %	0.11%
<b>Silica (Si)</b>		*
<b>Oxygen (O)</b>	-	0.67%
<b>Cr,Ni,Ca, Na</b>	0.01%	*
<b>Mg, Mn</b>	0.01%	0.002%
<b>Others</b>	0.001%	1.338%

Clearly there seems to exist a difference between what is stated by the company and our results. Although roughly 2% in absolute difference for the carbon content, this value can be used to justify some not well succeeded experiments, once the catalyst is extremely sensitive to its surroundings.

It is described in the patents and in the information provided by the company that the particles' size is in maximum 0.8 mm and, in this context, 95% of all particles are between 0.315 and 0.58 mm. Ref. 98 provides light microscopic images of different sizes of this spherical particles and scanning electronic microscopy (SEM) images. Figure 15 shows those experimental results. No doubts remain concerning the actual shape of the particles. Furthermore the process of synthesis associated with the particles' size and shape leads to an abrasion resistance much superior to typical values [98].



(a)



(b)

**Figure 15** – light microscopic images of different carbon particles (a) and SEM image (b); obtained from ref. 98

Surface area and pore size distribution are the two remaining key parameters to assess on the provided carbon. Table 12 shows the results obtained for the Commercial Carbon (CC). These values are good, once a considerable surface area and pore volume are available. It was also found that CC contains 60% mesopores and 40% micropores.

**Table 12** - BET measurements on pure carbon support.

Sample	BET surface area (m <sup>2</sup> /g)	Pore volume (cm <sup>3</sup> /g)
CC	1,420	1.11

Lastly, an insight into the carbon surface by means of X-ray photoelectron spectroscopy (XPS) provides a way of quantifying the total amount of surface oxygen. Reference 98 states the content to be lower than 5 wt-% with 4% C-O bond and 1% C=O bonds.

Table 13 quantifies that the surface (up to 10 nm deepness) of mesoporous carbon consist of 95.3 at% C and 4.7 at% O. The C 1s spectrum of the pristine carbon, Figure 16, quantifies the carbon bonds on the surface. It revealed that the mesoporous carbon shows mainly C–C (78 at.%), C–O (7 at.%), and C=O (4 at.%) signals. In addition we can also evidence the shakeup satellite peak around 290-291 eV.

**Table 13** - XPS surface elemental analysis; \* below detection limit.

Element	At. %
Carbon (C)	95.3
Iron (Fe)	*
Oxygen (O)	4.7

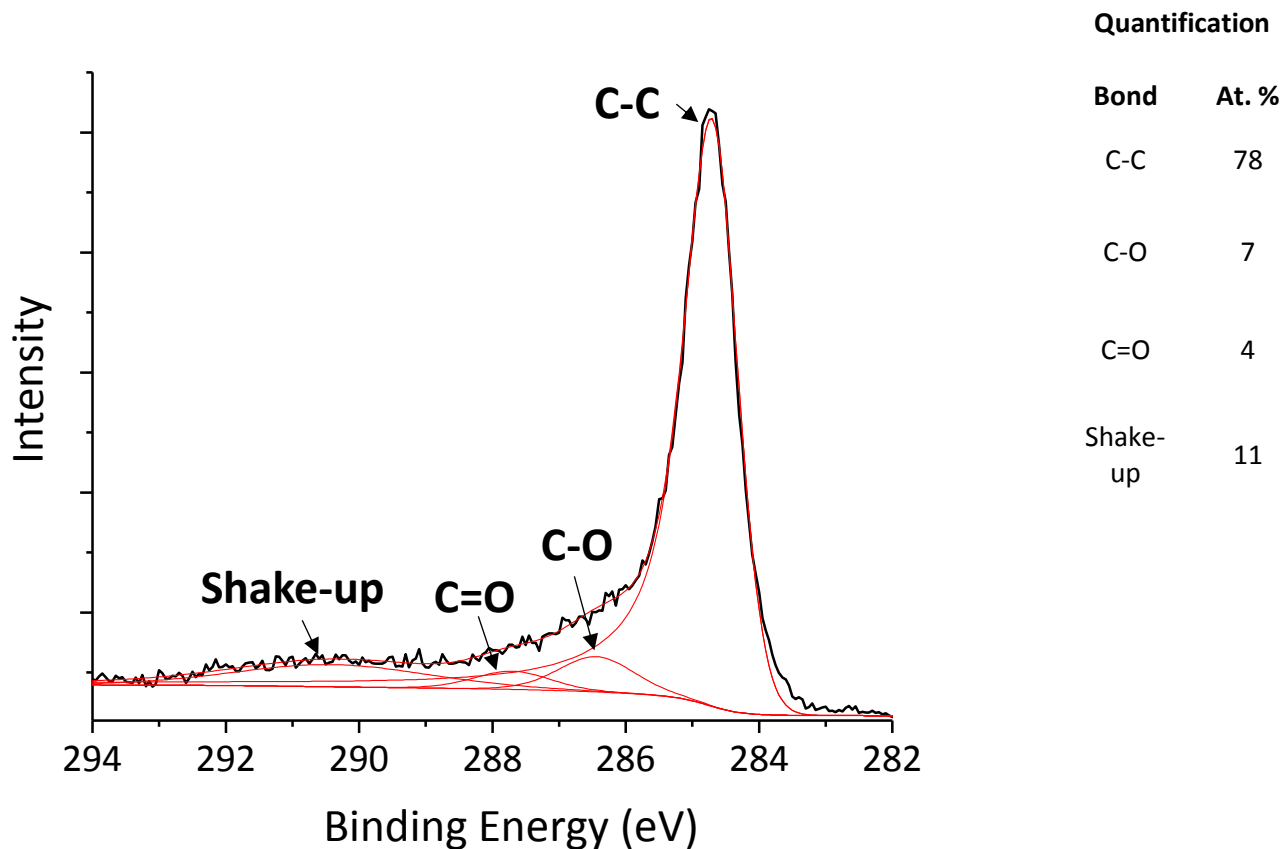


**Figure 16** - XPS pristine carbon surface spectra and quantification; Shake-up stands for other  $\pi$  interactions; black line represents experimental data and red lines the used fittings.

The immediate question is: How is the surface? What specific groups are there? It has been reported in a review on activated carbon [97] the astonishing quantity of surface groups available to interact with substrates, catalysts, solvents and products. Figure 17 illustrates what the previous review states about surface groups.

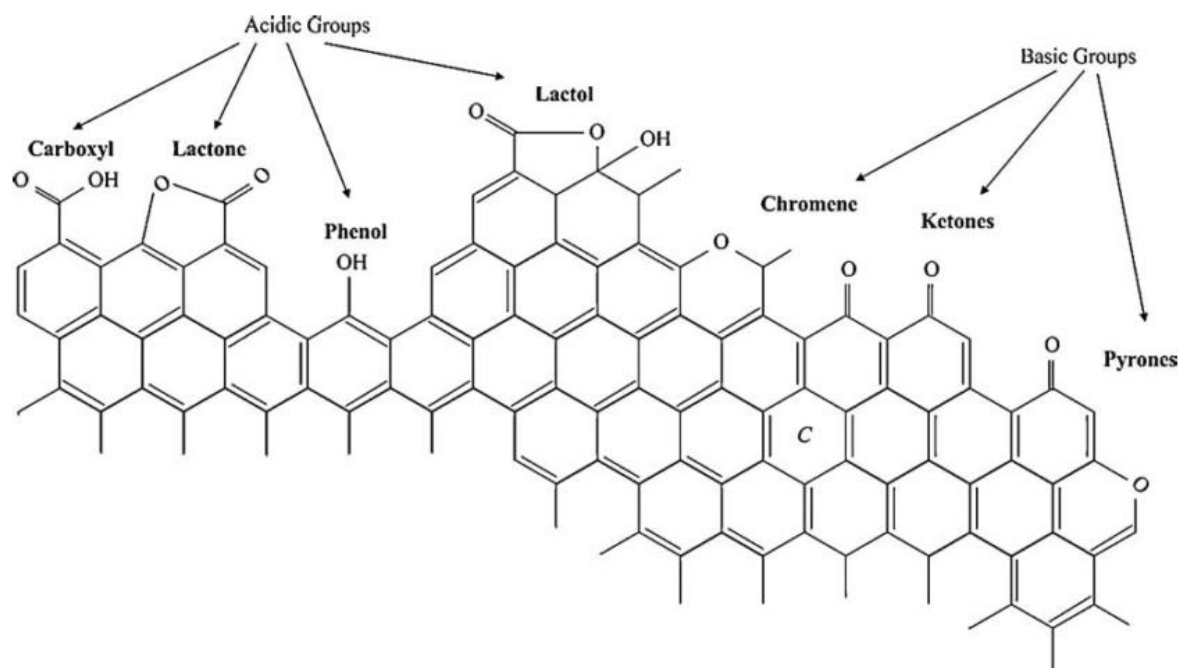


**Figure 17** - surface groups on activated carbon surface; image from ref. 97

On the one hand, basic groups are expected to cause no major problem on our catalyst's activity, once it has been reported to be fully active in basic environment. On the other hand, acidic groups are the cause of ready deactivation of our catalyst. XPS data shows that the surface does not contain O=C=O bonds, which belong to very acidic functionalities, such as carboxylic group, which in turn are extremely dangerous to our catalyst. This absence is in good agreement with the 900°C heat treatment used in the activation step of the carbon spheres, once this high temperature can selectively remove some of the acidic groups from the activated carbon surface [97]. However, some weakly acidic phenol groups can be imagined on the surface, since the carbon contains 7 At. % C–O bond which can be attributed to phenol and ether functionalities. By measuring CC pH it can be assessed whether it is rather basic or acidic. Table 14 shows the measured pH.

**Table 14** - Support used and respective pH.

Carbon	pH
Commercial Carbon – CC	8.4

Once the measured value for the CC lies in the basic region it can be assumed that the temperature treatment successfully removed the majority of acidic groups allowing the carbon to be suitable for catalytic applications.



## 4.6 Reaction optimization

Introducing the CC support may change dramatically the results based either on homogeneous or biphasic reactions. This interaction is still nowadays a difficult aspect to explain [77], once multiple factors are plausible to affect the outcome. For example the interaction support/IL/catalyst as well as changes in viscosity and density are possible factors.

Firstly, optimizing reaction conditions regarding pore filling degree and impregnation time were essential. The impregnation step of the IL inside the porous matrix is crucial to effectively allow for the catalytic phase to stay inside the structure. Ethanol was an easy choice for a solvent, once the catalyst is soluble in it and does not decompose. Furthermore, all the ILs studied are soluble in ethanol, making it the easiest choice. In accordance with previous good results, reactions' optimizations were achieved using IL#1.

In Figure 18 two pictures a) and b) are presented to illustrate the beginning and the end (after applying vacuum) of impregnation.

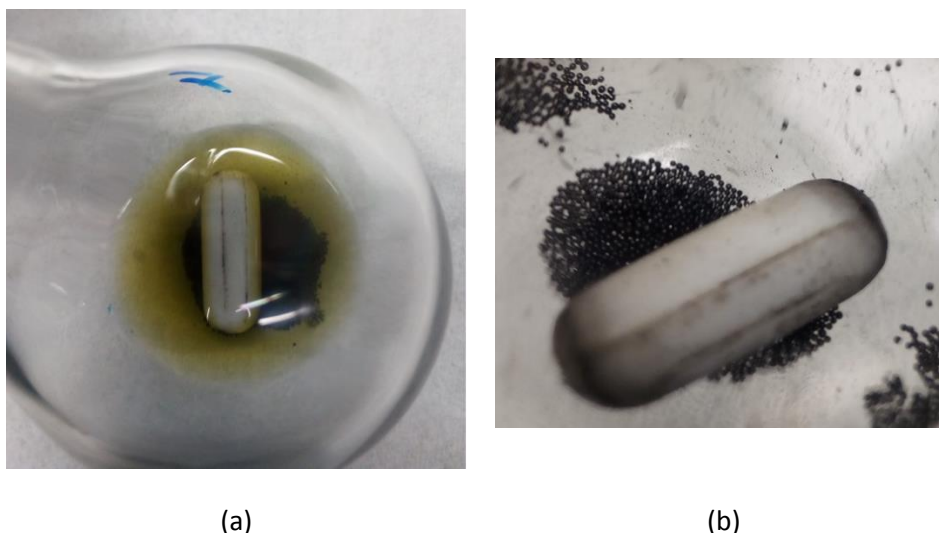


**Figure 18** – beginning (a) and the end (b) of impregnation step.

A way of assessing the impregnation is to look for an IL peak in NMR spectra after performing hydrogenations, since  $\text{NTf}_2$  anion has a strong peak at -78.1 ppm in  $^{19}\text{F}$  so is easily detected in case of leaching.

The general reaction in Figure 19 was used to optimize the supported reactions with different pore filling degrees ( $\alpha$ ). Taking into consideration that CC has a pore volume of  $1.11 \text{ cm}^3/\text{g}$ , the pore filling degree was tested starting from 20%, which means that the volume of IL is 20% of the total pore volume of CC. These initial experiments are included in Table 15 in order to provide a visually attractive way of summarizing the available information; any observations, when relevant, are provided in the comments section.

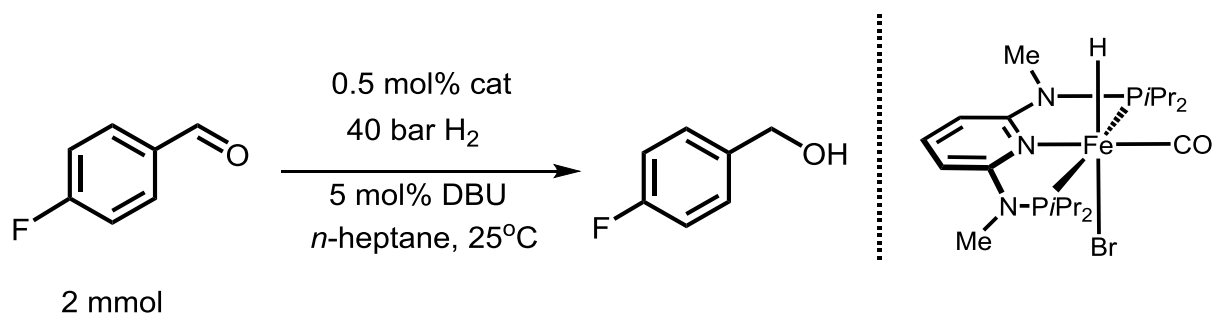
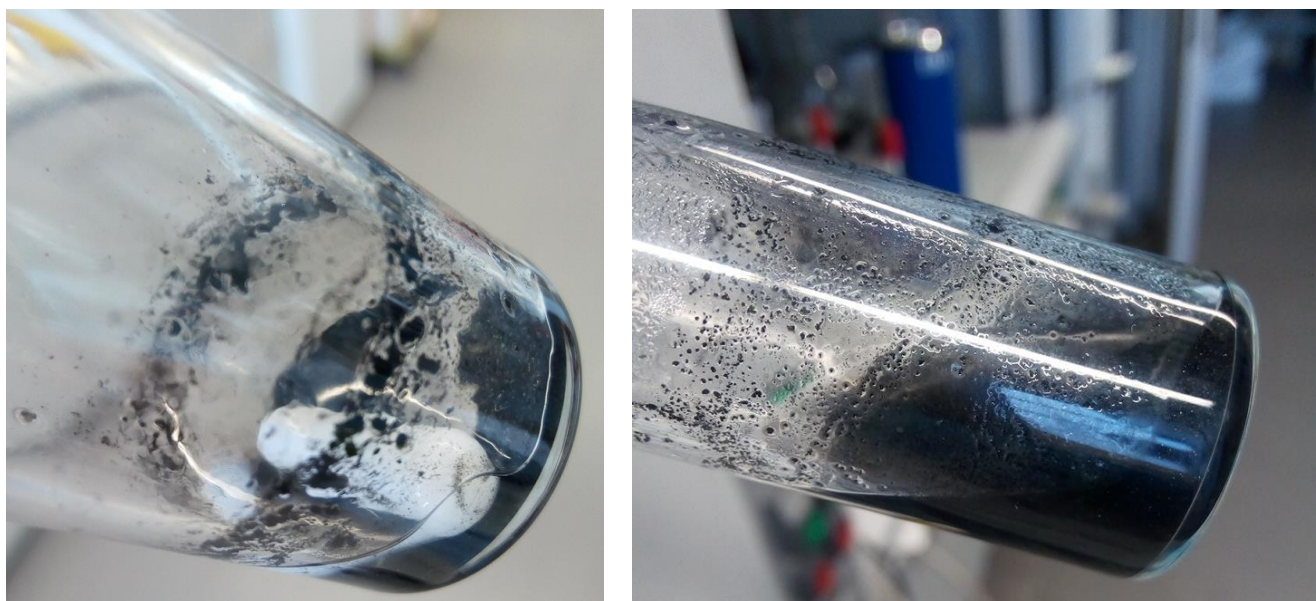


Figure 19 – model reaction for optimizing reaction conditions

Table 15 – pore filling degree testing on supported reactions; support: 100 mg of CC; IL#1: 50 $\mu$ L.

$\alpha$ (%)	Time (h)	Conversion (%)	Comments
20	24	0	--
30	24	0	--
40	24	0	--
50	24	0	IL leaching
60	24	0	Texture changed

The results clearly show that the SILPs did not catalyse the reaction at all. The addition of CC changed the previous results, suggesting that something poisoned the catalyst. However, the majority of impregnations were successful, meaning that indeed IL could enter the pores and get fixed inside the porous matrix. Moreover, different pore filling degrees can change the texture of the overall support. Figure 20 clearly illustrates this situation; on the one hand the desirable situation is depicted in Figure 20-a) where all the carbon particles stay in the bottom of the flask ( $\alpha = 20, 30, 40\%$ ) allowing for the recovery of the supernatant and allowing for recyclability of the SILP system. On the other hand, Figure 20-b) shows a total mixture between particles and supernatant making it much more difficult to recycle ( $\alpha = 60\%$ ). It is good to keep in mind that the recycle process must be as fast as possible, once contact with oxygen is lethal for the catalyst.



(a)

(b)

**Figure 20** – macroscopic view of 2 samples with (a) desirable and (b) undesirable texture.

One possible reason for the inactivity of the catalyst may be assigned to impurities found in the carbon as revealed by elemental analysis. In order to remove them, CC was treated with HCl and/or NaOH as described in the experimental part. Unfortunately, after the cleaning procedure the conversion was still 0%.

Another reason could be that the confinement of IL has changed its physical properties. Confinement effects on ILs have been widely reported. It is consensual that the viscosity of an IL strongly increases when confined inside a porous matrix [99,100,101]. The degree to which it increases is dependent on the IL nature and pore diameter. Not so consensual though, and an open field for further studies, is the effect on the melting point (MP) of the samples. On the one hand there are a considerable number of publications [102,103] that found a decrease in MP; on the other hand, at least one [104], found out an increase in MP, up to 200°C.

What if the Ionic Liquid is no longer a liquid but turns up in a solid inside the pores? What if, a crystallization or freezing step happens inside the pores, traps the catalyst and does not allow for penetration of DBU, hydrogen and aldehyde? This possibility might be responsible for the non-working experiments. If one considers this possibility, all the results could be explained by this phase transition on the IL phase. The catalyst would be trapped inside a solid, and neither Hydrogen nor substrate would reach the catalytic site.

In order to solve this question, Differential Scanning Calorimetry (DSC) measurements were performed. Two samples were analysed; one is a SILP with  $\alpha = 30\%$  and the other one is the pure IL#1, in order to have a control. IL#1 is relatively small and the impregnation was considered successful, with no leaching of IL detected by NMR measurement as discussed above. The experimental data is presented in Figure 21.

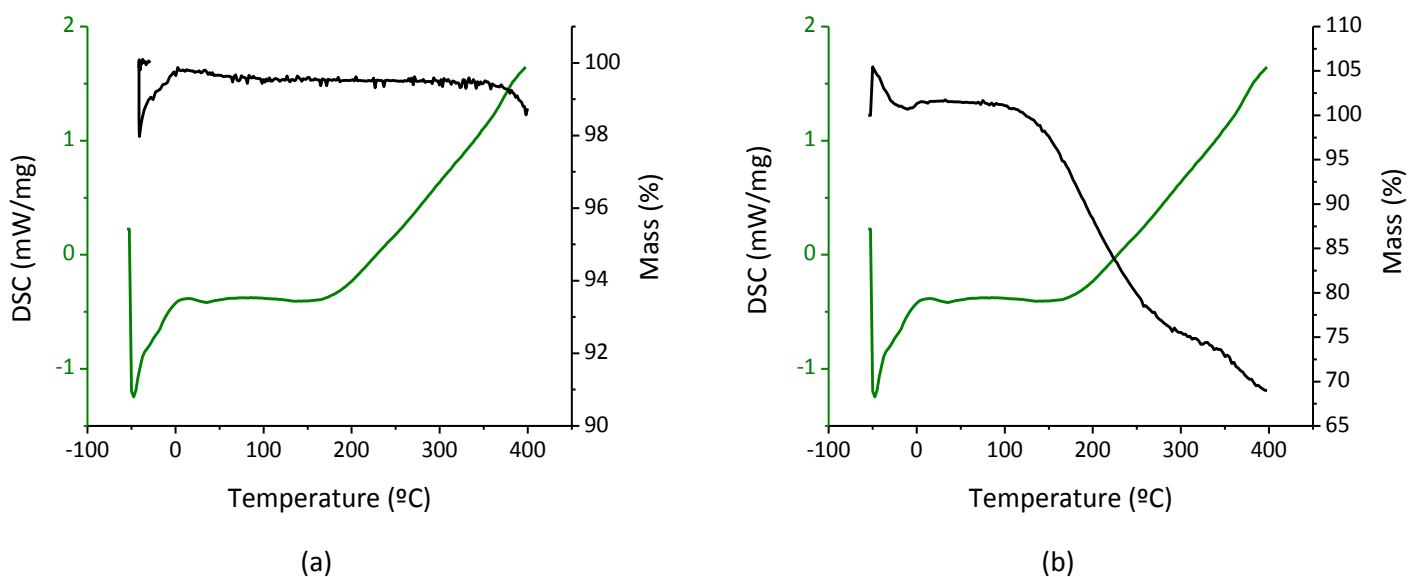


**Figure 21** – DSC (green) and mass percentage (black) plots for (a) pure IL#1 and (b) impregnated sample with  $\alpha = 30\%$

The analysis of the raw data allows for concluding that there is no IL freezing inside the pores. The DSC curves are very similar and, at lower temperatures (between  $-50^{\circ}\text{C}$  and  $0^{\circ}\text{C}$ ), the data is not consistent, once the heating rate was not stabilized. However, if a phase change was to happen, a big peak would be noticed. A final remark would go to some decomposition at high temperatures (about  $350^{\circ}\text{C}$ ) for the pure IL and a curious decomposition at much lower temperatures, starting at  $120^{\circ}\text{C}$  for the impregnated IL; although confinement clearly does not freeze the IL inside the porous structure, some change happened to allow for this lower degradation temperature.

Another reason for the SILPs' inactivity could be that the oxygen removal from the pores of the CC was not sufficient when applying vacuum for 24h at  $50^{\circ}\text{C}$ , once CC contains 40% of micropores, which adsorbs  $\text{O}_2$  strongly. This is why a  $300^{\circ}\text{C}$  thermal pre-treatment under vacuum conditions was used. After this pre-treatment, the reactions were performed again. The results are shown in Table 16.

**Table 16** - pore filling degree testing on supported reactions; support: 100 mg of CARB; IL#1:  $50\mu\text{L}$ .

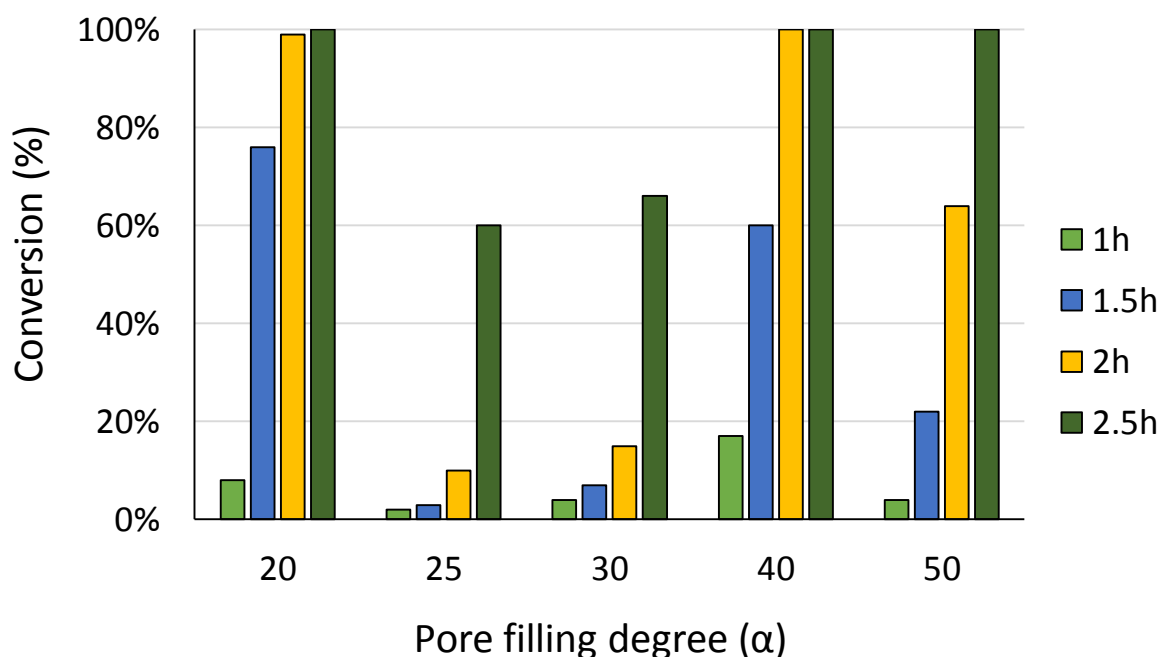
$\alpha$ (%)	Time (h)	Conversion (%)	Comments
20	24	>99	--
30	24	>99	--
40	24	>99	--
50	24	>99	IL leaching
60	24	>99	Texture changed

Finally, the inactivity problem was effectively solved, with all the SILPs catalysing the reaction. To confirm the presence of air in the micropores, BET measurements were performed using both 300 and 50 °C as degassing temperature. The results are depicted in Table 17, where it seems clear that 24h degassing at 50°C is not enough to remove the air from the micropores.

*Table 17 - BET results for CARB and CC.*

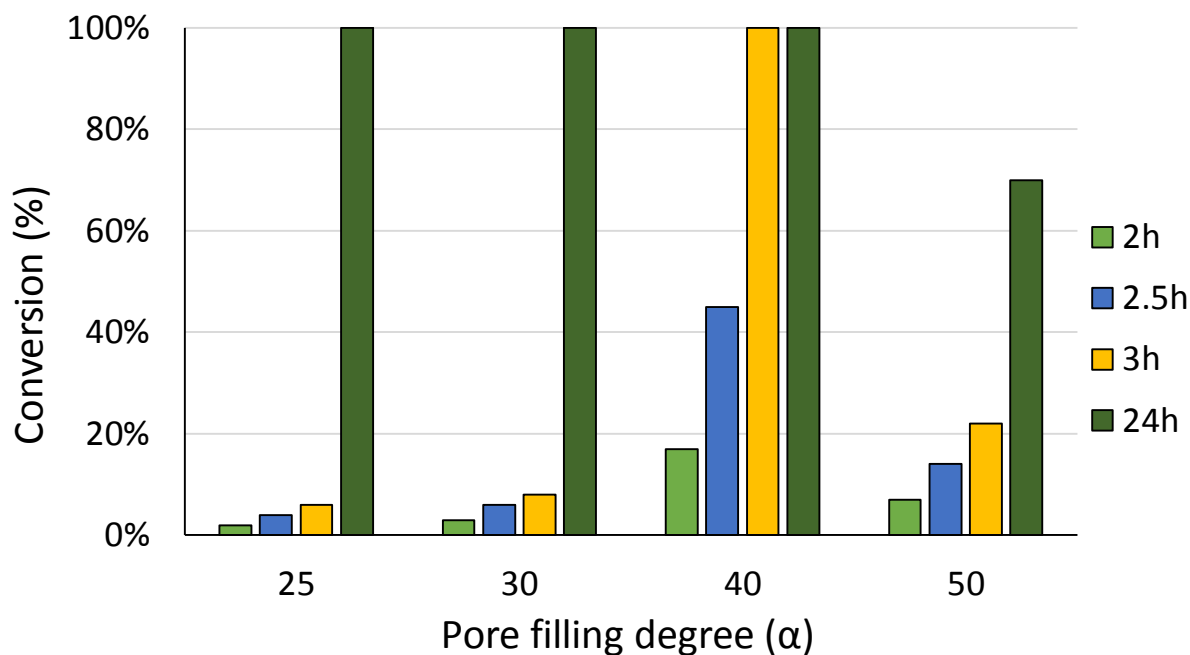
Sample	BET surface area (m <sup>2</sup> /g)	Pore volume (cm <sup>3</sup> /g)	Degassing temperature (°C)	Mesopores: Micropores (%)
CARB	1,728	1.18	300	50:50
CC	1,420	1.11	50	60:40

The optimum pore filling degree was still to be found. According to the previous results, it has to be between 20 and 50%. CARB 20, 25, 30, 40, and 50, corresponding to 20, 25, 30, 40, and 50 pore fillings respectively, were tested. The best catalytic phase amount was determined, meaning the one that maximizes conversion for a certain period of time. Experiments were made using 40 and 10 bar of pressure. The results are available in Figure 22 and Figure 23 respectively.



**Figure 22** - 40 bar pressure hydrogenation results; experimental condition: 100 mg of support; 2 mmol of substrate(4-FBA); 5 mg of catalyst; 2 ml of solvent (heptane); 16μL of DBU; 24-60 μL of IL#1.

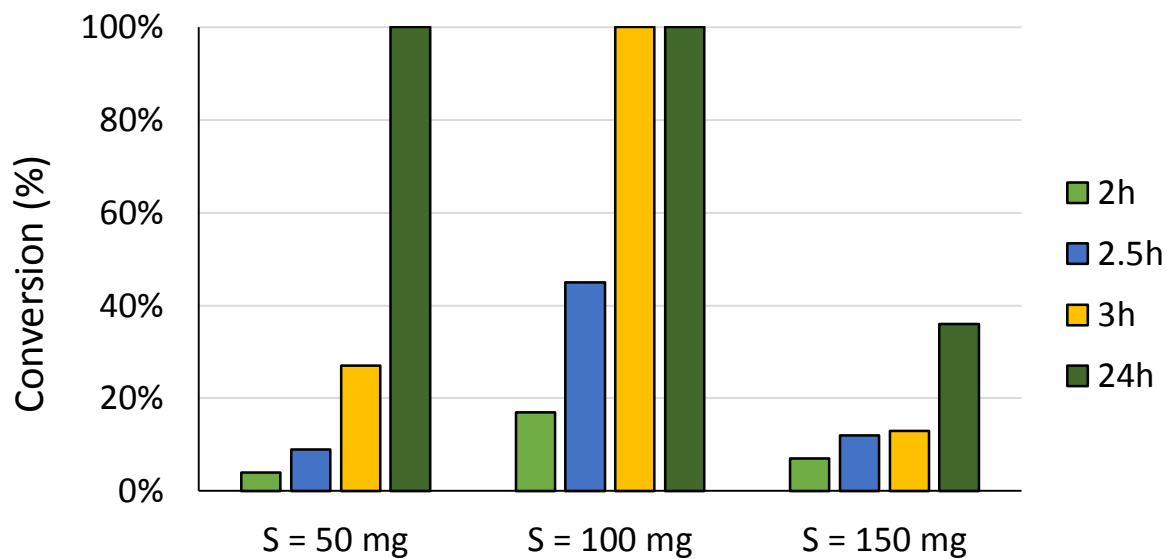
It is clearly seen that when using 40 bar H<sub>2</sub> pressure, both CARB 20 and 40, reach full conversion in approximately 2 hours. However, it must be noted, that for the preparation of CARB 20 only 24 μL of IL were used. This amount is not enough to dissolve the catalyst, meaning that the catalyst leached to the heptane phase and a homogeneous reaction was taking place as well, consequently 100% conversion was achieved. 10 bar pressure provided a slower reaction but was used to confirm the best volume amount; indeed CARB 40 seemed to be the optimum pore filling.



**Figure 23** – 10 bar pressure hydrogenation results; experimental condition: 100 mg of support; 2 mmol of substrate(4-FBA); 5 mg of catalyst; 2 ml of solvent (heptane); 16 $\mu$ L of DBU; 30-60  $\mu$ L of IL#1.

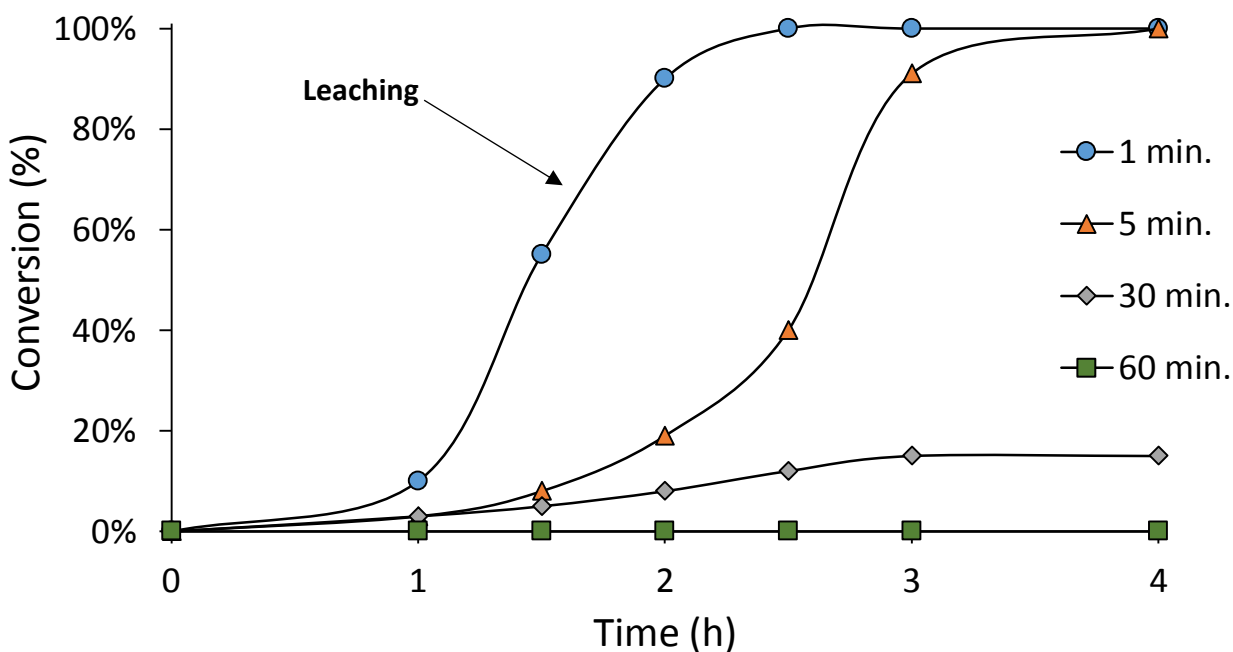
Two other important parameters were lacking: the support amount and the impregnation time. For the first, keeping the optimum IL:support ratio, thus using  $\alpha = 40\%$  and 10 bar pressure, the effect of support quantity was tested.

Figure 24 shows conversion results when using  $S = 50, 100$  and  $150$  mg of support and the results are awfully sensitive. When using 50 mg of support, the impregnation was not successful meaning that the yellow characteristic colour of the catalyst did not disappear during the process, leading, to some extent, to a homogenous reaction outside the porous matrix. Nevertheless, a foregone conclusion can be outdrawn; 100 mg support amount is the best choice available and the catalyst activity seems to be extremely sensitive to the amount of support.



**Figure 24** - support's amount results; experimental condition: 50-150 mg of support; 2 mmol of substrate (4-FBA); 5 mg of catalyst; 2 ml of solvent (heptane); 16 $\mu$ L of DBU; 24-70  $\mu$ L of IL#1; pressure: 10 bar.

Lastly, the impregnation time was meticulously tested in order to determine the best time to promote vacuum evaporation of the solvent. In Figure 25 conversion results are presented for 4 different impregnation times.



**Figure 25** – impregnation time experiment; experimental condition: 100 mg of support; 2 mmol of substrate (4-FBA); 5 mg of catalyst; 2 ml of solvent (heptane); 16 $\mu$ L of DBU; 50  $\mu$ L of IL#1; pressure: 10 bar; points represent experimental data; lines were created just to fit data.

It is readily comprehensible that, as impregnation time increases, IL and consequently the catalyst are allowed to penetrate deeper inside the porous matrix. On the one hand after only 1 minute, leaching was detected in  $^{19}\text{F}$  NMR, thus indicating that a substantial amount of catalytic phase lays outside the carbon support. On the other hand, after 60 minutes of impregnation, the phase is so deep in the pores that substrate and/or Hydrogen have a hard time reaching it, and consequently there is no conversion after 4h. From this set of experiments, it seems wise to consider 5 minutes the best impregnation time once no leach is detected, rolling spheres texture is kept and the conversion achieved is maximized.

Summarizing the results, the optimal determined conditions for SILP system using IL#1 are: 100 mg support, 50  $\mu\text{L}$  of IL ( $\alpha = 40\%$ ) with 5 minutes impregnation time. This material is referred as CARB 40.

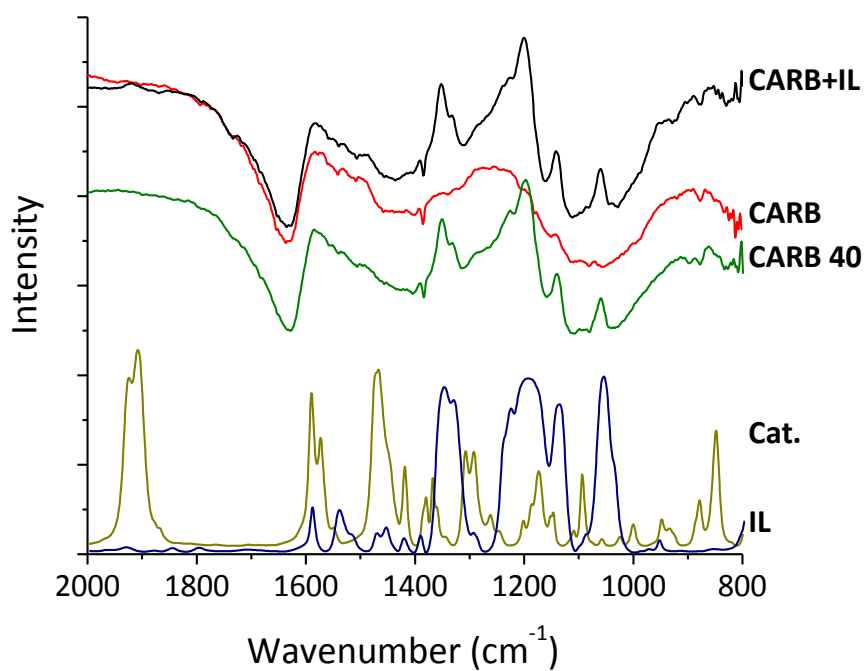
## 4.7 Characterization of CARB 40

### 4.7.1 FTIR measurements

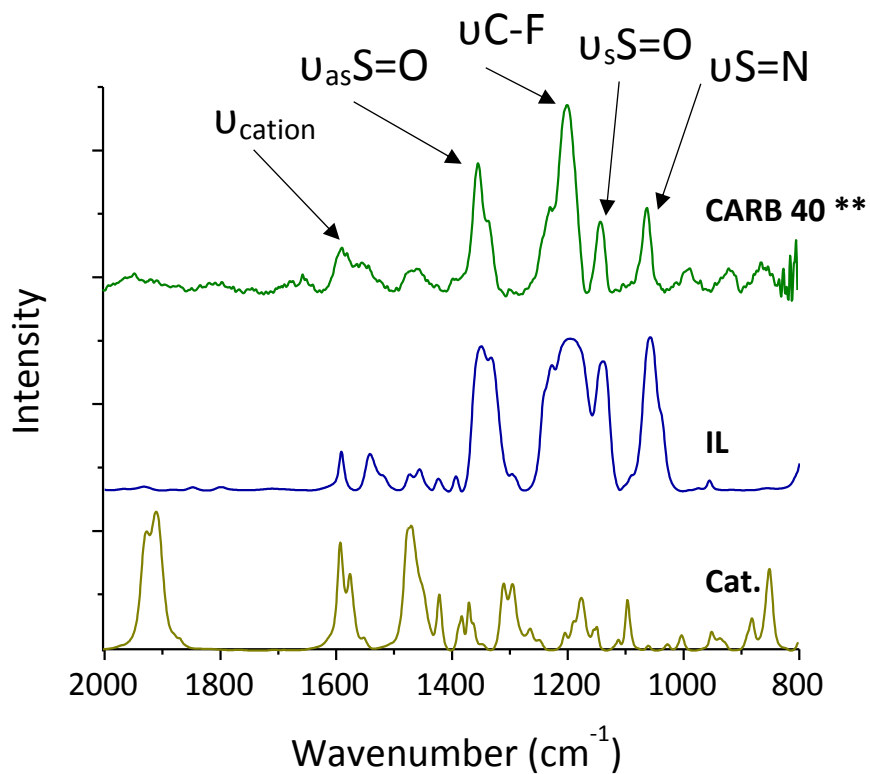
Infra-red measurements constitute a way of assessing the impregnation step and draw possible assumptions on whether, and how, does the IL and catalyst interact with each other and with the support itself. Being a vibrational spectroscopy, the information provided is on molecular bonds. For that purpose, the catalyst, IL#1 and CARB were analysed as well as CARB impregnated only with IL#1 (100 mg of carbon and 50 $\mu\text{L}$  of IL#1) and with IL#1 and catalyst (100 mg of carbon, 50 $\mu\text{L}$  of IL#1 and 5 mg of catalyst); the conditions pretend to imitate the compositions used in the reaction scenario. The results are provided in Figure 26.

The results provided clearly point for a successful impregnation of the IL and IL+Cat. inside the porous structure, since characteristic peaks of IL can be seen in the spectrum of CARB 40, Figure 26 – (b). The strong peaks between 1400 and 1000  $\text{cm}^{-1}$  are related to the vibrations of the anion. The peak at 1054  $\text{cm}^{-1}$  is assigned to the S=N stretch, the vibration at 1190  $\text{cm}^{-1}$  corresponds to the C–F stretch, while the bands at 1350 and 1140  $\text{cm}^{-1}$  belong to the asymmetrical and symmetrical S=O stretching vibration, respectively. The peaks between 1600 and 1400  $\text{cm}^{-1}$  are related to the cation as N–C–H and H–C–H vibrations [105]. However, the peaks of the catalyst are fairly seen when the catalyst is present in the impregnation medium, since its amount is 20 and 15 times lower than the support and IL respectively.





(a)



(b)

**Figure 26** – IR results of (a) all samples measured and (b) catalyst and IL in detail; \*\* - results from subtracting CARB spectrum from CARB 40 spectrum. In (b), the spectra were baseline corrected.

#### 4.7.2 BET and density measurements

An open question that was still remaining concerned the real pore filling degree of all the samples used. Table 18 provides BET measurements not only for the pure carbon support but also for carbon impregnated with IL and carbon impregnated with IL and catalyst. The amounts used were always 100 mg of support, 50  $\mu\text{L}$  of IL#1 and 5 mg of catalyst. Concerning the preparation of both impregnated samples, the procedure was exactly the same but for the fact that one contains catalyst.

*Table 18 - BET measurements on carbon samples.*

Sample	BET surface area ( $\text{m}^2/\text{g}$ )	Pore volume ( $\text{cm}^3/\text{g}$ )	Theoretical Pore filling (%)	Real Pore Filling (%)
CARB	1,728	1.18	-	-
CARB+IL	292	0.34	40	72
CARB 40	177	0.24	40	80

The volumes used of IL and IL+Catalyst correspond theoretically to 40% of the total free volume available inside the porous structure. Not surprisingly, when the impregnation is made, due to some clogging of the pores (Figure 27) the real impregnation percentage is 72 and 80%, respectively. It seems that when the catalyst is in the IL, there is a volume expansion, compatible with a conformational change in the IL structure and/or an effect on the viscosity and density of IL upon confinement [99].

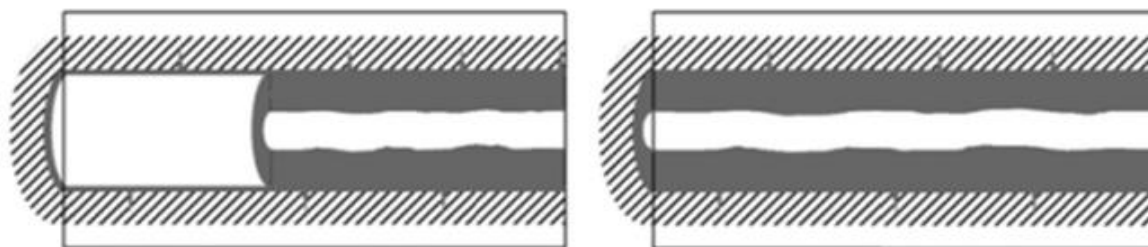


*Figure 27 - representation of possible pore clogging.*

Some basic density measurements were made to check for a sudden change in this property. Table 19 presents density results where it is possible to assess some changes in this property, corroborating the idea of an expansion due to the catalyst presence.

*Table 19 - Density results for IL and IL+Cat.*

Sample	Density ( $\text{g}/\text{cm}^3$ )	Error margin
IL#1	1.61	$\pm 0.05$
IL#1 + Catalyst	1.38	$\pm 0.09$

### 4.7.3 XPS results

Complementary to the empirical conclusion provided in Figure 20 and to NMR spectra, some XPS measurements were conducted in order to access not only the successful impregnation but also the proper dissolution of the catalyst in the IL structure. For that purpose CARB, CARB+IL, IL#1, Cat., IL#1+Cat and CARB 40 were used.

An overall elemental analysis (angle-integrated quantification) can be found in Table 20 which results from the integration of the full survey depicted in Figure 28. It is relevant to note that due to charging effects the results for the catalyst alone should only be considered an estimation. It is immediate that the impregnation of the IL inside the carbon was successful. Both CARB+IL and CARB 40 present a decrease in Carbon amount and an increase in Fluor, Nitrogen, Oxygen and Sulfur. Furthermore, the dissolution of the catalyst in the IL (IL+Cat.) is evident as well, with a significant increase in Fe content as well as P. The catalyst presence in the impregnated sample (CARB 40) is indisputable however its low amount does not allow to be detectable with XPS.

*Table 20 - XPS elemental analysis.*

<b>Sample / Elements (at. %)</b>	<b>Br</b>	<b>C</b>	<b>F</b>	<b>Fe</b>	<b>N</b>	<b>O</b>	<b>P</b>	<b>S</b>
<b>CARB</b>		95.3				4.7		
<b>IL</b>		36.8	25.6		12.8	16.4		8.3
<b>CARB+IL</b>		74.9	5.3		2.5	15.9		1.5
<b>Cat.</b>	5.1	65.0		2.4	7.2	15.5	4.8	
<b>IL+Cat.</b>	0.9	61.3	8.5	1.9	4.9	17.0	1.6	3.9
<b>CARB 40</b>		72.0	6.8		2.5	17.5		1.2

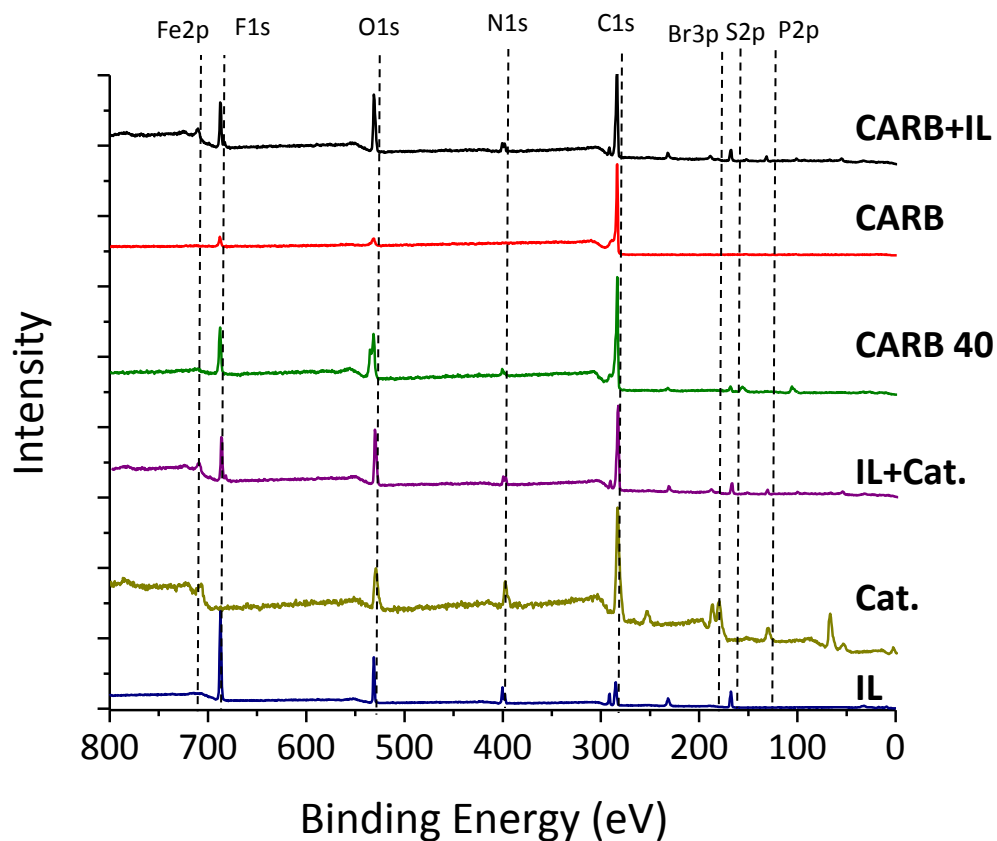


**Figure 28** – XPS survey scan spectra and elemental identification; measurements at 51° relative to sample surface normal.

All the peaks present in the survey scan (Figure 28) are compatible with the structure of the intervenient species, although with some minor cross-contaminations in the Carbon spectrum for Fluorine (e.g.). Taking the best of XPS technique, besides analysing the full survey, elemental spectra analysis provides a way of getting an insight into what is occurring in the near surface. Figure 29 considers C 1s and Figure 30 N 1s, F 1s and S 2p spectra of the relevant intervenients.

Concerning the IL, in C 1s region, a set of peaks are observed; the C 1s peak at the highest binding energy, that is, at 292.7 eV, is labelled as CF<sub>3</sub> in Figure 29. It arises from the two CF<sub>3</sub> groups of the [NTf<sub>2</sub>]<sup>-</sup> anion, corroborating previous results [106,107]. These carbon atoms are the most electropositive due to covalent bonding to fluorine atoms (electron withdrawing by nature) and were fitted accordingly. The carbon signals at lower binding energies are assigned to the imidazolium ring, where carbon atoms exist with different chemical environments. These environments are generally classified as C<sub>hetero</sub>, corresponding to carbon atoms bonded to heteroatoms, and C<sub>alkyl</sub>, corresponding to atoms bonded to other carbons and hydrogen. However, inside these categories a range of sub-categories are accepted [107,108], namely carbons that are classified as C<sub>alkyl</sub> and are next to the imidazolium ring, are logically assigned to higher binding energies, due to the presence of a more electronegative atom in its surroundings. A classification and deconvolution of the peaks is presented as well in Figure 29, with carbons labelled from C<sup>1</sup> to C<sup>5</sup> according to their chemical environment. The C<sup>1</sup>:C<sup>2</sup>:C<sup>3</sup>:C<sup>4</sup>:C<sup>5</sup> ratio obtained is 1:2:2.5:1.25:1.25, which is in line with the theoretical ratio of 1:2:2:1:1. Furthermore the experimental ratio CF<sub>3</sub>:C<sup>3</sup> is 1:1 in perfect agreement with theoretical expectations.

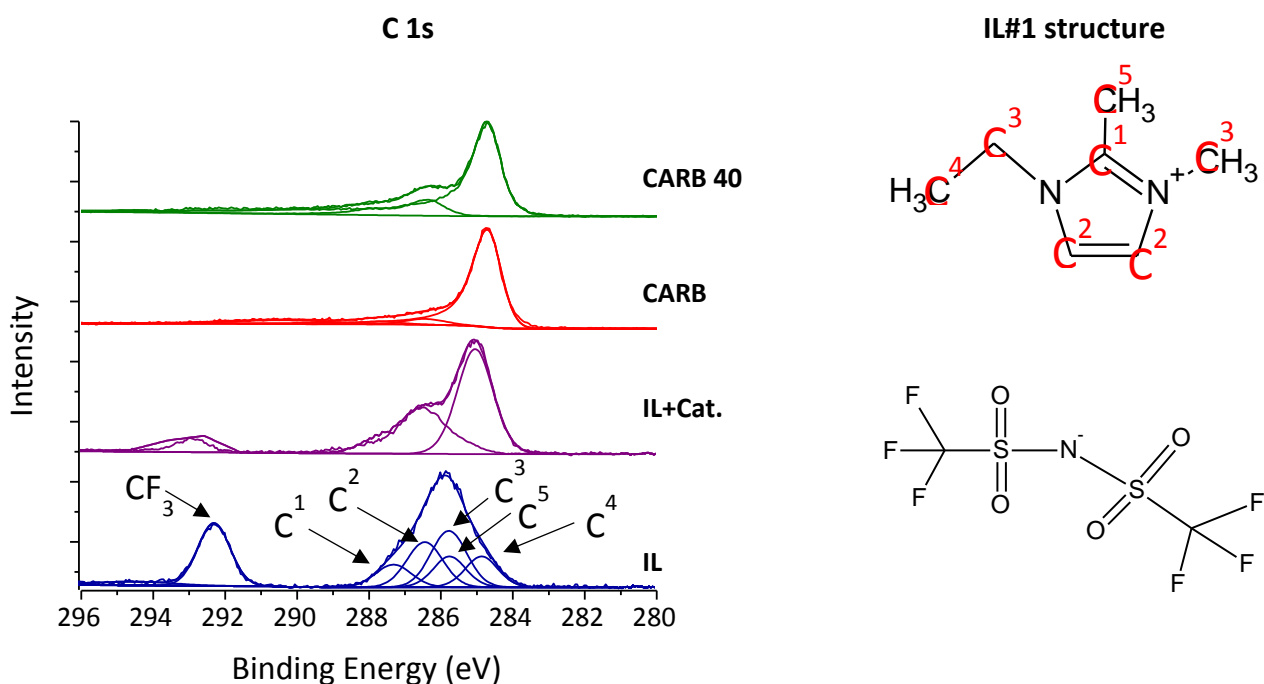
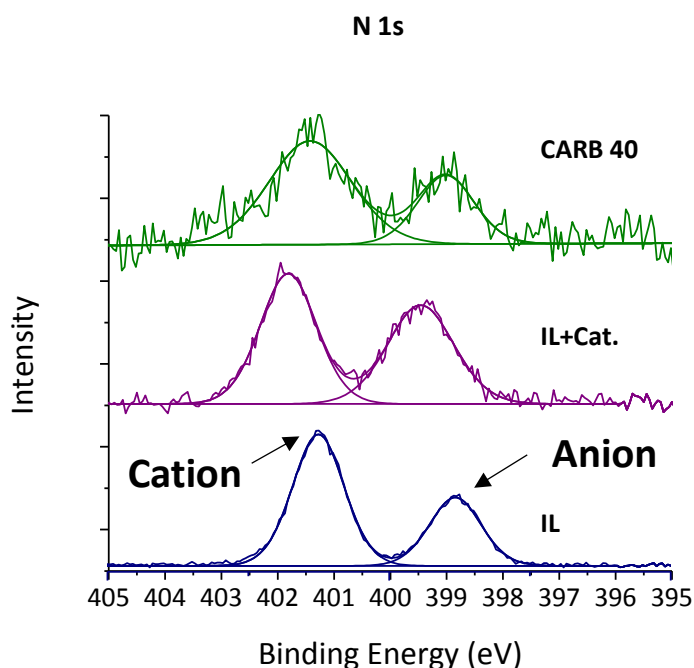
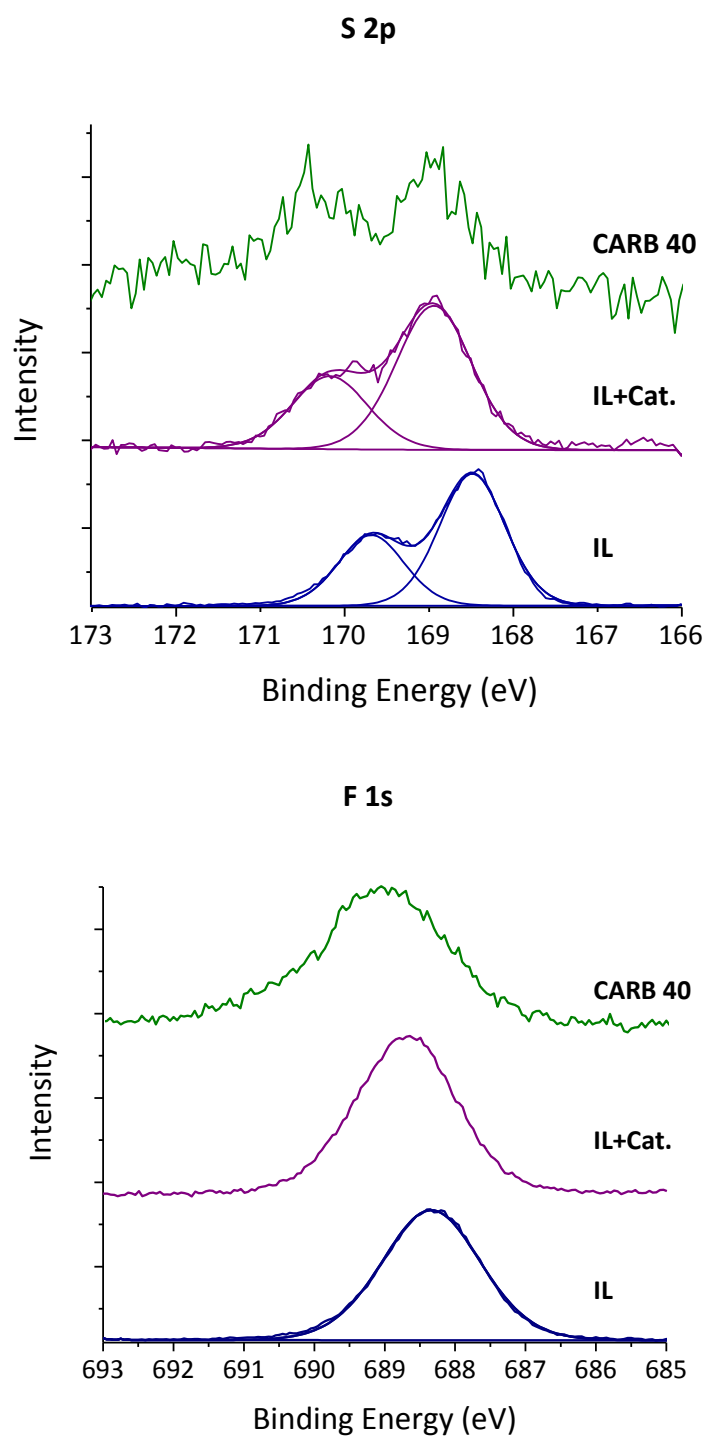


Figure 29 – XPS C 1s spectra and IL#1 structure and peak assignment; measurements at 51° relative to sample surface normal.

C 1s spectra contain more information, in particular for IL+Cat. and CARB 40. In the former, the dissolution of the catalyst is clear, once (e.g.) CF<sub>3</sub> peak intensity is decreased. In truth this peak comes only from the IL structure, and so the increase in other Binding Energies is due to the catalyst dissolution and interaction. Concerning the latter, and comparing with the pure Carbon spectrum, the impregnation step was successful, meaning that indeed the IL and the catalyst were able to penetrate the porous structure.





**Figure 30** – N1s, S2p and F 1s XPS spectra for major samples; measurements at 51° relative to sample surface normal.

Complementary to C 1s and the full survey, 3 other major elements were analysed and contributed to analyse the successful impregnation.

N 1s spectra emphasize again the success of the impregnation. On the one hand the IL spectrum shows both cation and anion peaks, in the ratio 2:1, which is compatible with the IL structure, once there are two equal Nitrogen in the imidazolium ring and a Nitrogen in the anion. The

dissolution of the catalyst changes this ratio to 1.1:1. The catalyst contributes with 3 Nitrogen atoms as previously shown in Figure 8. Finally for CARB 40 the ratio is roughly 2:1. This result points that indeed the IL is inside the carbon structure. One could advocate though, that the ratio should be closer to 1.1:1, once the catalyst is dissolved in the IL matrix. However, this situation is not necessary, once the amount of catalyst is below the detection limit.

For S 2p, it could be noted again a successful impregnation. However, there are two major peaks in the IL and IL+Cat. spectra. This could be misleading and as actually created, for years, erroneous publications on XPS studies on ILs [109]. The phenomena is known as spin orbit coupling. In this situation, for 2p level, there are two peaks,  $2p_{1/2}$  and  $2p_{3/2}$ , with different binding energies. In accordance with the degeneracy of the magnetic quantum numbers for  $j = 1/2$  ( $m_j = -1/2, +1/2$ ) and  $j = 3/2$  ( $m_j = -3/2, -1/2, +1/2, +3/2$ ), the intensity ratio is 1:2. This ratio is indeed confirmed in the present situation. A further detail to notice is the shifting in binding energy, namely towards higher values, when the catalyst is present. This shift is present as well for the impregnated sample.

F 1s spectra confirm that when the catalyst is added, higher values of binding energy are available. The shift is approximately 0.5 eV when the dissolution occurs. This situation is in agreement with a conformational change in the liquid structure when the catalyst is added and compatible with the cluster image already described by some authors [53,77] and discussed in the State of the art.

A deep understanding of the interface nature is of great interest not only for this specific application, but for a wide range of them [16]. Typically the discussion on IL surface structure involves two aspects: surface composition and molecular orientation. For the former, specific molecules may trigger special affinities towards a specific ion or group leading to preferential adsorption. This situation leads to a depletion of that ion in the bulk composition. For the latter, detailed and geometric ordering of the ions is relevant, even more when a foreign specie (like a catalyst) is present.

There are plenty of information and data concerning orientation of pure ILs when in contact with a support [109,110]. XPS has been widely used in order to show particular ionic distribution in ILs, with or without a solid support. However, a consensual explanation for that fact is still lacking. Rather some minor details are explored and explained. XPS is not very sensitive to meticulously describe geometry effects such as molecular orientation but is useful for determining the depth distribution of certain elements, in other words, the surface composition [111].

The colour maps depicted from Figure 31 to Figure 35, shed some light on how specific element changes in atomic percentage with increasing deepness. It should be noted that deepness values are not fixed for all the elements. Indeed they depend on the kinetic energy, which depends on the binding energy, which consequently depends on the element. For all the following Figures the smallest deepness corresponds to 75° and the biggest to an angle of 27°.

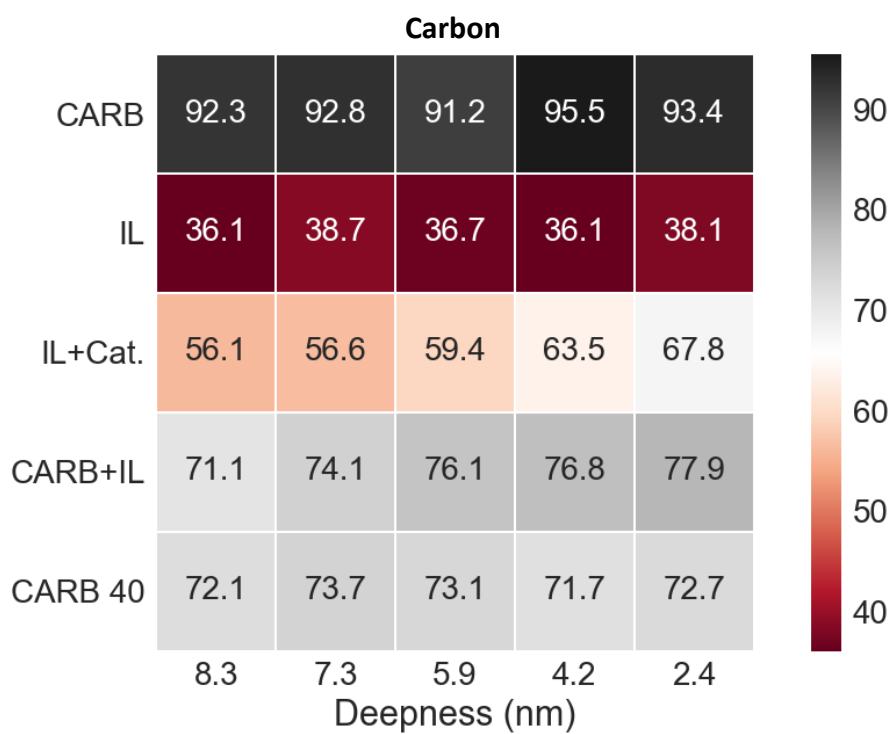


**Figure 31** – XPS angle dependant results for Carbon element; values in atomic percentage.

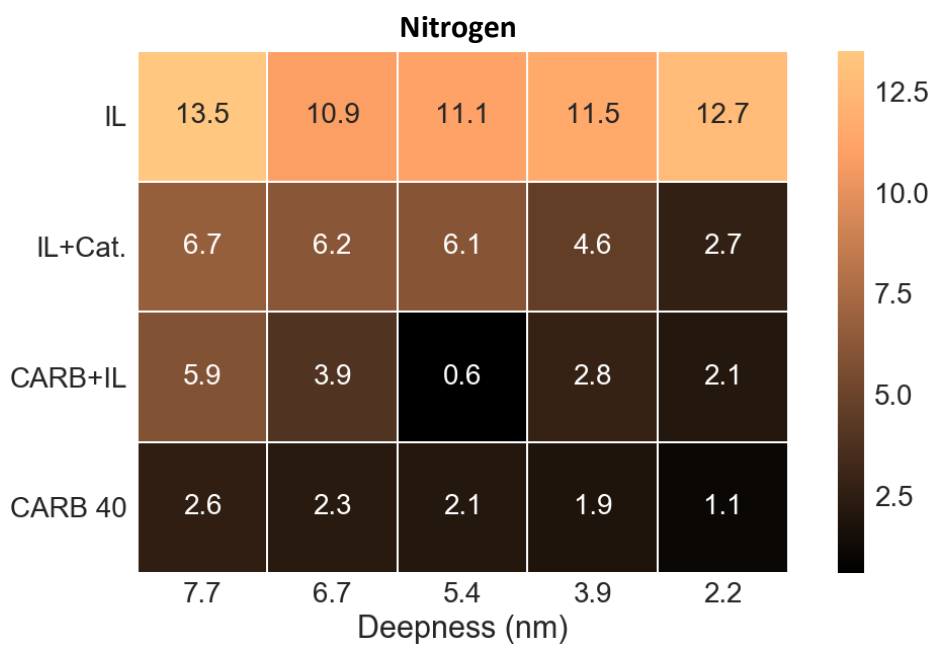


**Figure 32** - XPS angle dependant results for Nitrogen element; values in atomic percentage.



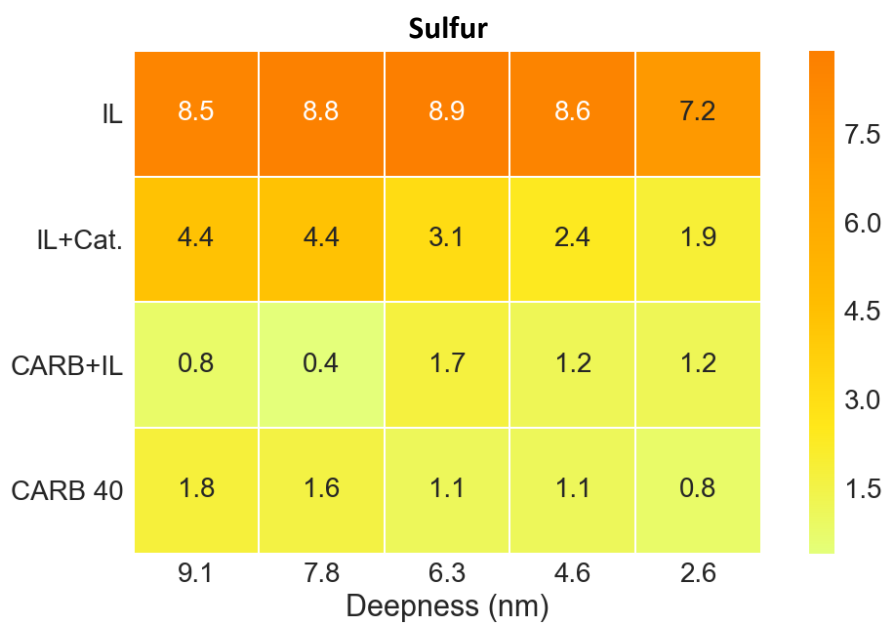


**Figure 33** - XPS angle dependant results for Sulfur element; values in atomic percentage.

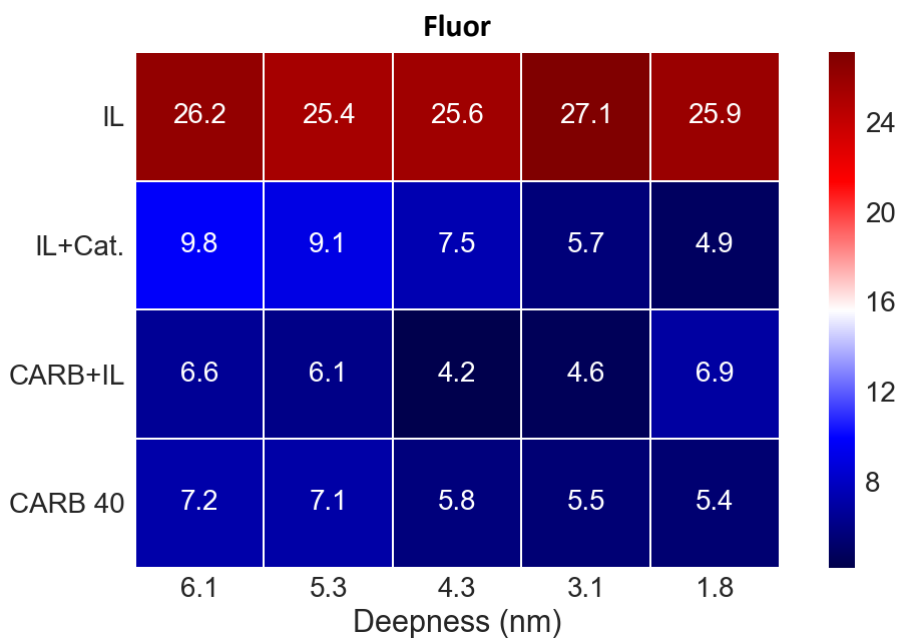


**Figure 34** - XPS angle dependant results for Fluor element; values in atomic percentage.

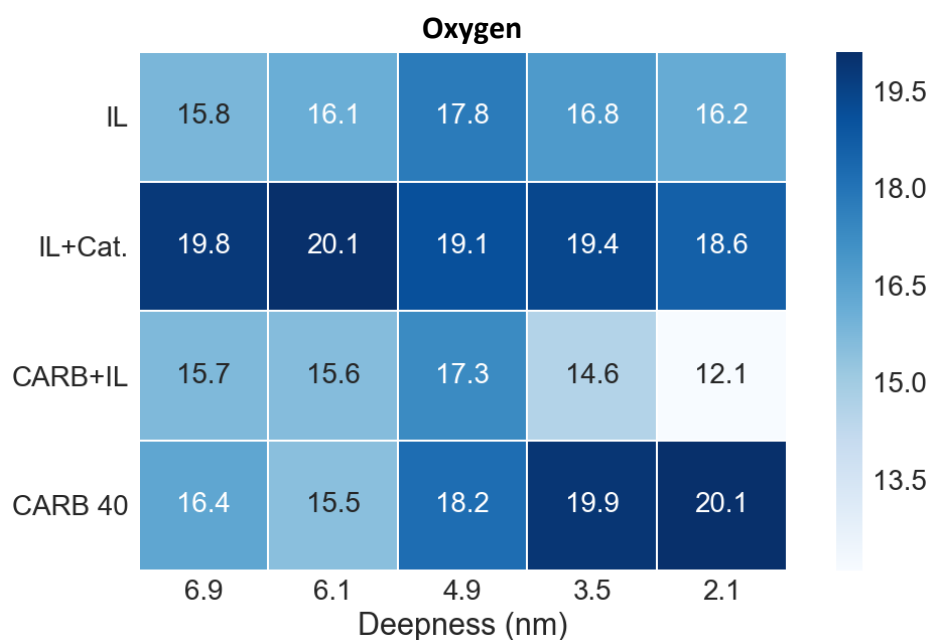


**Figure 35** - XPS angle dependant results for Oxygen element; values in atomic percentage.

The results could be no more interesting. Concerning elemental carbon, depicted in Figure 31, from both CARB+IL and CARB 40 it seems clear that the impregnation step was successful, with atomic percentages decreasing when compared to the carbon sample and increasing when compared to the IL. The curious effect of adding a catalyst to the IL is once again reported in this data. Without any support (IL+Cat.) there is a clear evidence of a preferential placement of carbon atoms in more superficial regions. Since carbon atoms are present in both IL and catalyst it is difficult to draw a definite conclusion based only in this spectrum. However, it is plausible to assume a higher amount of catalyst in the surface region, along with reported XPS carbon contamination [112]. It is relevant to note as well, that adding the support (containing a huge amount of carbon elements), associated with the experimental error associated with the technique, would reveal unwise any conclusions based on the supported samples.

Elemental nitrogen (Figure 32) displays the same problem as carbon, once it is present in both catalyst and IL. Nevertheless, the non-homogeneity of this element in all the scenarios (but for the IL, where it is homogeneous as expected) translate the idea that a change occurred not only because of the catalyst, but also in the impregnation step, with higher values of nitrogen in deeper regions.

The remaining 3 elements should be analysed simultaneously for a better picture of what is happening. Sulfur (Figure 33) and fluor (Figure 34) on the one hand, are only present in the IL anion (NTf<sub>2</sub>). On the other hand, oxygen (Figure 35) is present in the IL, catalyst and to some extent on the carbon surface.

For the IL, as a separate entity, the results are in perfect agreement with a homogeneous liquid, with all the elements equally distributed in both bulk and surface. When the catalyst is added (IL+Cat.) though, the bulk of the liquid is the preferred location for the anion, with significantly higher values compared to the surface. Adding a support to the homogeneous IL (CARB+IL) creates immediately a conformational adaption to the surface. This situation is known to happen [110] and is corroborated from the sulfur and fluorine maps where an increase with increasing deepness is obtained. The oxygen amount shows also an increase, although slight, with increasing deepness. The

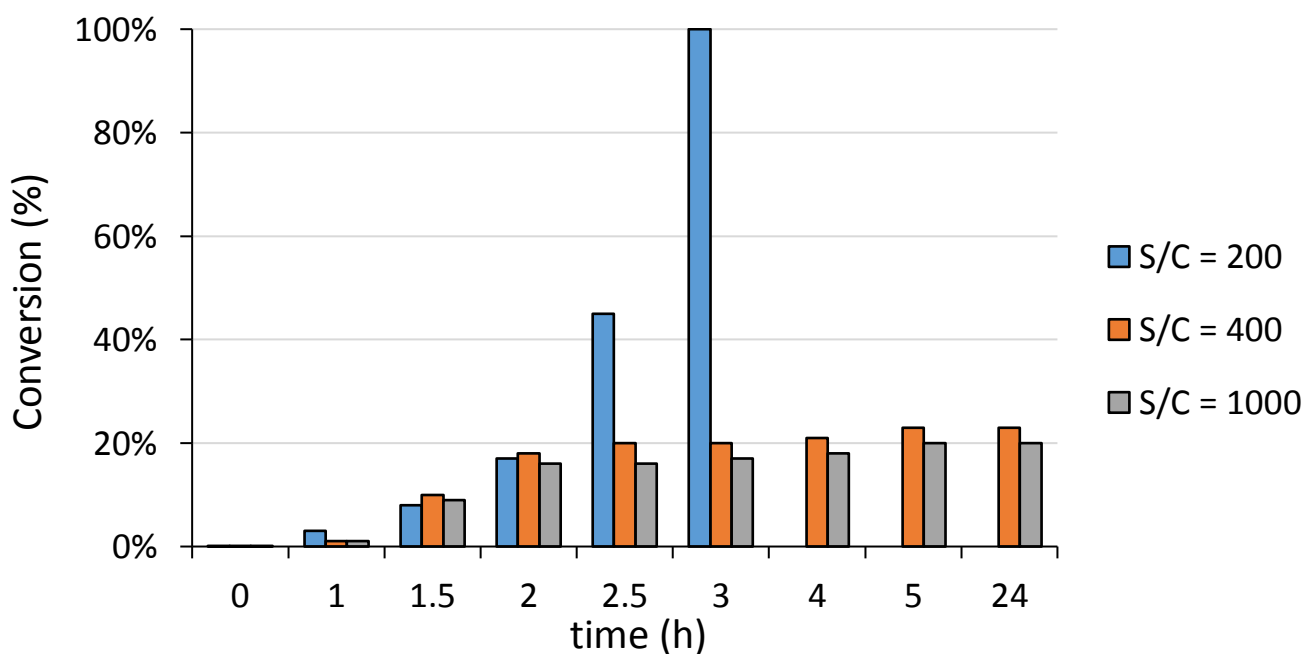
curious result arises from the supported sample impregnated with both the IL and catalyst (CARB 40). In this setting, sulfur and fluorine contents increase with increasing deepness, and oxygen values are the opposite of what would be expected, taking into consideration previous results. A possible interpretation would focus not only on the anion itself but on its groups' spatial orientation. It is described, for example, a particular orientation of  $CF_3$  groups towards the surface of the liquid when in contact with a surface [110]. This could be used to justify the rather amorphous result of fluorine. In addition, this interpretation could be also used for oxygen, where this element would have more affinity to be pushed to the outer space. However, up to now, there is no published data concerning this effect. The particular study of ILs on carbon surfaces is a somewhat emerging area, where a range of techniques may be applied.

In summa, it could be pointed from XPS data that the impregnation was deemed successful and that the IL structure, with catalyst alone and inside the porous structure (SILP), is totally heterogeneous, due to several interactions, ranging from electrostatic and Van der Waals forces to capillary and adsorption interactions.

## 4.8 Reactions using the optimized CARB 40

### 4.8.1 Substrate to catalyst ratio (S/C)

All the systems studied up to this point had a substrate to catalyst ratio (S/C) of 200. It is relevant to test the limits of the present SILP by increasing this ratio. In order to do so, the amount of substrate was increased to obtain ratios of 400 and 1000. Experiments were made at 10 and 40 bar (Figure 36).



(a)

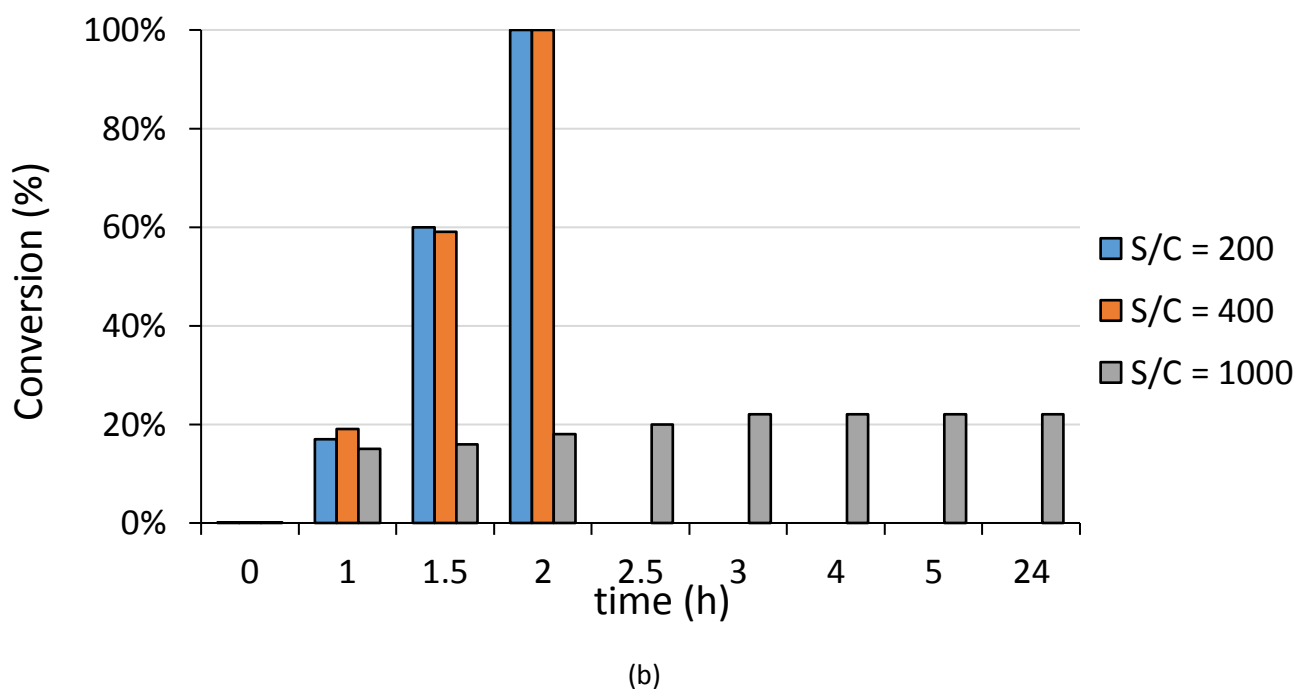


**Figure 36** - S/C ratio experiments at (a) 10 bar and (b) 40 bar; experimental condition: 100 mg of support; 2-10 mmol of substrate; 5 mg of catalyst; 2 ml of solvent (heptane); 16  $\mu$ L of DBU; 50  $\mu$ L of IL#1; pressure: 10;40 bar.

Not surprisingly, results at 40 bar are generally better than at 10 bar; moreover S/C ratios of 1000 are too harsh for the catalyst concentration. An interesting result is provided by S/C ratio of 400, where at 40 bar the reaction is completed after 2h. However, at 10 bar, after approximately 3 hours the conversion changes no more, stabilizing at approximately 20%. This result is tremendous to conclude that, for an optimum situation, the catalyst must be supplied with both Hydrogen and substrate in the right proportions, in order to avoid possible resting states.

#### 4.8.2 Mass transfer limitations

Homogeneous reactions using S/C ratio of 200 and using ethanol as solvent, achieve full conversion after only 6 minutes with 10 bar of pressure [76]. However, supported reactions here described at 10 bar, only achieve full conversion after 3h. It seems logical to assume severe mass transfer limitations on the overall process. In particular, 2 major limitations are immediate to identify and schematically represented in Figure 37. As a remark,  $C_{\infty}$  and  $C_{sat}$  are concentrations typically used when describing interfacial relations, and correspond to the concentration of  $H_2$  in the gas phase (given as  $C = P/RT$ ) and the maximum concentration of  $H_2$  achievable in heptane (well described by Henry's Law), respectively.

The first mass limitation is what is commonly known as external mass limitation, although in a rather broader way. It is firstly intended to describe the resistance experienced by the Hydrogen ( $H_2$ ) from the gas phase to the liquid medium and secondly the one from the bulk liquid to IL phase on the outer surface of the carbon sphere.  $H_2$  solubility in heptane can be excellently described by Henry's law, which predicts the amount of gas as a function of pressure [113,114]. However, this study goes beyond the scope of this work and the relevant conclusion is to acknowledge that the higher the

hydrogen pressure, the faster the reaction will be, once the saturation value ( $C_{sat.}$ ) will be higher. A second mass transfer limitation happens inside the IL, where Hydrogen must find the proper place to be part of the catalytic cycle.

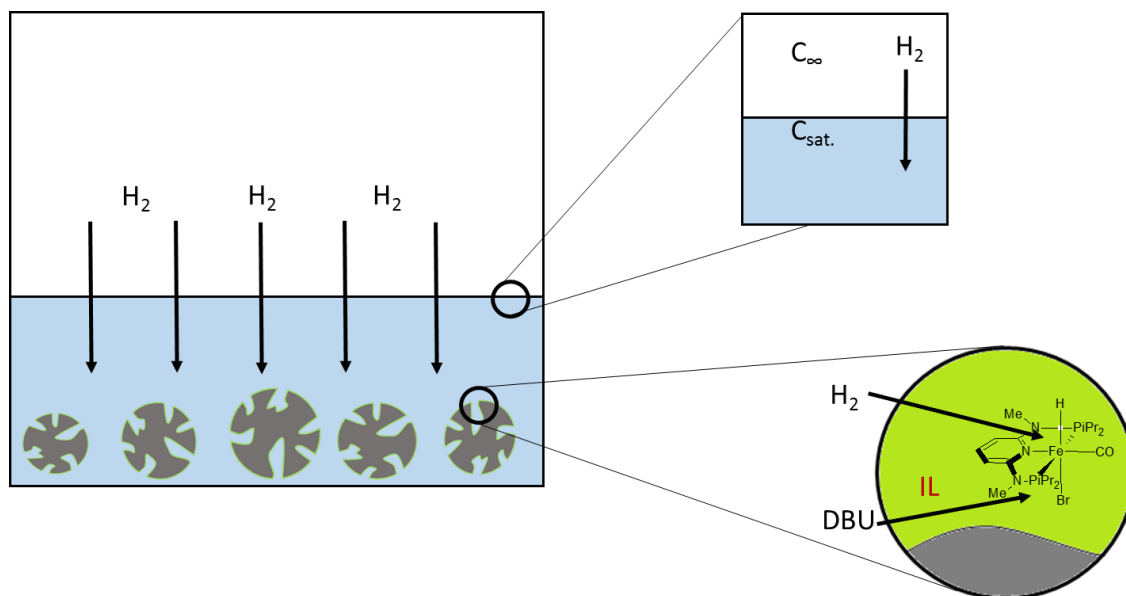


**Figure 37** - Schematic representation of major mass transfer limitations;  $C_{\infty}$  - concentration of H<sub>2</sub> in the gas phase;  $C_{sat.}$  - maximum concentration of H<sub>2</sub> in heptane.

Figure 38 shows the effect of changing pressure, and consequently the maximum bulk concentration of H<sub>2</sub> in the hydrogenations studied.

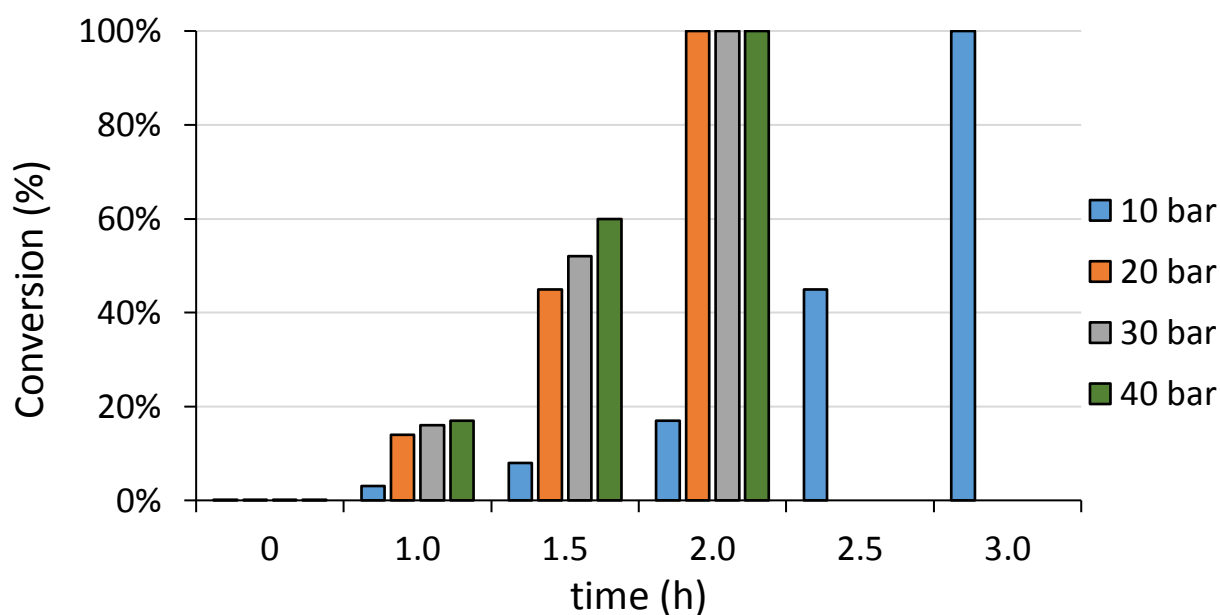


**Figure 38** - effect of changing H<sub>2</sub> pressure; experimental condition: 100 mg of support; 2 mmol of substrate(4-FBA); 5 mg of catalyst; 2 ml of solvent (heptane); 16 $\mu$ L of DBU; 50  $\mu$ L of IL#1; pressure: 10-40 bar.

Unexpectedly, Hydrogen pressure and consequently concentration in the heptane phase seem to be only relevant below 20 bar of working pressure. This result is a clear demonstration that, although H<sub>2</sub> plays its part for mass limitations problems, when reaching 20 bar, the limitation is no longer present. Effectively, the diffusivity of gases in liquids is known to be higher than that of liquids in liquids. This leads to the conclusion that mass transfer limitation is more serious with the process of admitting the substrate inside the IL phase and liberating the alcohol.

### 4.8.3 Leaching

The extension of leaching was necessary to have a qualitative interpretation of how severe the loss of catalyst/IL was and how this loss could affect the reaction results in subsequent experiments. ICP results for iron are provided in Table 21. Leaching percentage was calculated knowing the amount of iron determined by ICP in the heptane phase and the original amount inside the SILP.

**Table 21** - ICP results for leaching detecting; \*\* - leaching was detected by NMR.

Sample	Pressure (bar)	IL	Substrate	Leaching (%)
CARB 25	10	IL#1	4-FBA	0.2
CARB 25	40	IL#1	4-FBA	0.4
CARB 30	40	IL#1	4-FBA	0.1
CARB 40	10	IL#1	4-FBA	0.3
CARB 40	40	IL#1	4-FBA	0.3
CARB 60	40	IL#1	4-FBA	**1.2

It was found that the new SILP catalyst, with the optimum pore filling CARB 40, was highly active in the hydrogenation of 4-FBA without significant leaching of both the complex and the IL.

### 4.8.4 Recyclability

One of the biggest issues concerning supported ILs has to do, besides being able to perform the reaction, with being recyclable. Figure 39 presents recyclability results, under the best possible tested conditions. Conversions were obtained after exactly 2 hours from the addition of fresh substrate and two experimental sets were made, named #1 and #2.

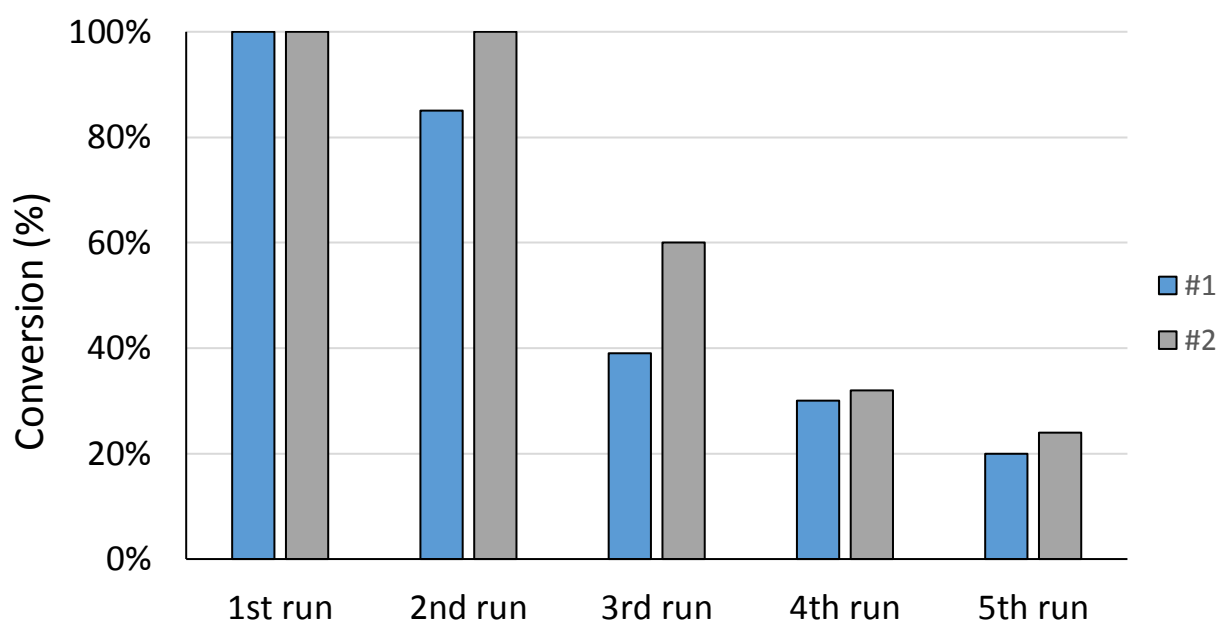


**Figure 39** - recyclability tested; experimental conditions: 100 mg of support; 2 mmol of substrate (4-FBA); 5 mg of catalyst; 2 ml of solvent (heptane); 16  $\mu$ L of DBU; 50  $\mu$ L of IL#1; pressure: 40 bar.

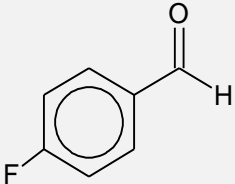
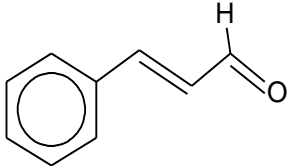
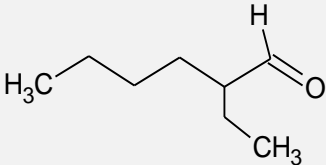
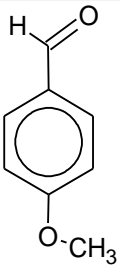
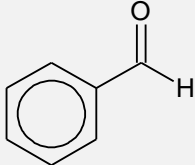
In absolute analysis the results obtained are not the best possible; indeed a severe decrease in conversion is identifiable after the 2<sup>nd</sup>/3<sup>rd</sup> run. However, the protocol followed and described in the experimental section partially allows for justification. The fully converted supernatant is pulled out with a syringe, which in turn is not able to remove all the liquid. This situation (of not removing all the product) has consequences in the subsequent run. Moreover, this step has to be performed as quickly as possible in order to avoid the infiltration of oxygen. Furthermore, once the substrate is fully consumed, the catalyst is thought to reach a resting state [76,80], which in turn may lead to the results presented.

A possible solution would be a continuous flow reactor, for example a plug flow, where the catalyst is constantly in contact with fresh substrate, avoiding reaching a resting state.

#### 4.8.4.1 Substrate screening

In all the experiments, 4-fluorobenzaldehyde was the elected substrate, once it is known to yield excellent results with the catalyst. In order to enlarge the spectra of possible, and useful reactions, several others were tested. Table 22 depicts the obtained results.

**Table 22** - Substrate screening; experimental condition: 100 mg of support; 2 mmol of substrate; 5 mg of catalyst; 2 ml of solvent (heptane); 16  $\mu$ L of DBU; 50  $\mu$ L of IL#1; pressure: 10 bar.

Substrates	Time	Conversion
 4-FBA	3 h	>99%
 Cinnamaldehyde	4 h	>99%
 2-Ethyl-Hexanal	24 h	0 %
 4-Anisaldehyde	4 h	>99%
 Benzaldehyde	3 h	>99%



Under these reaction conditions, aromatic substrates without substituent (benzaldehyde) or bearing both electron withdrawing halogen substituents such as p-fluorbenzaldehyde or electron donating groups such as OMe in 4-anisaldehyde are susceptible of being easily hydrogenated by the supported iron(II) complex catalyst. Moreover, after the hydrogenation of a challenging  $\alpha,\beta$ -unsaturated substrates (cinnamaldehyde), the C=C double bond remained unaffected. This emphasizes the high chemoselectivity of the present system. The liquid reaction mixtures were analysed again after the reaction and it was found that merely 0.2 mol% Fe leached with respect to the initial loading in all cases.

#### 4.8.4.2 IL screening

Hitherto it was made clear that using 50  $\mu$ L of IL and 100 mg of support (CARB 40) are the best conditions for the reaction. Moreover, the amount of support is as important as the pore filling degree. The second important parameter to check is the IL influence on the overall conversion. As already discussed, the structure of the IL plays a significant role in the catalyst stability and, as a consequence, on the catalyst activity. All ILs that would have a chance to work well with the catalyst were tested and results are displayed in Figure 40. Predictably, all the “small” ILs, namely IL#1, 2, 4 and 6 were able to perform well, showing no measurable leaching. For the “big” ILs (IL#7 and 8), a degree of leaching was expected, since they are soluble in heptane and entering the pores is a difficult task when having big chains attached. This situation allows for the IL to stay poorly adsorbed in the outer surface of the support, thus being easily removed once the reaction starts. As it was expected, detectable leaching, both with  $^{19}\text{F}$  NMR and ICP (1.7 %), was affecting big ILs. A final remark on these figures goes for comparing IL#1 and IL#2; they are exactly the same but for the lateral chain. The former has an ethyl and the later a butyl chain; this small difference affects the overall result of the reaction. First, catalyst’s solubility is different and second the increase in length may affect the filling of the pores, eventually leading to different degrees of clogging, not allowing for all the reaction to take place inside the porous matrix but only in the entrance of the pores. Unfortunately basic ILs, showed no conversion without adding DBU, which is the opposite of the homogeneous results.

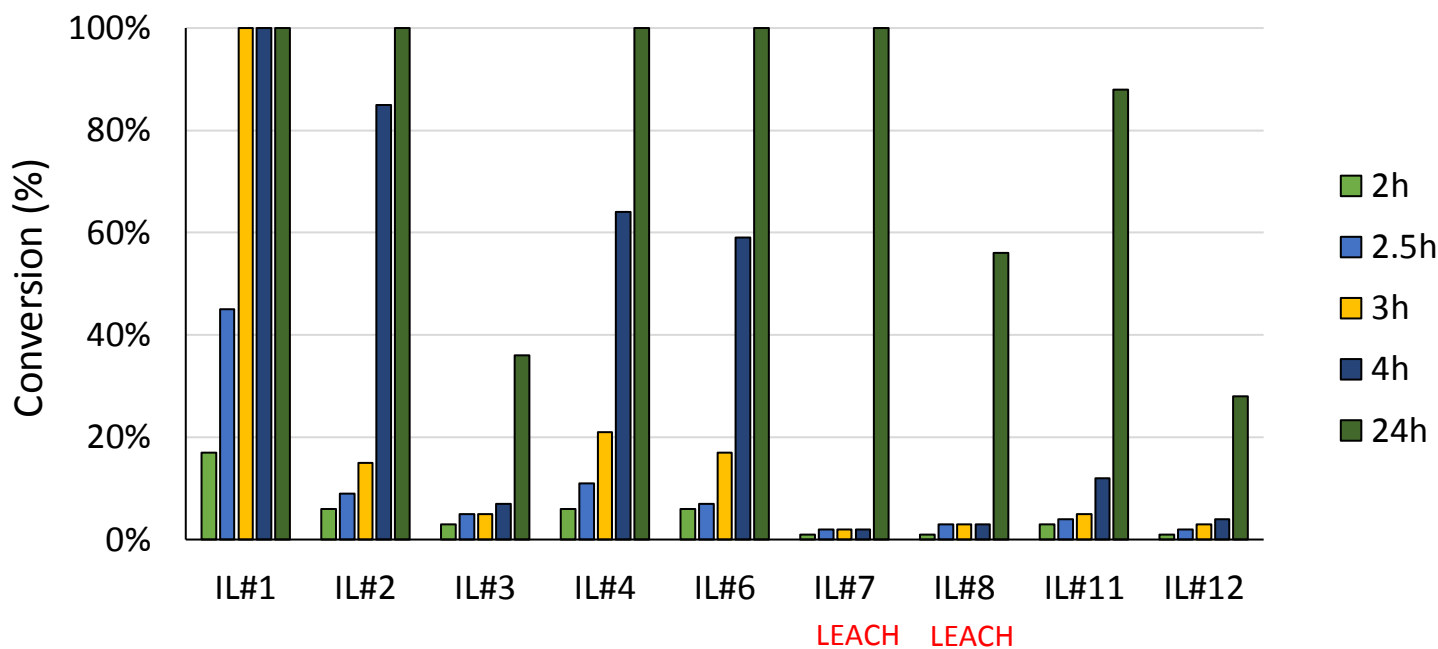


**Figure 40** - ILs testing; experimental condition: 100 mg of support; 2 mmol of substrate(4-FBA); 5 mg of catalyst; 2 ml of solvent (heptane); 16 $\mu$ L of DBU; 50  $\mu$ L of IL; pressure: 10 bar.

Up to this point all possible questions regarding the choice of IL, amount of support and IL seem to have been extensively discussed and settled, with all data pointing towards small ILs, in particular CARB 40 using 50  $\mu$ L of IL#1 and 100 mg of support.

#### 4.9 Carbon Cloth – Activated carbon fibers

Carbon fibers used were made available by Kynol<sup>®</sup> company; the carbon cloth consists of highly porous carbon fibers with specific surface areas ranging from 700 to 3000 m<sup>2</sup>/g and pore volume from 0.4 to 0.8 cm<sup>3</sup>/g. Fiber's diameter is typically 10  $\mu$ m and the pore structure is essentially micropores, with an average pore width of 1 nm. Having this into consideration, adsorption dynamics are expected to be much superior to those of conventional (granulated or powdered) activated carbons. Applications are several and range from electrical/electronic applications to a more conventional filtration medium. Nowadays it has been explored as a useful coating for hunters in order to avoid having their scent detected by the preys.

The raw material is a *novolac* resin, made by polymerization of phenol and formaldehyde and containing approximately 78% carbon. This resin suffers a series of transformations releasing some functional groups as the temperature is increased until the desired result is obtained and the fiber is completed. Figure 41 shows a picture of the fibers used while Table 23 summarizes the relevant information on the 4 kinds of carbon cloth available.

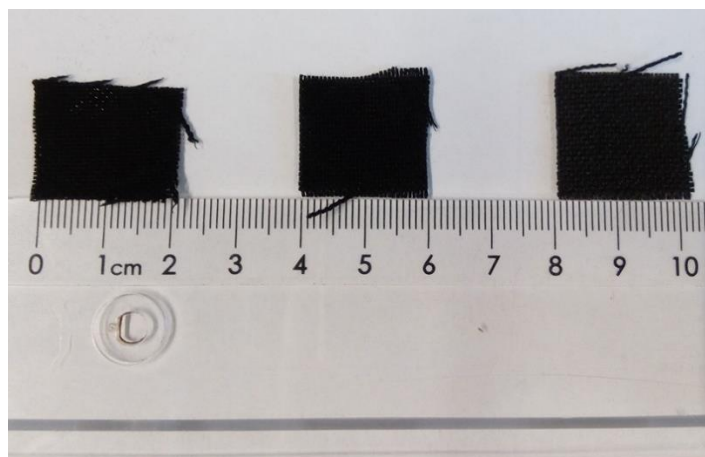


**Figure 41** - Carbon cloth example.

**Table 23** - Carbon cloths main characteristics.

Carbon Cloth Ref.	ACC-5092-10	ACC-5092-20	ACC-507-15	ACC-507-20
<b>Specific Surface Area (m<sup>2</sup>/g)</b>	1,000	2,000	1,500	2,000
<b>Carbon Fiber Content (%)</b>	100	100	100	100
<b>Thickness (mm)</b>	0.66	0.55	0.47	0.43
<b>Pore volume (cm<sup>3</sup>/g)</b>	0.4	0.8	0.5	0.7
<b>Weight (g/m<sup>2</sup>)</b>	205	150	115	105
<b>I<sub>2</sub> adsorption (mg/g)</b>	1,300	1,700	1,500	1,700
<b>pH</b>	6.5	7.5	7.1	8.0

Mikkola and co-workers [62] used Pd catalyst with ionic liquid supported carbon cloths in the hydrogenation of citral. Their results are very interesting, however it seems that carbon cloths are not suitable supports in the present case. They do not reach the desired aim in terms of reaction conversion. Table 24 shows the results obtained. It is noteworthy that the procedure followed was exactly the same used for carbon spheres, including several optimization steps.

**Table 24** - Carbon cloths results. Experimental conditions: 100 mg of support; 1 mmol of substrate (4-FBA); 2.5 mg of catalyst; 2 ml of solvent (heptane); 8  $\mu$ L of DBU; 40  $\mu$ L of IL#1; pressure: 40 bar.

Sample designation	Time	Conversion
ACC-5092-10	24 h	1 %
ACC-5092-20	24 h	2 %
ACC-507-15	24 h	2 %
ACC-507-20	24 h	3 %

These results are disappointing, but relatively easy to explain. The cloth is 100% microporous, which means that the IL completely fills the pores, leaving no space for the starting materials to reach the catalyst. Since the pores are clogged, the reaction does not take advantage of the incredible surface area available inside.

#### 4.10 Overall resume

The best results concerning experiments performed in homogeneous, biphasic and supported reactions are compiled in

Table 25. Furthermore, for all data, TON and TOF values were calculated, according to Eq. (2) and (3) respectively.

$$TON = \frac{\text{mol of product}}{\text{mol of catalyst}} \quad (2)$$

$$TOF = \frac{TON}{\text{time reaction (h)}} \quad (3)$$

**Table 25** – Resume Conditions: Biphasic: 2 mmol of substrate; 5 mg of catalyst; 2 ml of solvent (heptane); 16  $\mu$ L of DBU; IL according to Table 7; Supported: 100 mg of support; 2 mmol of substrate; 5 mg of catalyst; 2 ml of solvent (heptane); 16  $\mu$ L of DBU; 50  $\mu$ L of IL; pressure: 10/40 bar. \* - no DBU added.

Condition	Substrate	S/C	P (bar)	Time (min)	Conversion (%)	TON	TOF (h <sup>-1</sup> )
<b>Homogeneous IL#1</b>	4-FBA	200	10	7	>99	200	1714
<b>Biphasic IL#1</b>	4-FBA	200	10	60	> 99	200	200
<b>Biphasic IL#2</b>	4-FBA	200	10	60	> 99	200	200
<b>Biphasic IL#6</b>	4-FBA	200	10	60	> 99	200	200
<b>Biphasic IL#11*</b>	4-FBA	200	10	60	> 99	200	200
<b>Biphasic IL#12*</b>	4-FBA	200	10	60	> 99	200	200
<b>CARB 40 IL#1</b>	4-FBA	<b>200</b>	<b>10</b>	<b>180</b>	<b>&gt; 99</b>	<b>200</b>	<b>67</b>

<b>CARB 40 IL#1</b>	4-FBA	<b>200</b>	<b>40</b>	<b>120</b>	<b>&gt; 99</b>	<b>200</b>	<b>100</b>
<b>CARB 40 IL#1</b>	4-FBA	<b>400</b>	<b>40</b>	<b>120</b>	<b>&gt; 99</b>	<b>400</b>	<b>200</b>
<b>CARB 40 IL#1</b>	4-Anisaldehyde	200	10	240	> 99	200	50
<b>CARB 40 IL#1</b>	Benzaldehyde	200	10	180	> 99	200	67
<b>CARB 40 IL#1</b>	Cinnamaldehyde	200	10	240	> 99	200	50
<b>CARB 40 IL#2</b>	4-FBA	200	10	240	85	170	43

From all the successful SILPs performed using activated carbon spheres, the best results are the ones with 40% theoretical pore filling degree. This new SILP catalyst, with the optimum pore filling, was highly active in the hydrogenation of aromatic aldehydes, exhibiting TONs and TOFs of up to 400 and 200 h<sup>-1</sup>. TON and TOF values for supported reactions are more modest than those of homogenous and biphasic, in accordance with mass transfer limitations experienced by the SILP; however, it eliminates their main drawbacks, i.e., difficult separation and large amounts of IL needed, thus making the SILP catalyst more sustainable.

## 5. Conclusions and future work

SILP catalysis has a lot to offer to both academic and industrial applications. In the present work a successful SILP system was created, comprising mesoporous carbon spheres, an iron(II) complex catalyst and an imidazolium based IL. As major results, full conversion was achieved after 3 and 2 hours at 10 and 40 bar, respectively, using 4-Fluorobenzaldehyde as a substrate. Furthermore TONs and TOFs up to 200 and 400 h<sup>-1</sup>, respectively were attained. Pressure was found to be important up to 20 bar, situation when mass transfer limitation is no longer on the Hydrogen but on the aldehyde/alcohol movement. Another major result concerns the amount of support used. In truth, the SILP system is extremely sensitive to that parameter, with a small variation leading to huge changes in overall conversion. Recyclability was tested and, due to catalyst deactivation, progressive loss of activity was found out.

Some curious results concern the structure of the IL when the catalyst is dissolved, and when this mixture is successfully impregnated/confined in the carbon porous structure. Indeed all the employed techniques reveal some curious data concerning this interaction. BET results point for the fact that, when the same amount of IL and IL+catalyst are impregnated, the former has an effective occupied volume that is below that of the latter. XPS data provides an incredible range of data. On the one hand, binding energies shifting towards higher energies and, on the other hand, angle dependent analysis of all the elements, clearly shows a special adaptation of the system when the catalyst is present. IR measurements go again in the way of showing the same as the previous techniques. DSC shows a decrease in decomposition temperature, of approximately 200°C, when the IL is present in the porous carbon, in comparison with a pure IL sample.

A very interesting side result is the overall reaction conversion dependency with the impregnation time. From a hypothetical point of view, the longer the impregnation, the deeper will both IL and catalyst be. However, there is no major reason for showing no conversion at all after 4h.

Concerning future work, there are a lot of interesting possibilities. For a start it would be interesting to have, in place of a batch reactor, a continuous one, for example a plug flow reactor. This situation would be suitable to test for recyclability conditions. The catalyst would be fixed inside the reactor, and a continuous source of substrate would be always available, avoiding a possible deactivation of the catalyst due to lack of substrate. Another interesting possibility would be to explore all the side data concerning the structure of samples when the catalyst is present. As an example, some electrochemical techniques to explore charge distributions inside the IL containing catalyst would be relevant, as well as using these techniques to study what is happening indeed in the deepness of the porous structure.

## 6. References

1. Bolm, C. & Gladysz, J. A. Introduction: Enantioselective catalysis. *Chem. Rev.* **103**, 2761–2762 (2003).
2. Anastas, P. T. & Kirchhoff, M. M. Origins, current status, and future challenges of green chemistry. *Acc. Chem. Res.* **35**, 686–694 (2002).
3. Wang, X. & Ding, K. Self-Supported Heterogeneous Catalysts for Enantioselective Hydrogenation. *J. Am. Chem. Soc.* **126**, 10524–10525 (2004).
4. Hu, A., Ngo, H. L. & Lin, W. Chiral porous hybrid solids for practical heterogeneous asymmetric hydrogenation of aromatic ketones. *J. Am. Chem. Soc.* **125**, 11490–11491 (2003).
5. Song, C. E., Lee, S., Song, C. E. & Lee, S. Supported Chiral Catalysts on Inorganic Materials Supported Chiral Catalysts on Inorganic Materials. **102**, 3495–3524 (2002).
6. Li, X. *et al.* Asymmetric Hydrogenation of Ketones with Polymer-Supported Chiral 1, 2-Diphenylethylenediamine. *Orgn. Lett.* **24**, 4559–4561 (2003).
7. Murzin, D. Y., Mäki-Arvela, P., Toukoniitty, E. & Salmi, T. Asymmetric Heterogeneous Catalysis: Science and Engineering. *Catal. Rev.* **47**, 175–256 (2005).
8. Mehnert, C. P. Supported ionic liquid catalysis. *Chem. - A Eur. J.* **11**, 50–56 (2005).
9. Rodgers, R. D. & Seddon, K. R. Ionic Liquids--Solvents of the Future? *Science* **302**, 792–793 (2003).
10. Plechkova, N. V & Seddon, K. R. Applications of ionic liquids in the chemical industry. *Chem Soc Rev* **37**, 123–150 (2008).
11. Wasserscheid, P. & Welton, T., *Ionic Liquids in Synthesis*, Wiley-VCH, pp 369–463 (2007).
12. Riisager, A., Eriksen, K. M., Wasserscheid, P. & Fehrmann, R. Propene and 1-octene hydroformylation with silica-supported, ionic liquid-phase (SILP) Rh-phosphine catalysts in continuous fixed-bed mode. *Catal. Letters* **90**, 149–153 (2003).
13. Mehnert, C. P., Cook, R. A., Dispenziere, N. C. & Afeworki, M. Supported ionic liquid catalysis - A new concept for homogeneous hydroformylation catalysis. *J. Am. Chem. Soc.* **124**, 12932–12933 (2002).
14. Steinrück, H.-P. & Wasserscheid, P. Ionic Liquids in Catalysis. *Catal. Letters* **145**, 380–397 (2015).
15. Camper, D., Becker, C., Koval, C. & Noble, R. Diffusion and solubility measurements in room temperature ionic liquids. *Ind. Eng. Chem. Res.* **45**, 445–450 (2006).
16. Werner, S., Haumann, M. & Wasserscheid, P. Ionic Liquids in Chemical Engineering. *Annu. Rev. Chem. Biomol. Eng.* **1**, 203–230 (2010).
17. Carmichael, A. J. & Seddon, K. R. Polarity study of some 1-alkyl-3-methylimidazolium ambient-temperature ionic liquids with the solvatochromic dye, Nile Red. *J. Phys. Org. Chem.* **13**, 591–595 (2000).
18. Cevasco, G. & Chiappe, C. Are ionic liquids a proper solution to current environmental challenges? *Green Chem.* **16**, 2375 (2014).
19. Smiglak, M. *et al.* Ionic liquids for energy, materials, and medicine. *Chem. Commun.* **50**, 9228–

- 9250 (2014).
20. Conrad Zhang, Z. Catalysis in Ionic Liquids. *Adv. Catal.* **49**, 153–237 (2006).
  21. Welton, T. Ionic liquids in catalysis. *Coord. Chem. Rev.* **248**, 2459–2477 (2004).
  22. Miao, W. & Tak, H. C. Ionic-liquid-supported synthesis: A novel liquid-phase strategy for organic synthesis. *Acc. Chem. Res.* **39**, 897–908 (2006).
  23. Corma, A. & Garcia, H. Lewis acids: From conventional homogeneous to green homogeneous and heterogeneous catalysis. *Chem. Rev.* **103**, 4307–4365 (2003).
  24. Olivier-Bourbigou, H., Magna, L. & Morvan, D. Ionic liquids and catalysis: Recent progress from knowledge to applications. *Appl. Catal. A Gen.* **373**, 1–56 (2010).
  25. Seddon, K. R. Ionic liquids: A taste of the future. *Nat. Mater.* **2**, 363–365 (2003).
  26. Galinski, M., Lewandowski, A. & Stepniak, I. Ionic liquids as electrolytes. *Electrochim. Acta* **51**, 5567–5580 (2006).
  27. Pandey, S. Analytical applications of room-temperature ionic liquids: A review of recent efforts. *Anal. Chim. Acta* **556**, 38–45 (2006).
  28. Jork, C., Seiler, M., Beste, Y.-A. & Arlt, W. Influence of Ionic Liquids on the Phase Behavior of Aqueous Azeotropic Systems. *J. Chem. Eng. Data* **49**, 852–857 (2004).
  29. Minami, I. Ionic liquids in tribology. *Molecules* **14**, 2286–2305 (2009).
  30. Walden, P. Ueber die Molekulargröße und elektrische Leitfähigkeit einiger geschmolzener Salze (Molecular weights and electrical conductivity of several fused salts). *Bull Acad. Imper. Sci. St. Petersburg.* **8**, 405–422 (1914).
  31. Wilkes, J. S., Levisky, J. A., Wilson, R. A. & Hussey, C. L. Dialkylimidazolium Chloroaluminate Melts: A New Class of Room-Temperature Ionic Liquids for Electrochemistry, Spectroscopy, and Synthesis. **237**, 1263–1264 (1982).
  32. Wilkes, J. S. & Zaworotko, M. J. Air and water stable 1-ethyl-3-methylimidazolium based ionic liquids. *J. Chem. Soc. Chem. Commun.* **2**, 965–967 (1992).
  33. Plechkova, N. V. & Seddon, K. R. Ionic Liquids: ‘Designer’ Solvents for Green Chemistry. *Methods Reagents Green Chem. An Introd.* **2000**, 103–130 (2007).
  34. Tanner, E. E. L. *et al.* Probing the importance of ionic liquid structure: a general ionic liquid effect on an SNAr process. *Org. Biomol. Chem.* **11**, 7516 (2013).
  35. Wang, Z., Yan, J., Zhang, X. & Wang, L. Merrifield resin supported ionic liquids/L-proline as efficient and recyclable catalyst systems for asymmetric aldol reaction. *Synthesis (Stuttg.)* **22**, 3744–3750 (2009).
  36. Hagiwara, H., Sasaki, H., Hoshi, T. & Suzuki, T. Sustainable click reaction catalyzed by supported ionic liquid catalyst (Cu-SILC). *Synlett* **4**, 643–647 (2009).
  37. Breitenlechner, S., Fleck, M., Müller, T. E. & Suppan, A. Solid catalysts on the basis of supported ionic liquids and their use in hydroamination reactions. *J. Mol. Catal. A Chem.* **214**, 175–179 (2004).
  38. Shi, F., Zhang, Q., Li, D. & Deng, Y. Silica-gel-confined ionic liquids: A new attempt for the development of supported nanoliquid catalysis. *Chem. - A Eur. J.* **11**, 5279–5288 (2005).
  39. Selvam, T., MacHoke, A. & Schwieger, W. Supported ionic liquids on non-porous and porous



- inorganic materials - A topical review. *Appl. Catal. A Gen.* **445**, 92–101 (2012).
40. Volland, S. *et al.* Encapsulation of Pd(OAc)<sub>2</sub> catalyst in an ionic liquid phase confined in silica gels. Application to Heck-Mizoroki reaction. *New J. Chem.* **33**, 2015–2021 (2009).
  41. Sievers, C. *et al.* Palladium catalysts immobilized in thin films of ionic liquid for the direct addition of aniline to styrene. *J. Mol. Catal. A Chem.* **279**, 187–199 (2008).
  42. Lemus, J., Palomar, J., Gilarranz, M. A. & Rodriguez, J. J. Characterization of Supported Ionic Liquid Phase (SILP) materials prepared from different supports. *Adsorption* **17**, 561–571 (2011).
  43. Yu, N. *et al.* Gold nanoparticles supported on periodic mesoporous organosilicas for epoxidation of olefins: Effects of pore architecture and surface modification method of the supports. *Microporous Mesoporous Mater.* **143**, 426–434 (2011).
  44. Chun, Y. S., Shin, J. Y., Song, C. E. & Lee, S. G. Palladium nanoparticles supported onto ionic carbon nanotubes as robust recyclable catalysts in an ionic liquid. *Chem. Commun.* **7345**, 942–944 (2008).
  45. Burguete, M. I. *et al.* Pd catalysts immobilized onto gel-supported ionic liquid-like phases (g-SILLPs): A remarkable effect of the nature of the support. *J. Catal.* **269**, 150–160 (2010).
  46. Burguete, M. I. *et al.* Development of efficient processes under flow conditions based on catalysts immobilized onto monolithic supported ionic liquid-like phases. *Pure Appl. Chem.* **81**, 1991–2000 (2009).
  47. Xu, Z. *et al.* Reusable and efficient polystyrene-supported acidic ionic liquid catalyst for esterifications. *J. Mol. Catal. A Chem.* **332**, 152–157 (2010).
  48. Sievers, C., Jimenez, O., Müller, T. E., Steuernagel, S. & Lercher, J. A. Formation of solvent cages around organometallic complexes in thin films of supported ionic liquid. *J. Am. Chem. Soc.* **128**, 13990–13991 (2006).
  49. Knapp, R. *et al.* Corrugated ionic liquid surfaces with embedded polymer stabilized platinum nanoparticles. *J. Phys. Chem. C* **114**, 13722–13729 (2010).
  50. Jutz, F., Andanson, J. M. & Baiker, A. Ionic liquids and dense carbon dioxide: A beneficial biphasic system for catalysis. *Chem. Rev.* **111**, 322–353 (2011).
  51. Chen, P. & Meyer, T. J. Medium Effects on Charge Transfer in Metal Complexes. *Chem. Rev.* **98**, 1439–1477 (1998).
  52. Crowhurst, L., Lancaster, N. L., Pérez Arlandis, J. M. & Welton, T. Manipulating solute nucleophilicity with room temperature ionic liquids. *J. Am. Chem. Soc.* **126**, 11549–11555 (2004).
  53. Fow, K. L., Jaenicke, S., Müller, T. E. & Sievers, C. Enhanced enantioselectivity of chiral hydrogenation catalysts after immobilisation in thin films of ionic liquid. *J. Mol. Catal. A Chem.* **279**, 239–247 (2008).
  54. Atkin, R. & Warr, G. G. Self-assembly of a nonionic surfactant at the graphite/ionic liquid interface. *J. Am. Chem. Soc.* **127**, 11940–11941 (2005).
  55. Mantz, R. & Trulove, P. ROESY NMR of basic ambient-temperature chloroaluminate ionic liquids. *Inorg. Chem.* **34**, 3846–3847 (1995).
  56. Migowski, P. & Dupont, J. Catalytic applications of metal nanoparticles in imidazolium ionic liquids. *Chem. - A Eur. J.* **13**, 32–39 (2007).

57. Huang, J. *et al.* Pd nanoparticles immobilized on molecular sieves by ionic liquids: Heterogeneous catalysts for solvent-free hydrogenation. *Angew. Chemie - Int. Ed.* **43**, 1397–1399 (2004).
58. CATALYTIC HYDROGENATION USING SUPPORTED IONIC LIQUID MEMBRANES. *High Temp. Mater. Process. (An Int. Q. High-Technology Plasma Process.* **2**, 543–558 (1998).
59. Hagiwara, H., Nakamura, T., Hoshi, T. & Suzuki, T. Palladium-supported ionic liquid catalyst (Pd-SH-SILC) immobilized on mercaptopropyl silica gel as a chemoselective, reusable and heterogeneous catalyst for catalytic hydrogenation. *Green Chem.* **13**, 1133 (2011).
60. Kernchen, U., Etzold, B., Korth, W. & Jess, A. Solid catalyst ionic liquid layer (SCILL) - A new concept to improve selectivity illustrated by hydrogenation of cyclooctadiene. *Chem. Eng. Technol.* **30**, 985–994 (2007).
61. Rodríguez-Pérez, L., Teuma, E., Falqui, A., Gómez, M. & Serp, P. Supported ionic liquid phase catalysis on functionalized carbon nanotubes. *Chem. Commun. (Camb)*. 4201–4203 (2008).
62. Mikkola, J., Virtanen, P., Karhu, H., Salmi, T. & Murzin, D. Y. Supported ionic liquids catalysts for fine chemicals : citral hydrogenation. *Green Chem.* **8**, 197–205 (2006).
63. Nassor, E. C. O. *et al.* Magnetic Carbon Nanofiber Networks as Support for Ionic Liquid Based Catalyst. *Catal. Letters* **145**, 505–510 (2015).
64. Schsner, E., Schneider, M. J., Meyer, C., Haumann, M. & Wasserscheid, P. *Challenging the scope of continuous, gas-phase reactions with supported ionic liquid phase (SILP) catalysts - Asymmetric hydrogenation of methyl acetoacetate.* *Applied Catalysis A: General* **399**, 35-41 (2011).
65. Jimenez, O., Müller, T. E., Sievers, C., Spirkl, A. & Lercher, J. a. Markownikoff and anti-Markownikoff hydroamination with palladium catalysts immobilized in thin films of silica supported ionic liquids. *Chem. Commun. (Camb)*. 2974–2976 (2006).
66. Jakuttis, M. *et al.* Rhodium-phosphite SILP catalysis for the highly selective hydroformylation of mixed C4 feedstocks. *Angew. Chemie - Int. Ed.* **50**, 4492–4495 (2011).
67. Schneider, M. J., Haumann, M., Stricker, M., Sundermeyer, J. & Wasserscheid, P. Gas-phase oxycarbonylation of methanol for the synthesis of dimethyl carbonate using copper-based Supported Ionic Liquid Phase (SILP) catalysts. *J. Catal.* **309**, 71–78 (2014).
68. Riisager, A., Jørgensen, B., Wasserscheid, P. & Fehrmann, R. First application of supported ionic liquid phase (SILP) catalysis for continuous methanol carbonylation. *Chem. Commun.* 994–996 (2006).
69. Wang, J. Q., Yue, X. D., Cai, F. & He, L. N. Solventless synthesis of cyclic carbonates from carbon dioxide and epoxides catalyzed by silica-supported ionic liquids under supercritical conditions. *Catal. Commun.* **8**, 167–172 (2007).
70. Gu, Y., Ogawa, C. & Kobayashi, S. Silica-supported sodium sulfonate with ionic liquid: a neutral catalyst system for Michael Reactions of Indoles in Water. *Org. Lett.* **9**, 175–178 (2007).
71. Gu, Y., Ogawa, C., Kobayashi, J., Mori, Y. & Kobayashi, S. A heterogeneous silica-supported scandium/ionic liquid catalyst system for organic reactions in water. *Angew. Chemie - Int. Ed.* **45**, 7217–7220 (2006).
72. Kim, D. W. & Chi, D. Y. Polymer-Supported Ionic Liquids: Imidazolium Salts as Catalysts for Nucleophilic Substitution Reactions Including Fluorinations. *Angew. Chemie - Int. Ed.* **43**, 483–485 (2004).

73. Lozano, P. *et al.* On the importance of the supporting material for activity of immobilized *Candida antarctica* lipase B in ionic liquid/hexane and ionic liquid/supercritical carbon dioxide biphasic media. *J. Supercrit. Fluids* **40**, 93–100 (2007).
74. Lozano, P., De Diego, T., Carrié, D., Vaultier, M. & Iborra, J. L. Lipase catalysis in ionic liquids and supercritical carbon dioxide at 150 degrees C. *Biotechnol. Prog.* **19**, 380–2 (2003).
75. Johnson, N. B., Lennon, I. C., Moran, P. H. & Ramsden, J. A. Industrial-scale synthesis and applications of asymmetric hydrogenation catalysts. *Acc. Chem. Res.* **40**, 1291–1299 (2007).
76. Gorgas, N., Stöger, B., Veiros, L. F. & Kirchner, K. Highly Efficient and Selective Hydrogenation of Aldehydes: A Well-Defined Fe(II) Catalyst Exhibits Noble-Metal Activity. *ACS Catal.* **6**, 2664–2672 (2016).
77. Fehrmann, R., Riisager, A. & Haumann, M. *Supported Ionic Liquids - Fundamentals and Applications.*, Wiley-VCH, 2014.
78. Doorslaer, C. Van *et al.* Catalytic Hydrogenolysis of Aromatic Ketones in Mixed Choline – Betainium Ionic Liquids. *ChemSusChem* **1**, 997–1005 (2008).
79. Van Doorslaer, C., Schellekens, Y., Mertens, P., Binnemans, K. & De Vos, D. Spontaneous product segregation from reactions in ionic liquids: application in Pd-catalyzed aliphatic alcohol oxidation. *Phys. Chem. Chem. Phys.* **12**, 1741–1749 (2010).
80. Gorgas, N. *et al.* Efficient Hydrogenation of Ketones and Aldehydes Catalyzed by Well-Defined Iron(II) PNP Pincer Complexes: Evidence for an Insertion Mechanism. *Organometallics* **33**, 6905–6914 (2014).
81. Clark, K. D., Nacham, O., Purslow, J. A., Pierson, S. A. & Anderson, J. L. Magnetic ionic liquids in analytical chemistry: A review. *Anal. Chim. Acta* **934**, 9–21 (2016).
82. Joseph, A. *et al.* Paramagnetic ionic liquids for advanced applications: A review. *J. Mol. Liq.* **218**, 319–331 (2016).
83. Taylor, A. W. & Licence, P. X-ray photoelectron spectroscopy of ferrocenyl- and ferrocenium-based ionic liquids. *ChemPhysChem* **13**, 1917–1926 (2012).
84. Hayashi, S. & Hamaguchi, H. Discovery of a Magnetic Ionic Liquid [bmim]FeCl<sub>4</sub>. *Chem. Lett.* **33**, 1590–1591 (2004).
85. Yoshida, Y. *et al.* Conducting and magnetic properties of 1-ethyl-3-methylimidazolium (EMI) salts containing paramagnetic irons: Liquids [EMI][MIII Cl<sub>4</sub>] (M = Fe and Fe<sub>0.5</sub>Ga<sub>0.5</sub>) and solid [EMI] 2[FeII Cl<sub>4</sub>]. *Bull. Chem. Soc. Jpn.* **78**, 1921–1928 (2005).
86. Del Sesto, R. E. *et al.* Structure and magnetic behavior of transition metal based ionic liquids. *Chem. Commun.* 447–449 (2008).
87. Erto, A. *et al.* Carbon-supported ionic liquids as innovative adsorbents for CO<sub>2</sub> separation from synthetic flue-gas. *J. Colloid Interface Sci.* **448**, 41–50 (2015).
88. Wang, Y., Li, C., Guo, X. & Wu, G. The influence of silica nanoparticles on ionic liquid behavior: A clear difference between adsorption and confinement. *Int. J. Mol. Sci.* **14**, 21045–21052 (2013).
89. Joni, J., Haumann, M. & Wasserscheid, P. Continuous gas-phase isopropylation of toluene and cumene using highly acidic Supported Ionic Liquid Phase (SILP) catalysts. *Appl. Catal. A Gen.* **372**, 8–15 (2010).

90. Armarego, W. L. . & Perrin, D. . *Purification of Laboratory Chemicals*. 4th ed., Pergamon: New York, 199.
91. Shirley, D. A. High-resolution x-ray photoemission spectrum of the valence bands of gold. *Phys. Rev. B* **5**, 4709–4714 (1972).
92. Scofield, J. H. Hartree-Slater subshell photoionization cross-sections at 1254 and 1487 eV. *J. Electron Spectros. Relat. Phenomena* **8**, 129–137 (1976).
93. Liquids, I. & Gmbh, T. *Ionic Liquids*. Wiley-VCH, 0–76 (2016).
94. Rufete-Beneite, M. & Román-Martínez, M. C. Support effects on SILP hybrid catalysts prepared with carbon materials and the RhCOD complex. *RSC Adv.* **6**, 100976–100983 (2016).
95. Blucher H.V., inventor; 2007 Aug. 6 Process for producing spherical activated carbon. United States Patent US 2008/0171648A1
96. Schonfeld M., inventor; 2003 Nov. 20 Spherical active carbon. United States Patent US 2006/0148645A1
97. Shafeeyan, M. S., Daud, W. M. A. W., Houshmand, A. & Shamiri, A. A review on surface modification of activated carbon for carbon dioxide adsorption. *J. Anal. Appl. Pyrolysis* **89**, 143–151 (2010).
98. Boehringer, B. *et al.* Polymer-based spherical activated carbons-from adsorptive properties to filter performance. *Chemie-Ingenieur-Technik* **83**, 53–60 (2011).
99. Singh, M. P., Singh, R. K. & Chandra, S. Ionic liquids confined in porous matrices: Physicochemical properties and applications. *Prog. Mater. Sci.* **64**, 73–120 (2014).
100. Perkin, S. Ionic liquids in confined geometries. *Phys. Chem. Chem. Phys.* **14**, 5052 (2012).
101. Rajput, N. N., Monk, J. & Hung, F. R. Ionic Liquids Confined in a Realistic Activated Carbon Model: A Molecular Simulation Study. *J. Phys. Chem. C* **118**, 1540–1553 (2014).
102. Hayes, R. *et al.* Pronounced Structure in Confined Aprotic Room-Temperature Ionic Liquids. *Technology* 7049–7052 (2009).
103. Chen, S. *et al.* Morphology and melting behavior of ionic liquids inside single-walled carbon nanotubes. *J. Am. Chem. Soc.* **131**, 14850–14856 (2009).
104. Chen, S., Wu, G., Sha, M. & Huang, S. Transition of Ionic Liquid [bmim][PF6] from Liquid to High-Melting-Point Crystal When Confined in Multiwalled Carbon Nanotubes. *J. Am. Chem. Soc.* **129**, 2416–2417 (2007).
105. Dong, K., Zhao, L., Wang, Q., Song, Y. & Zhang, S. Are ionic liquids pairwise in gas phase? A cluster approach and in situ IR study. *Phys. Chem. Chem. Phys.* **15**, 6034 (2013).
106. Höfft, O. *et al.* Electronic structure of the surface of the ionic liquid [EMIM][Tf2N] studied by metastable Impact Electron Spectroscopy (MIES), UPS, and XPS. *Langmuir* **22**, 7120–7123 (2006).
107. Smith, E. F., Rutten, F. J. M., Villar-Garcia, I. J., Briggs, D. & Licence, P. Ionic liquids in vacuo: Analysis of liquid surfaces using ultra-high-vacuum techniques. *Langmuir* **22**, 9386–9392 (2006).
108. Lockett, V., Sedev, R., Bassell, C. & Ralston, J. Angle-resolved X-ray photoelectron spectroscopy of the surface of imidazolium ionic liquids. *Phys. Chem. Chem. Phys.* **10**, 1330 (2008).

109. Lovelock, K. R. J., Villar-Garcia, I. J., Maier, F., Steinrück, H. P. & Licence, P. Photoelectron spectroscopy of ionic liquid-based interfaces. *Chem. Rev.* **110**, 5158–5190 (2010).
110. Steinrück, H. P. *et al.* Surface science and model catalysis with ionic liquid-modified materials. *Adv. Mater.* **23**, 2571–2587 (2011).
111. Lovelock, K. R. J. *et al.* Influence of Different Substituents on the Surface Composition of Ionic Liquids Studied Using ARXPS Influence of Different Substituents on the Surface Composition of Ionic Liquids Studied. *J. Phys. Chem. B* **113**, 2854–2864 (2009).
112. Taylor, C. E., Garvey, S. D. & Pemberton, J. E. Carbon Contamination at Silver Surfaces: Surface Preparation Procedures Evaluated by Raman Spectroscopy and X-ray Photoelectron Spectroscopy. *Anal. Chem.* **68**, 2401–2408 (1996).
113. Ji, S., Wang, Z., Guo, A., Zhou, Y. & Chen, K. Determination of hydrogen solubility in heavy fractions of crude oils by a modified direct method. *J. Chem. Eng. Data* **58**, 3453–3457 (2013).
114. Trinh, T. K. H., De Hemptinne, J. C., Lugo, R., Ferrando, N. & Passarello, J. P. Hydrogen Solubility in Hydrocarbon and Oxygenated Organic Compounds. *J. Chem. Eng. Data* **61**, 19–34 (2016).